KU LEUVEN

FACULTY OF SCIENCE

Neuropeptidergic circuitry governing arousal in *C. elegans*

Majdulin Nabil ISTIBAN

Supervisor: Prof. Dr. W. Schafer
Animal physiology and Neurobiology

Co-supervisor: Dr. I. Beets
Animal physiology and Neurobiology

Mentor: K. Venkatesh
Animal physiology and Neurobiology

Thesis presented in
fulfillment of the requirements
for the degree of Master of Science
in Biology

Academic year 2021-2022

Host lab information page

Master theses performed in the Beets lab comply with following house rules:

1. *Maximal education and scientific self-empowerment of students*

   Students are encouraged to learn from their mistakes through dialogue, rather than by simply being corrected by their supervisors. All writing in this document is the result of this process.

   Students get two feedback moments with respect to their writing process. One from their daily supervisor, who will advise them on format and content (*e.g.* scientific language, proper representation of results and structure of their interpretations). For this, daily supervisors interact either in person with the student, or via comments added to the manuscript. Under no circumstances do they rephrase sections of the text, which is entirely the student's wording. A second feedback session includes comments from (co)supervisors and only focuses on content. This implicates additional input with regards to the student's findings and the final discussion of results. The student's interpretation of this feedback is integrated in the final version of this manuscript, as it is presented here.

2. *Authenticity in science*

   Potential plagiarism was verified using TurnItIn. This work overall scored 6% of potential plagiarism. Sections underlying this result were manually verified by the daily supervisor, as such supporting the authenticity of this work.

Acknowledgements

I would like to express my sincere appreciation to Dr. William Schafer and Dr. Isabel Beets for their continuous support and subject matter expertise. Thank you for inviting me into such a warm and welcoming research environment!

To my supervisor Keertana Venkatesh: your help and feedback was invaluable, and I appreciate your mentorship deeply. I am thankful for my lab colleagues, too many to list, for their guidance and companionship during our lab duties.

To my parents, Suhad and Nabil Istiban: your constant encouragement and profound belief in my abilities got me to where I am today. Any accomplishment gained through this period is the summation of a lifetime's worth of boundless love.

To my partner Aaron Wright: thank you for being a constant in my life, through time and across continents. I cherish our years of sharing late-night calls, laughter, tears, fears, and frustrations. Happy four years! I love you so much.

Finally, I would like thank KU Leuven and its faculty of science for facilitating this wonderful learning experience. I am incredibly grateful for being awarded the Science@Leuven scholarship. Lightening my financial burden allowed me to dive headlong into my studies. I hope someday I can repay even a fraction of that goodwill to others like myself and to this prestigious institution.

Thank you all.

Table of Contents

Abbreviations

5-HT	*5-hydroxytryptamine*
ATGL-1	adipocyte triglyceride lipase-1
C. elegans	*Caenorhabditis elegans*
CAPS	calcium-dependent activator protein for secretion
CenGen	*C. elegans* Neuronal Gene Expression Network
CGC	*Caenorhabditis* Genetics Centre
cGMP	cyclic guanylyl monophosphate
ChR2	channelrhodopsin2
cM	centiMorgan
CPE	carboxypeptidase E
CRISPR	clustered regularly interspaced short palindromic repeats
crRNA	CRISPR RNA
D. melanogaster	*Drosophila melanogaster*
DCV	dense core vesicle
DMSO	Dimethylsulfoxide
DSB	double stranded break
E. coli	*Escherichia coli*
EMS	Ethyl methane sulphonate
ER	Endoplasmic reticulum
FLP	FMRFamide-related peptide
G protein	heterotrimeric guanine nucleotide-binding protein
GFP	Green fluorescent protein
GPCR	G-protein-coupled receptor
Hcrt	Hypocretin
HDR	homology directed repair
ILP	insulin-like peptides
KO	Knockout
MRN	Mechanoreceptor neuron
NCBI	National Center for Biotechnology Information
NEP	neprilysin
NeuroPal	neuronal polychromatic atlas of landmarks
NGM	Nematode Growth Medium
NLP	neuropeptide-like proteins
NmU	Neuromedin U
Orx	Orexin
PAM	Protospacer Adjacent Motif

PC	prohormone convertase
PCR	polymerase chain reaction
PDMS	Polydimethylsiloxane
PRLHR	prolactin releasing hormone receptor
sc	single cell
sGC	Soluble guanylyl cyclase
SNARE	N-ethylmaleimide-sensitive factor attachment receptor
SSV	small clear synaptic vesicle
TAE	Tris-acetate-EDTA
TPM	transcripts per million
tracrRNA	*trans*-activating CRISPR RNA
TRN	touch receptor neurons
UV	Ultraviolet

Summary

Arousal is a primitive behavioral trait that organisms need in order to survive harsh conditions and threatening encounters. When an organism faces an arousing cue, it becomes primed to respond to subsequent stimuli. This readiness is evident in its heightened responses to sensory stimulation, thereby it is said to be sensitized.

Stimulus-evoked arousal has been explored in various organisms, and neuromodulators seem to be important, if not required in some cases. However, the complete underlying cellular and molecular circuitry is yet to be discovered.

Using the model organism *Caenorhabditis elegans* (*C. elegans*), we set out to investigate potential neuropeptidergic regulators of the arousal state.

Based on previous work done in our lab, two candidates were chosen for further investigating their role in mediating arousal responses. Both candidate mutants, the neuropeptide *flp-7* and the neuropeptide receptor *npr-13*, exhibited altered ASH-dependent sensitization responses following mechanical stimulation. This combined with their expression pattern, made them good candidates to investigate locomotor arousal in response to aversive cues. In addition, from their expression data, we suspected both candidates might be involved in mediating responses to hyperoxic conditions.

Partial and complete gene deletion mutants of our candidates were tested in two behavioral assays. One behavioral assay probed for changes in locomotor arousal after plate taps and a second assay involved tracking worms for hyperoxic escape responses. Using the locomotor (taps) assay, we were able to infer the non-involvement of both candidates in locomotor hyperactivity after taps. However, their role in ASH-mediated cross-modal sensitization still needs to be investigated. On the other hand, our data suggests a possible role of *flp-7* as a repressor of hyperoxic escape responses.

By conducting more trials for both behavioral assays and performing more detailed experiments, future research will validate our preliminary results and shed more light on the molecular pathways governing these behaviors.

Introduction

1. Arousal and sensitization

To survive, organisms need to properly respond and adapt to their changing environment. This is especially important in the context of dangerous encounters. Ideally, the animal's behavioral state is adjusted to allow its escape from current conditions and be more aware of their environment. In other words, an organism is said to be in an aroused state.

Arousal is a general behavioral state that can be quantitatively measured; this is possible because it represents trackable changes in behavior (Pfaff *et al.*, 2008; Pfaff, 2006).

To have a clear behavioral interpretation of arousal, a universal definition was proposed by Pfaff. Pfaff (2006) describes an aroused organism as an individual that shows increased alertness in response to stimulation of different sensory inputs, heightened motor activity, and elevated emotional responsiveness. It is noteworthy that this definition includes reflex motor activity as well as voluntary activity (Pfaff, 2006). This is evident in various organisms where the aroused state leads to prolonged hyperactivity that persists after the stimuli termination (Chew, Tanizawa, *et al.*, 2018; Yokogawa *et al.*, 2012).

Within the context of this definition, an increase in responsiveness to repeated stimuli reflects a type of behavioral plasticity referred to as sensitization (Chew, Tanizawa, *et al.*, 2018). Sensitization is a characteristic feature of arousal. The sensitized input does not have to be the same as the initial stimuli; indeed, an initial stimulus could lead to an increased response to a secondary stimulus engaging a different sensory modality. This type of behavioral plasticity is referred to as cross-modal sensitization (Chew, Tanizawa, *et al.*, 2018; Govindaraju *et al.*, 2006). The underlying cellular and molecular players governing arousal and sensitization are still not fully understood.

1.1 Arousal across the phylogenic tree

Arousal has been studied in a variety of organisms, ranging from invertebrates to mammals. In humans, a malfunctioning arousal system can play a role in cognition-related disorders like attention deficit hyperactivity disorder and autism (Garey *et al.*, 2003). Changes in responsiveness and neurocognitive disorders may also reveal a potential role of arousal in more complex models of memory and learning (Chew, Tanizawa, *et al.*, 2018; Garey *et al.*, 2003).

Food arousal and the gill withdrawal reflex in *Aplysia* has also been studied extensively in the past as one of the earliest models for arousal (Carew *et al.*, 1971; Susswein *et al.*, 1978). One of the arousal states in *Aplysia* include food responses, found by measuring the strength and

quickness of the biting behavior alongside increased heart rate and blood pressure (Dieringer *et al.*, 1978; Koch & Koester, 1982; Susswein *et al.*, 1978).

Arousal states can also be endogenously regulated, like in a sleep-wake cycle. This cycle is an oscillation of wakefulness and sleep/quiescent phases (Jones, 2020). The waking period is usually associated with hyperactivity and cortical activation, while the sleep phase is regarded as the low motor and neuronal activity phase (Chiu *et al.*, 2016; Iannacone *et al.*, 2017; Jones, 2020; Lebestky *et al.*, 2009).

Organisms may share similar behavior in an aroused state or active wakefulness. For example, Sorribes *et al.* (2013) have shown that the amount of overnight sleep decreases with age while causing longer waking bouts in both humans and zebrafish. Similarities are also found in invertebrate models like *Drosophila melanogaster (D. melanogaster)*. Comparable to mammals, *D. melanogaster* show varying degrees of responsiveness depending on their internal state. For example, fruit flies exposed to vibratory stimuli after a quiescent period longer than five minutes show an increased arousal threshold compared with behaviorally awake flies (Shaw *et al.*, 2000). This was also shown in *C. elegans*, where worms subjected to the noxious chemical stimulus 1-octanol showed increased latency in their withdrawal response during the lethargus state (behavioral quiescence period) compared with adults (Raizen *et al.*, 2008). These studies highlight the importance of the endogenous state of increased alertness and readiness for follow-up responses. In both vertebrate and invertebrate models, being in active wakefulness is necessary for the organism to properly respond.

Additionally, exogenous stimuli can also trigger an arousal response in organisms which in turn contributes to survival. In addition to *Aplysia*, stimulus-driven arousal has been studied in other organisms like *C. elegans* and *D. melanogaster*. In *C. elegans*, Chew, Tanizawa, *et al.* (2018) confirmed that noxious stimuli including taps, heat, and odorants like 2-nonanone lead to an increase in forward locomotor speed that persists for about 120 seconds after stimulation. This highlights the importance of a functional arousal system to mediate escape behaviors following the onset or persistent noxious cues in *C. elegans*. In *D. melanogaster*, arousal stimuli include Ultraviolet (UV)-exposure, changes to thermal conditions, and environmental changes leading to male aggression (Asahina *et al.*, 2014; Im *et al.*, 2015). Both UV-exposure (254nm) and high temperatures (48°C) elicited withdrawal response in *Drosophila* larvae which can be described as a corkscrew-like rolling along their anterior-posterior axis (Im *et al.*, 2015). Eight hours after UV-induced tissue damage, flies showed thermal hyperalgesia, with 95% of irradiated animals responding in less than 5 seconds compared with 26% in the control group (Babcock *et al.*, 2009). Here, thermal hyperalgesia is an aroused behavioral state in the form of nociceptive sensitization (Babcock *et al.*, 2009; Im *et al.*, 2015). Another form of arousal is male-specific aggression in *Drosophila*. This type of

behavioral arousal, inter-male aggression, is measured by the number of lunges performed (Asahina *et al.,* 2014). Both male-specific aggression and heat-induced nociceptive sensitization involve the tachykinin neuropeptide (Asahina *et al.*, 2014; Im *et al.,* 2015). However, the complete underlying molecular mechanisms required to drive arousal states mentioned above are still incomplete.

1.2 Sensitization and cross-modal sensitization

An arousal-inducing stimulus readies an organism to respond to successive stimulation. These future responses are characterized by a reduced response threshold and heightened reaction to aversive stimulation (Gold & Gebhart, 2010; Chen & Chalfie, 2014). A documented analogue to the coined 'arousal state' is nociceptive sensitization in the presence of chronic pain or injury. In some cases, sensitization following chronic pain is irreversible even after the initial insult has passed. This is evident in individuals that have undergone limb amputations or nerve transection (Gold & Gebhart, 2010). Hypersensitivity is not necessarily specific to chronic pain or tissue injury. In experiments done by Hubbard *et al.* (2011), test subjects were issued a display that delivered a 'safe' message and a threat message. A safe message meant no impending electric shock, while a 'threat' message signaled the possibility of a future shock. The electric shock was delivered through abdominal electrodes. Subjects showed significantly higher startle reactivity when anticipating a threat compared to safe periods where no threat was issued. Modulation of this defensive reflex is indicative of an upregulated, sensitized response.

This response to threatening external cues can be extrapolated to invertebrates like *C. elegans*. Rankin *et al.* (1990) observed that animals exposed to a delayed tap two minutes after a series of taps showed significantly higher response levels. This illustrates generalized, parallel cross-species behavior to the Hubbard pilot study. Other forms of mechano-sensory stimulation in *C. elegans* led to increased sensitivity even in very subtle background changes. Chen & Chalfie (2014) used 50 Hz vibrations to induce mechanical stimulation; the ALM sensory neurons showed spontaneous calcium spikes even when no vibrational stimulus was applied. The authors claim that their worms were sensitized to such high levels that they detected otherwise imperceptible background vibrations.

Forms of sensitization were also observed in other invertebrates like *Aplysia*. Cellular investigations by Carew *et al.* (1971) measured the gill-withdrawal response. In their work, *Aplysia* showed sensitization to test stimuli following four brush strokes to the neck. This is important because even organisms with a compact nervous system like *Aplysia*, with ~10,000 neurons, still exhibit basal arousal behavior (Moroz L., 2011).

Arousal-associated plasticity extends beyond pure repetition. This is important for survival because exposure to dangerous situations is not limited to a single type of cue. Cross-modal sensitization is represented in both vertebrates and invertebrates. In rats, hypersensitivity to both gentle touch and thermal stimuli is observed following intermittent vibrations of the tail (Govindaraju *et al.*, 2006). In *C. elegans*, hypoxic conditions lead to enhanced gustatory perception through the upregulation of serotonin and neuropeptide signaling (Pocock & Hobert, 2010). Although some molecular factors have been identified, the complete underlying arousal circuitry is still not fully characterized.

1.3 Neuromodulation of arousal

Organisms are not constantly in an aroused state; they regulate their sensory systems' responsiveness according to their environmental demands. Refining the neuronal networks helps modulate observed activity as it provides stronger responses necessary for correct behavior (elevated alertness and hyperactivity). Although neuronal networks are typically defined in terms of synaptic connectivity, non-synaptic signal transmission by neuromodulators can regulate these networks and ultimately change behavioral outputs (Diao *et al.,* 2017). Neuromodulatory molecules include neuropeptides and monoamines, both of which can mediate their effects extrasynaptically (Bentley *et al*., 2016). In many species, both monoamines and neuropeptides seem to be involved and, in some cases, required for an aroused state (Ahnaou & Drinkenburg, 2011; Branch *et al.*, 2016; Chen & Chalfie, 2014; Chiu *et al.*, 2016; Libersat & Pflueger, 2004; Mochizuki *et al.*, 2004; Muschamp *et al.*, 2007; Pocock & Hobert, 2010; Prober *et al.*, 2006; Yokogawa *et al.*, 2012).

A system that has been linked to multiple arousal states is the Hypocretin or Orexin (Hcrt/Orx) system. It has been implicated in male sexual arousal in mice, and the sleep-wake cycle in multiple organisms (Muschamp *et al.*, 2007). In mammals, Orexin knockout (KO) mice have been shown to generate narcoleptic behavior, suggesting disruption of the sleep-wake system (Branch *et al*., 2016). In humans, degenerative Hcrt neurons have been linked to adult narcolepsy (Mochizuki *et al.*, 2004). In invertebrates, the overexpression of Hcrt has been shown to induce an insomnia-like phenotype in adult zebrafish (Prober *et al.*, 2006). This conservation of hcrt peptides demonstrates the importance of vigilance and mediating various arousal behaviors. Despite intensive cross-species effort to map the Hcrt system's circuitry, it is still unknown how it regulates changes in arousal state (Tyree *et al.*, 2018).

Arousal systems are also modulated by different circuitry; this leads to compounding signal complexity while refining behavioral output. Chiu *et al.* (2016) have shown that overexpression of neuromedin U (NmU) led to hyperactivity in zebrafish. They also studied the effects of this overexpression on a normal sleep-wake framework, resulting in the reduction of sleep time and frequency. This can be expressed as a phenotype similar to

insomnia. This neuropeptide may be responsible for regulating arousal by increasing motor activity. Similarly, the administration of NmU23 peptide led to hyperactivity with shorter sleep periods in rats (Ahnaou & Drinkenburg, 2011). This shows that a combination of regulatory inputs is required to drive changes in behavioral states; a single molecule does not modulate a behavioral state on its own. Other modulatory molecules are involved, whether they're supporting the same activity or inhibiting it.

Neuropeptidergic regulation is also involved in stimulus-driven arousal. As mentioned before, the Hcrt system has been implicated in is male sexual arousal in mice. Another system that seems to be conserved among different species is Substance P in mammals and its homolog tachykinin in invertebrates. Both have been implicated in arousal forms related to aggression behaviors and post tissue-damage sensitization (Asahina *et al.*, 2014; Im *et al.*, 2015; Sahbaie *et al.*, 2009). This shows the involvement of a single neuropeptide regulatory signal in both endogenously and exogenously generated arousal states as well as different behavioral arousal forms within the same category.

The regulation of the organisms' behavioral response by multiple neuromodulators and the involvement of these molecules in multiple arousal responses further complicates the underlying circuits. Nonetheless, a detailed understanding of the circuitry involved could allow for manipulation of alertness and vigilance, enhance sleep at night, and advance anesthesiology precision (Garey *et al.*, 2003; Pfaff *et al.*, 2008).

Performing behavioral genetic screening in mammalian models continues to be a challenge. This calls for a model organism that is genetically amenable, responsive to arousal, and can be screened for behavioral state changes like the nematode *C. elegans*.

2. *C. elegans* as a model organism

The nematode *C. elegans* was first isolated by Emile Maupas as mentioned in his 1900 publication; he described them as self-fertilizing hermaphrodites for the first time (Nigon & Felix, 2017). As a small, free-living nematode, *C. elegans* does not require the presence of a host (Corsi *et al.*, 2015). It sports a rapid lifecycle, genetic toolbox, complete genome sequence, connectome, and an extensive neuromodulatory system (Alcedo & Prahlad, 2020; Nigon & Felix, 2017). *C. elegans* is the model of choice in thousands of laboratories worldwide.

2.1 *C. elegans* in neuroscience and genetics

Multiple characteristics of *C. elegans* make it a suitable model for genetics and studies of the nervous system. These include its transparency and large mutant library.

In 1965, Brenner (1974) picked up *C. elegans* due to his interest in development of the nervous system and the characterization of its genetics. He generated and mapped Ethyl methane sulphonate (EMS)-induced mutants with a wide range of phenotypes. He characterized around 100 genes and their mutagenesis phenotypes. Mutants identified by Brenner are still used today as markers in genetic screens of *C. elegans* (Arribere *et al.*, 2014a). Mutants can also be generated using targeted gene editing tools like the clustered regularly interspaced short palindromic repeats (CRISPR)-Cas system.

The maintenance of these mutant strains requires little effort as *C. elegans* can be frozen and recovered for long periods (Corsi *et al.*, 2015). Its life cycle is short, spanning 3 days from egg to egg-laying adult when kept at 25°C (Corsi *et al.*, 2015). In addition, their small size allows for propagation in containers that require little space; an adult is about 1 mm long (Corsi *et al.*, 2015). It can be observed, transferred, and manipulated under a dissecting microscope (Corsi *et al.*, 2015). The transparency of *C. elegans* allows for labeling and observation of single cells using fluorescent markers. Subcellular details like protein localization, metabolic molecules, and cell signaling propagation like genetically-encoded Ca^{2+} indicators can be directly observed (Chew, Tanizawa, *et al.*, 2018; Maulik *et al.*, 2017). No surgical interference is required to visualize specific cells or their activity.

C. elegans was the first multicellular model organism to have its whole genome sequenced (*C. elegans* Sequencing Consortium, 1998). This allowed the discovery of key genes in the development and growth process, alongside the linkage of specific behavioral states with their underlying genetic players.

Maintaining strains for their genotype is challenging in other model organisms where breeding plans are required. Using self-fertilizing organisms like *C. elegans* makes it easier to generate genetically uniform populations. Through this process, mainly hermaphrodites are produced with the probability of males being lower than 0.2% (Corsi *et al.* 2015). Males are often used in crossings and genetic screens.

These features combined made the nematode *C. elegans* a powerful tool for genetic studies. Its significance in biology has also extended to neuroscience due to the complete synaptic wiring diagram of the nervous system that is available. The complete nervous system of the adult hermaphrodite consisting of 302 neurons has been fully mapped (Cook *et al.*, 2019; White *et al.*, 1986; Witvliet *et al.*, 2021). The adult male mating circuit was reconstructed as well (Jarrell *et al.*, 2012). These connectomes are a starting point for decoding neuronal activity in behavioral states. This makes *C. elegans* a model that is ideal for circuit-level analysis. Figure (1) shows the whole-body connectome of both an adult hermaphrodite and male. To understand how a cohesive behavioral output is generated, an extensive wiring diagram of the whole animal is a big advantage. The *C. elegans* wiring connectome provides

cellular-level networks leading to specific response and more importantly how these cellular units consolidate various sensory input to orchestrate a comprehensive output leading to changes in behavior. It can also be used to further investigate the wireless neuromodulatory system which is more difficult to map out due to its long range.

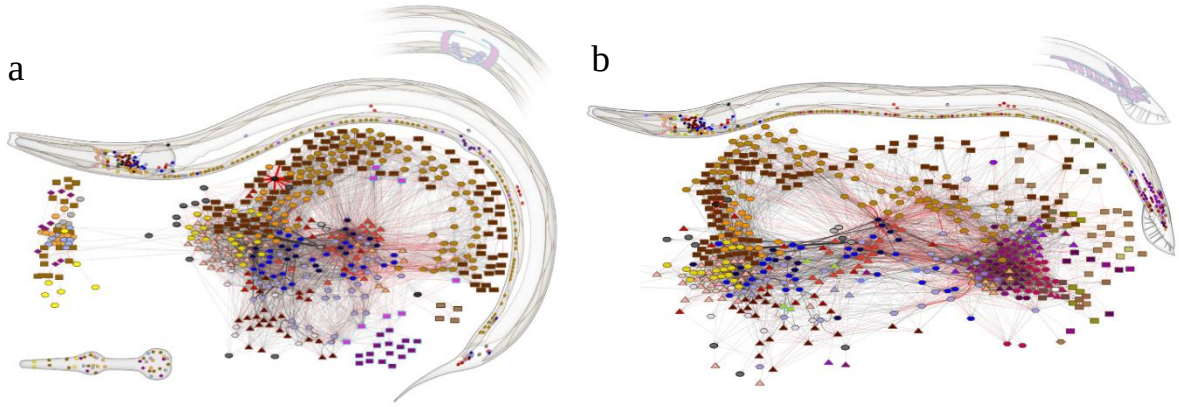

Figure 1: Whole-body connectome of the center and left-side nuclei of the nervous system in adult *C. elegans*. (a) Adult hermaphrodite and **(b)** Adult male. Different shapes represent cell types and the shades of the same color indicate different modalities, connectivity, and layer for a certain cell type. Black, white, and grey shapes represent non-muscular end organs. The type of connections wiring is also depicted where the black arrows delineate chemical synapses and red lines delineate gap junctions. The thickness and transparency of each line corresponds to the connection weight. Key: rectangles are muscles, ovals as motor neurons, triangles as sensory neurons, and hexagons as interneurons. The faded insets show the sex muscles of each animal. Adopted from (Cook *et al.*, 2019).

C. elegans' adaptability and plasticity to complex behavioral states combined with its sophisticated and well-established neurobiology and genetics allows for the study of various systems and circuits at a molecular and cellular level. To better understand underlying circuitry networks involved in arousal, the modulation of sensory systems is the first step to fill in the gaps.

2.2 Sensory input and processing in *C. elegans*

Perceiving and integrating external stimuli is important for an organism to adapt to changes in their surroundings. The nervous system has evolved multiple neuronal circuits to integrate different sensory modalities allowing the organism to mount the proper response for survival and reproduction.

Functioning of all sensory modalities in *C. elegans* have a similar behavior that can be described as a motor outcome to a sensory input. Sensory input is perceived and processed mainly by ion channels or heterotrimeric guanine nucleotide-binding proteins (G proteins) (Allen *et al.*, 2015). On the output end, the signal to change behavior is delivered by different categories of motor neurons to the head and body muscles.

C. elegans' sensory inputs can be categorized into aversive and attractant molecules. Both of which the worm would respond to in the form of changes in locomotor activity, whether moving away or travelling towards the stimuli (Bargmann *et al.*, 1993; Nuttley *et al.*, 2001). In terms of movement, there are two kinds of turns that *C. elegans* perform when exposed to stimuli. Reversals are when the animal "reverses" backwards for a couple of seconds and then proceeds to move forward. On the other hand, omega turns are when the animal reorients its direction of forward movement by bending its body, with the front end almost touching the tail end forming the Greek letter omega (Ω) (Croll, 1975). These turns happen in bursts or sharp changes of movements that Pierce-Shimomura *et al.* (1999) described as pirouettes.

It has been well established that *C. elegans* can sense volatile and water-soluble odorants, mechanical, chemical, and thermal stimuli as well as proprioception (Bargmann, 2006). Impressively, *C. elegans* have also been shown to be capable of detecting other sensory cues including humidity, electric fields, magnetic fields, airborne sounds, short wavelengths of light, and gases like oxygen and carbon dioxide (Bretscher *et al.*, 2011; Gabel *et al.*, 2007; Gong *et al.*, 2016; Iliff *et al.*, 2021; Russell *et al.*, 2014; Vidal-Gadea *et al.*, 2015). Our work will focus mainly on responses to aversive mechanosensory stimuli and varying oxygen levels.

2.2.1 Mechanosensory circuit

To survive, it is important for organisms to detect any surface tension on their bodies. In the case of nematodes like *C. elegans*, they should be able to detect when bumping into other animals or particles in their environment. This requires specialized neurons to detect mechanical stimulation which are called Mechanoreceptor neurons (MRNs) (Bargmann, 2006). MRNs differ in number between hermaphrodites and males. Male-specific MRNs lie in the spicule, hook, and fan in addition to the 30 MRNs present in the hermaphrodite (Bargmann, 2006). Structurally, depending on the presence of cilia, MRNs can be divided into two groups, non-ciliated and ciliated MRNs. Non-ciliated MRNs include six touch-sensitive neurons and one body stretch-sensitive receptor neuron (Bargmann, 2006). Ciliated MRNs include male specific MRNs, four CEP neurons, ADE, PDE, and ASH (Bargmann, 2006). Touch-sensitive neuron response depends on the location of stimulus on the animal's body and its magnitude.

The six posterior/anterior touch sensitive MRNs are ALML, ALMR, AVM, PVM, PLML, and PLMR (Chalfie & Thomson, 1979) (Fig. 2). The role of these neurons has been studied in both gentle posterior/anterior body touches and plate taps. The neurons PLML/R are essential for a posterior touch response and ALML/R and AVM are required for anterior touch responses (Chalfie *et al.*, 1985; Wicks *et al.*, 1996). In plate taps, the observed escape

response is described as a sub-circuits activation imbalance, wherein head sensory neurons promote backward locomotion and tail sensory neurons promote forward locomotion (Chalfie *et al.*, 1985; Wicks & Rankin, 1995). This imbalance is mainly due to the presence of the three sensory neurons (ALML, ALMR, and AVM) in the anterior end of the worm and two sensory neurons (PLML and PLMR) in the posterior end (Bozorgmehr *et al.*, 2013). Hence, the tap stimuli lead to a balanced response with 50% forward and 50% reverse movements before the post-embryonic development of AVM (Bozorgmehr *et al.*, 2013; Chiba & Rankin, 1990). Other types of mechanosensory stimulation involve other sensory neurons. For example, harsh prodding like using a platinum wire requires a different mechanosensory neuron called PVD (Way & Chalfie, 1989).

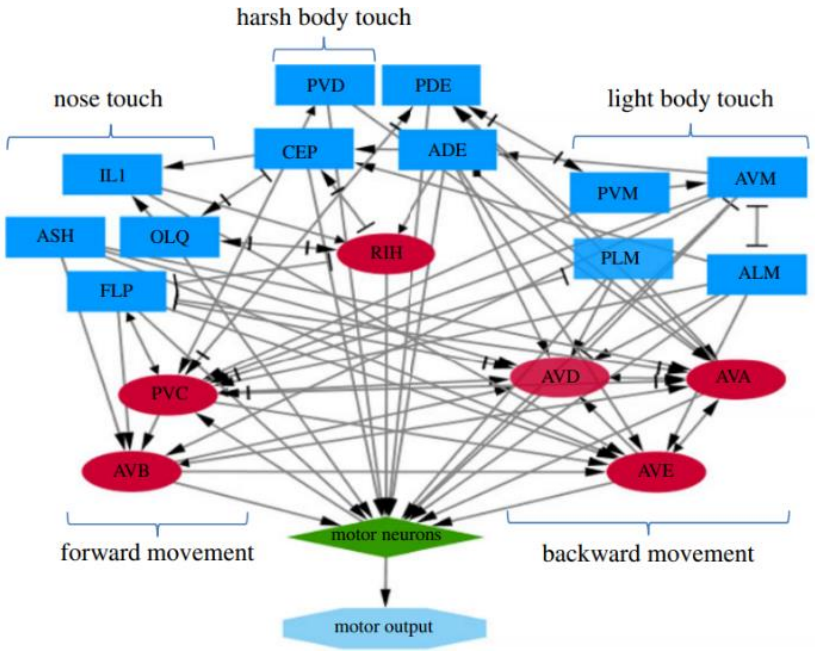

Figure 2: Overview of the different mechano-sensory neuronal circuits. Sensory neurons responsible for the detection of nose, harsh and light body touch are portrayed along with their synaptic connections with other sensory neurons and downstream interneurons. Key: sensory neurons represented as blue rectangles, interneurons as red ovals, and motor neurons as green diamond shape. The types of synapses are denoted as arrows for chemical synapses and bars for gap junctions. Adopted from (Metaxakis *et al.*, 2018).

Mechanical stimuli detection requires mechanoreceptor channel complexes which involve at least five proteins (Bounoutas & Chalfie, 2007). In these channels, two DEG/ENaC proteins, MEC-4 and MEC-10, make up the mechanoreceptor's pore (Bounoutas & Chalfie, 2007; Goodman *et al.*, 2002; O'Hagan *et al.*, 2004). The onset of a mechanical stimulus like plate taps results in a mechanoreceptor current in PLM cells. This is primarily due to the inward currents mediated by Na^+ (O'Hagan *et al.*, 2004). The propagation of the action potential may be mediated through voltage-gated calcium channels which would trigger the release of neurotransmitters to activate or inhibit different cell targets (Bounoutas & Chalfie, 2007).

C. elegans have a specialized neuron pair dedicated for pain-associated nociception called ASH. The ASH neurons are considered polymodal as they are involved in mechano-, osmo-, chemo-, photo-, and electrosensation for which an avoidance behavior is elicited (Altun & Hall, 2011). In mechanosensation, ASH Ca^{2+} transients were observed using genetically encoded Ca^{2+} indicators as a response to nose touch only in the presence of the neuromodulator serotonin (Hilliard *et al.*, 2005b). The observable escape response initiated by ASH can be described as the animal stops moving, reverses, and changes direction of movement often by performing an omega turn (Bargmann, 2006).

2.2.2 Oxygen-sensing circuit

As aerobic animals, *C. elegans* need to be able to sense available oxygen levels and avoid hyperoxia to survive. According to Gray *et al.* (2004), worms prefer an oxygen concentration around 7%. The authors suggest that this might be a protection strategy against both molecular and environmental conditions. Molecularly, they avoid reactive oxygen species formation as oxygen can easily diffuse through small bodies like *C. elegans.* Environmentally, lower oxygen levels serve as an indicator of growing bacteria and lower risk of predation compared to being on the surface.

Atmospheric levels of oxygen, 21%, act as a noxious stimulus for *C. elegans*. Worms would navigate to find an environment with lower more preferred oxygen levels. When not found, the worms exhibit increased locomotor activity (Laurent *et al.*, 2015). This increase in speed persists for at least 2 hours and may be sustained until the worms find an environment with lower oxygen levels (Busch *et al.*, 2012). The three main neurons implicated in sensing atmospheric oxygen levels are URX, AQR, and PQR (Busch *et al.*, 2012; Gray *et al.*, 2004; Rogers *et al.*, 2003). Among these oxygen-sensitive neurons, the pair of URX neurons are required and sufficient to mediate the avoidance and escape response (Laurent *et al.*, 2015). Oxygen detection by these neurons relies on the activation of soluble oxygen-binding guanylyl cyclases (sGCs) with two subunits encoded by *gcy-35* and *gcy-36* (Gray *et al.*, 2004). Its activation leads to the production of cyclic guanylyl monophosphate (cGMP) as a second messenger (Gray *et al.*, 2004). This leads to the activation of the cGMP-gated cation channel *tax-2/tax-4* which is suggested to be responsible for the avoidance response at 21% oxygen levels (Gray *et al.*, 2004).

Downstream of the oxygen sensing neurons the RMG interneurons seem to be a core part in oxygen-evoked escape responses. Based on calcium imaging, the RMG interneurons show increased activity in response to a 7-21% oxygen concentration change which returns to baseline levels after returning to 7% oxygen (Busch *et al.*, 2012). Whereas ablating these neurons disrupts the hyperactivity response at 21% oxygen (Busch *et al.*, 2012). The RMG oxygen-elicited calcium response is lost when the URX neurons are ablated (Laurent *et al.*,

2015). This suggests that the URX neurons may be the main oxygen-related input to the RMG interneurons. Also, solely activating the RMG neurons was sufficient to induce hyperactivity and impede reversals in the absence of all oxygen-sensing neurons under both 7% and 21% oxygen conditions (Laurent *et al.*, 2015). This long-lasting increased forward locomotion at 21% oxygen is mainly driven by the AIY and AVB interneurons which function downstream of the URX-RMG signaling circuit (Laurent *et al.*, 2015).

Ablating all three oxygen sensors, URX, AQR, and PQR does not completely obliterate hyperoxia avoidance responses which suggests the presence of other oxygen-sensitive neurons in *C. elegans* (Chang *et al.*, 2006). Other neurons involved in mediating oxygen responses include SDQ, ALN, BDU, ASH, ADF, ADL, and ASK (Chang *et al.*, 2006; Laurent *et al.*, 2015). Like URX, AQR, and PQR, the neurons ALN, BDU, and SDQ all express the sGC subunit *gcy-35* (Chang *et al.*, 2006). In aerotaxis defective *gcy-35* mutants, the expression of *gcy-35* in ALN, BDU, and SDQ was sufficient to restore oxygen sensitivity (Chang *et al.*, 2006). On the other hand, the nociceptive neurons ASH, serotonergic neurons ADF, and ADL seem to be involved in hyperoxia avoidance through the transient potential vanilloid channel subunits, *osm-9* and *ocr-2* (Chang *et al.*, 2006; Laurent *et al.*, 2015). Lastly, ASK is not required for oxygen-escape responses, however, it might act as a shunt for RMG (Laurent *et al.*, 2015). Based on these results, Laurent *et al.* (2015) suggested an oxygen-evoked behavioral switch that *C. elegans* undergo when exposed to a 7-21% oxygen concentration change (Fig. 3).

The ability of *C. elegans* to change their behavioral state in response to increased oxygen levels depends on the NPY/RFamide-like neuropeptide receptor, NPR-1. Two *npr-1* receptor variants have a different amino acid encoded on position 215 leading to different behavioral responses (De Bono & Bargmann, 1998). The standard lab strains carry the allelic variant *npr-1(215V)* which acts as gain-of-function allele whereas *npr-1(215F)* allele is commonly found in wild isolates (Chang *et al.*, 2006; De Bono & Bargmann, 1998). The presence of the *npr-1(215V)* variant abolishes the oxygen-evoked responses by altering the function of several neurons involved in the circuit; the inhibition mechanism is not clear (Chang *et al.*, 2006; Coates & De Bono, 2002; Laurent *et al.*, 2015). This inhibition explains the solitary behavior seen in lab strains and their insensitivity to culturing oxygen levels.

Modulation of the circuit's activity is evident at multiple layers. The activity of the hyperoxia avoidance inhibitor, *npr-1*, is regulated by two neuropeptide ligands, *flp-18* and *flp-21* (Gray *et al.*, 2004). Also, in the oxygen-sensitive neurons, neuropeptides seem to play an important role in sustained acceleration response to increased oxygen levels. Neuropeptide biogenesis interference by performing targeted RNAi knockdown in URX, PQR, and AQR strongly reduced locomotor arousal at 21% oxygen without affecting their movement at 7% oxygen

(Busch *et al.*, 2012). Finally, Laurent *et al*. (2015) suggest that neuropeptide secretion might mediate oxygen concentration information from the URX-RMG circuit to AVB and AIY to evoke increased locomotor activity.

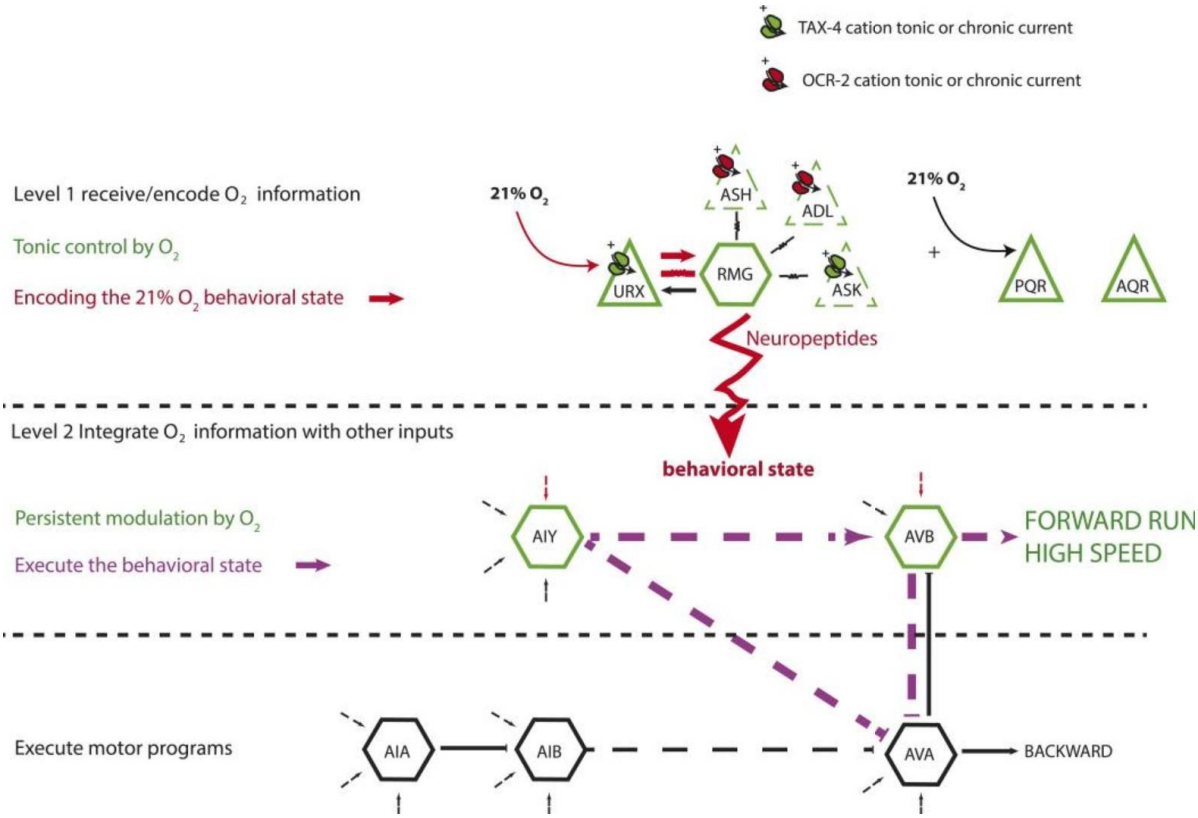

Figure 3: Oxygen-evoked behavioral switch model. The model is divided into three levels: receiving, integrating, and responding to increased oxygen concentrations. On the receiving level, the URX-RMG signaling encode oxygen concentrations tonically. RMG also forms gap junction with ASH, ADL, and ASK neurons which regulate RMG activity by acting as shunts. Downstream executors of the behavioral shift include AIY, AVB, AIA, AIB, and AVA. However, only AIY and AVB activity reflects changes in oxygen concentrations. It is suggested that neuropeptidergic inputs from the URX-RMG circuit to mainly AIY and AVB leads to locomotor arousal. Adopted from (Laurent *et al.*, 2015).

Although the wired mechanical and oxygen-sensing circuits are well-characterized, underlying regulatory sub-circuits are yet to be defined. Therefore, circuit diagrams showing established gap junctions and chemical synapses do not tell the full story and lack regulatory components like neuromodulators. We seek to further investigate neuropeptides regulatory roles in *C. elegans'* arousal.

2.3 Arousal paradigm in *C. elegans*

Organisms from invertebrates to mammals exhibit an elevated state of alertness in response to aversive arousing stimulation (Carew *et al.*, 1971; Govindaraju *et al.*, 2006; Yokogawa *et al.*, 2012). In *C. elegans*, Chew, Tanizawa, *et al.* (2018) have established an arousal paradigm

that includes both mechanical and chemical stimulation. In this paradigm, an initial mechanical stimulation in the form of plate taps serves as the arousal stimulus. When worms are exposed to mechanical vibrations in the form of taps, they pause, move backwards for some distance, and then resume forward locomotion (Rankin *et al.*, 1990; Wicks *et al.*, 1996). This is due to the nature of this stimuli, wherein anterior and posterior vibration-sensitive neurons in the worm's body are activated leading to reflexes by both sets of neurons antagonistically (Fig. 2) (Wicks *et al.*, 1996). The anterior touch-sensitive cells promote a reversal reflex while the posterior cells promote forward acceleration (Wicks & Rankin, 1995). Following this initial reflex, animals undergo an increase in speed that lingers for around two minutes after the delivery of tap stimuli (Chew, Tanizawa, *et al.*, 2018). During this phase of aroused locomotion, the nociceptive responses mediated by the ASH neurons are also sensitized. Chew, Tanizawa, *et al.* (2018) quantified cross-modal sensitization using ASH calcium level fluctuations and reversal distance. The ASH escape responses to the repellent glycerol were enhanced after the arousing tap stimulation. This sensitization seems to be specific to a prior noxious mechanical stimulus and hereby cross-modal. When worms were exposed to an initial aversive chemical cue followed by ASH activation, the ASH responses were not sensitized. This means that ASH responses are not sensitized by noxious odorants like nonanone.

A candidate screen was performed to identify possible regulators of this arousal state. Chew, Tanizawa, *et al.* (2018) identified the neuropeptide *flp-20* and its receptor *frpr-3* to be required in mediating the arousal signal. Both *flp-20* and *frpr-3* mutant strains portrayed defective acceleration after tap delivery and ASH-dependent sensitization (discussed in more detail in section 3.2.1. of the *Introduction*). This highlights the importance of neuromodulators, specifically neuropeptides, in regulating neuronal networks involved in tap-evoked arousal. Therefore, although neuronal networks are typically defined in terms of synaptic connectivity, non-synaptic signal transmissions by neuromodulators can regulate these networks and ultimately change behavioral outputs (Diao *et al.*, 2017).

3. Beyond wired signaling: Neuropeptidergic modulation

In a partially constructed neuropeptidergic network by Bentley *et al.* (2016), out of the 302 neurons in an adult *C. elegans*, 239 neurons were found to be involved in neuropeptide signaling. Although this is not the complete network of all neuropeptides, the number of potential connections between neurons involved in neuropeptidergic signaling (7035 connections) seems to be much higher than synaptic wiring (4887 chemical synapses and 1447 gap junctions).

The analysis also showed that 60% of the receptor-expressing neurons did not have synaptic input from the ligand-expressing neurons. This suggests that most of the neuropeptide

network functions extrasynaptically. Although the connectome is very valuable and provides important information about neuronal circuitry that gives rise to a variety of behaviors, it might underestimate the complexity of such networks.

3.1 Neuropeptides in *C. elegans*

Neuropeptides are small molecules of short amino acid sequences that have a large variation of functions, from autocrine regulators to long range hormones (Burbach, 2011; Li & Kim, 2008). The term "neuropeptides" was devised by David de Wied in the 1970s to describe peptide hormones that are neuroactive (Burbach, 2011).

C. elegans have at least 153 neuropeptide-encoding genes that are predicted to produce more than 300 different bioactive neuropeptides (Peymen *et al.*, 2019; Van Bael, Watteyne, *et al.*, 2018; Van Bael, Zels, *et al.*, 2018). They can be grouped into three distinct families, the FMRFamide (Phe-Met-Arg-Phe-NH2)-related peptides (FLPs), insulin-like peptides (ILPs), and neuropeptide-like proteins (NLPs) (Li & Kim, 2008).

Candidates of all these neuropeptide families have been shown to regulate various biological processes during *C. elegans* lifecycle. For instance, insulin-like peptides have been implicated in regulating dauer lifecycle, developmental growth, pathogen resistance, thermotolerance, lifespan, and associative learning (Fernandes de Abreu *et al.*, 2014; Li, 2005; Matsunaga *et al.*, 2017; Tomioka *et al.*, 2006; Zheng *et al.*, 2018). The NLP family is involved in different behaviors based on their expression in chemosensory neurons and have been associated with antimicrobial activity (Couillault *et al.*, 2004; Li, 2005). Lastly, the FLP neuropeptide family is involved in a wide array of behaviors like locomotion, reproduction, sleep, and arousal (Chang *et al.*, 2015; Chew, Tanizawa, *et al.*, 2018; Nath *et al.*, 2016; Turek *et al.*, 2016).

3.1.1 Neuropeptide processing

Neuropeptides are processed from a larger precursor molecule called the pre-pro-neuropeptide (Li & Kim, 2014). The production of active neuropeptides involves the processing and modification of the larger precursor molecules. These precursor molecules do not necessarily code for a single peptide, rather they may include multiple distinct neuropeptides produced by different cleavage patterns, multiple copies of the same neuropeptide, or a combination of both (Li, 2005) (Fig. 4A).
The processing of neuropeptide precursor molecules yielding active peptides is summarized in figure 4B using the FLP-16 precursor as an example. Every pre-pro-neuropeptide contains a 20-25 amino acid extension on the N-terminus called the signal peptide which allows for

the peptide's entry into the endoplasmic reticulum (ER) where it is cleaved (Li & Kim, 2008).

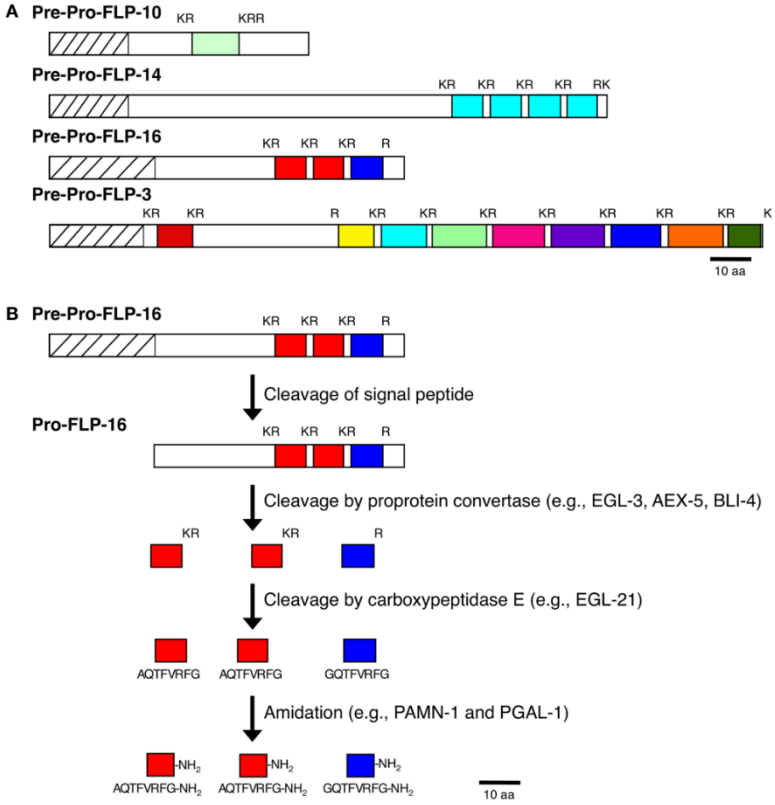

Figure 4: FMRFamide-related peptide precursors structure and processing. (A) Different pre-pro-FLP neuropeptides containing the sequence of a single peptide (Pre-Pro-FLP-10), multiple copies of the same peptide (Pre-Pro-FLP-14), a combination of both options (Pre-Pro-FKP-16), and a single copy of multiple peptides (Pre-Pro-FLP-3). **(B)** Overview of neuropeptide precursor processing and modification to yield an active FLP neuropeptide. Adopted from (Li & Kim, 2014).

This yields a pro-neuropeptide which is then further processed by a proteolytic enzyme called prohormone convertases (PCs). PCs are serine endo-proteases that typically recognize and cleave after specific dibasic residues like lysine and arginine (Steiner, 1998). Although rare, cleavage of mono-, tri-, and non-basic residues by PCs is also possible in *C. elegans* (Li & Kim, 2014). In *C. elegans*, there are four PC genes, *bli-4/kpc-4*, *aex-5/kpc-3*, *egl-3/kpc-2*, and *kpc-1* (Thacker & Rose, 2000). Using immunochemistry experiments and mass spectrometry data on PC mutants in *C. elegans*, it was deduced that pro-peptides are mainly cleaved by EGL-3/KPC/2 (Husson *et al.*, 2006). However, other nematode PCs are involved but to a lesser extent. Following the pro-protein cleavage by PCs, the enzyme carboxypeptidase E (CPE) removes the basic residues from the pro-peptide sequence (Li & Kim, 2008). FLPs are substrates of the *egl-21* CPE which is expressed in around 60% of neurons in *C. elegans*, this includes motor neurons, sensory neurons, and interneurons (Jacob & Kaplan, 2003). Two carboxypeptidase genes are predicted to be present in the *C. elegans* genome, but no association with neuropeptides processing has been reported (Jacob & Kaplan, 2003). Post-

translational modifications are common to protect the neuropeptides from degradation and prolong their half-life (Li & Kim, 2008, 2014). Post-translational modifications are found in both secreted and stored neuropeptides including phosphorylation, acetylation, sulfation, and N- and O-glycosylation (Li & Kim, 2008). The most common post-translational modification is amidation (Van Bael, Watteyne, *et al.*, 2018). In *C. elegans*, amidation could be mediated by two distinct enzymes that are thought to catalyze the amidation process based on their similarity to the mammalian bifunctional protein peptidylglycine-α-amidating monooxygenase (Li & Kim, 2008).

3.1.2 Neuropeptide packaging and release

Neuropeptide precursor modification starts in the ER, continues in the Golgi network, and ends in large vesicles called the dense core vesicles (DCVs) (Li & Kim, 2014). In neurons that produce more than one type of neuropeptides, DCVs co-store and co-release these neuropeptides upon stimulation (Salio *et al.*, 2006). On the contrary to the more abundant small clear synaptic vesicles (SSVs), DCVs are not localized at synaptic zones, rather they are unsystematically scattered further away from the axo-dendritic synapses (Salio *et al.*, 2006). In *C. elegans*, DCVs are primarily localized in the axons and their transport is dependent on two motor proteins UNC-104/KIF1A/kinesin-3 and UNC-116/kinesin-1 (Li & Kim, 2008). The complete mechanism of how DCVs are translocated to the plasma membrane is not clear.

The release of neuropeptides from DCVs in triggered by a diffused increase of calcium in the axonal terminal rather than a focal elevation in the case of SSVs (Salio *et al.*, 2006). The neuropeptides discharge from their vesicles is a multistep regulated process that is comprised of docking, priming, fusion, and the release of vesicle content (Li & Kim, 2014). As in the release of SSVs, DCVs make use of the core soluble N-ethylmaleimide-sensitive factor attachment receptor (SNARE) complex in addition to DCV-specific proteins (Richmond & Broadie, 2002). Vesicle docking and release is promoted by a cytoplasmic calcium-dependent activator protein for secretion (CAPS) called UNC-31; It bridges between the plasma membrane and the DCV (Sieburth *et al.*, 2006). Unlike SSVs, DCVs do not dock at dense projections active zones, but are more evenly spread-out along the axon (Hammarlund *et al.*, 2008). Upon release, recycling and reuptake of neuropeptides is not possible. They are degraded by a class of proteolytic enzymes called neprilysin (NEP) zinc metallopeptidases (Li & Kim, 2014). Therefore, vesicle stores need to be replenished by *de novo* synthesis and packaging of neuropeptides.

3.1.3 Neuropeptide receptor signaling

Most neuropeptides signal through G-protein-coupled receptors (GPCRs) that are expressed on the membrane of target cells (Frooninckx *et al.*, 2012; Li & Kim, 2014). GPCRs are seven transmembrane proteins through which intracellular signal transduction is conveyed by G-proteins (Frooninckx *et al.*, 2012). GPCRs have been classified into six distinct families: Secretin, Rhodopsin, Adhesion, Frizzled, and Glutamate receptor family (Munk *et al.*, 2016). Two families are involved in neuropeptide signaling, the rhodopsin and secretin families (Frooninckx *et al.*, 2012).

Although most neuropeptide signaling seems to be conveyed by GPCRs, there has been work that shows the involvement of other receptor types. For example, some FLPs are involved in inducing fast depolarizing responses by gating ion-channels (Lingueglia *et al.*, 1995). Since we still do not know all target receptors of *C. elegans* peptides, this mode of signaling might also apply to other neuropeptides.

The signaling complexity of neuropeptides is remarkably increased by the multiple couplings of both neuropeptide receptors and peptides. Our understanding of *C. elegans'* neuropeptide signaling repertoire is far from complete. This also serves as an extra complication to be solved when deciphering neuromodulatory circuitries that drive behavioral states.

3.2 Neuropeptidergic regulation of arousal in *C. elegans*

Different stimuli are perceived as a threat by *C. elegans*, and the worms respond in a manner that leads to changes in its global state. In the case of plate taps, the arousal state is characterized by locomotor acceleration and the enhancement of escape responses to successive noxious chemical stimuli. Using a candidate screen approach, Chew, Tanizawa, *et al.* (2018) further shed light on the afferent pathway mediating this behavior.

3.2.1 The afferent FLP-20/FRPR-3 pathway

Arousal in the form of hyperactivity and cross-modal sensitization following mechanosensory stimulation were recently investigated by Chew, Tanizawa, *et al.* (2018). The administration of plate taps as a noxious mechanical stimulus resulted in a dosage-dependent arousal response. This response was measured as increased speed that lasted for around two minutes and a heightened ASH-dependent escape behavior.

To identify potential underlying neuromodulators, a candidate screen was performed for animals with altered arousal responses. In this screen, deletion mutant worms in the neuropeptide-precursor gene *flp-20* showed significantly lower locomotor arousal and sensory sensitization of the ASH-mediated reversal response following mechanical

stimulation. ASH neurons were excited using a glycerol drop test or optogenetic stimulation. A transgene that expresses channelrhodopsin2 (ChR2), a light-gated cation channel with blue-shifted absorption, was integrated to optogenetically excite the ASH neurons by blue light illumination (Nagel *et al.*, 2003, 2005). To avoid the activation of intrinsic short-wave escape response, a mutant allele of the *lite-1* gene was included in the worms' background. Edwards *et al.* (2008) showed that *lite-1* mutants have extremely dampened locomotor responses when exposed to blue light. The light-responsiveness measured in body bends/minute was the lowest in the amino acid substitution mutant *lite-1(ce314)* (Edwards *et al.*, 2008). The same *lite-1* mutant allele was incorporated in the background of optogenetically assayed strains.

Using neuron-specific rescue experiments in *flp-20* mutants, the touch receptor neurons (TRNs) were identified as the source of FLP-20 released after mechanical stimulation. The FMRFamide-like peptide GPCR *frpr-3* expressed on the neuroendocrine cell RID, was found to be the main receptor mediating *flp-20* arousal effects. The optogenetic activation of RID prior to ASH activation was sufficient to mediate the cross-modal sensitization of ASH and magnify forward locomotion speed (Lim *et al.*, 2016). The signal mediated by RID to sensitize ASH and potentiate hyperactivity after mechano-stimulation may involve both neuropeptides release and wired connections. However, the efferent signaling pathways regulating this are not clear.

These results led to a new afferent neuropeptide paradigm governing locomotor arousal and cross-modal sensitization in response to aversive stimuli (Fig. 5). Additionally, in the same candidate screen that was used to identify *flp-20* and *frpr-3* mutants to be arousal defective, other FLPs and neuropeptide receptor mutants also exhibited altered arousal and sensitization responses. Validating and further examining these potential candidates would help better understand how arousal is regulated on the cellular and molecular level.

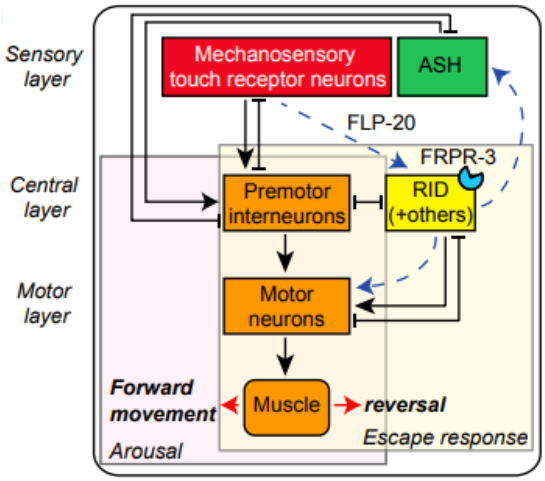

Figure 5: *C. elegans'* behavioral arousal paradigm in the form of hyperactivity and ASH-specific cross-modal sensitization following mechanosensory stimulation. The sensory, central, and motor layers depict the

main neural and molecular aspects of this arousal paradigm. Upon delivery of mechanical stimuli, the touch receptor neurons, TRNs, release *flp-20* which mainly acts on RID through the receptor *frpr-3*. The activated RID cell in turn heightens forward movement and sensitizes the escape response of ASH. Adopted from (Chew, Tanizawa, *et al.*, 2018).

3.2.2 Other FLP neuropeptide candidates for mediating arousal

Besides *flp-20*, other FLP neuropeptide mutants were also screened for locomotor activity and ASH-sensitization after mechanical stimulation. The mutant strains that were identified in the candidate screen to be defective in arousal are shown in figures 6 and 7. Based on this screen, another FLP mutant exhibited a similar degree of ASH cross-modal sensitization defectiveness as *flp-20* mutants which is the *flp-7* mutant (Fig. 7a).

flp-7 is a tachykinin-like peptide that has been implicated in gut metabolism through the work of Palamiuc *et al.* (2017). *flp-7* secreted from the ASI sensory neurons was found to act through the receptor *npr*-22 (tachykinin 2 receptor orthologue) to mobilize fat stores in the intestinal cells of *C. elegans*. The release of *flp-7* from ASI acts as a communication point between neural signaling fluctuations in the form of serotonin or 5-hydroxytryptamine (5-HT) and intestinal fat loss (Palamiuc *et al.*, 2017). The *flp-7*/*npr*-22 signaling leads to fat oxidation by transcriptionally activating a lipolytic enzyme called adipocyte triglyceride lipase-1 (ATGL-1) (Palamiuc *et al.*, 2017). Littlejohn *et al.* (2020) proposed that *flp-7* secretion leads to fat loss by repressing the expression of the transcription factor HLH-11 (negative regulator of ATGL-1).

Based on the *C. elegans* Neuronal Gene Expression Network (CenGen) RNA sequencing data, *flp-7* is expressed in various sensory neurons (Taylor *et al.*, 2021). Hence, it might be involved in the regulation of a wide range of behaviors. This combined with the altered sensitization response of *flp-7* mutants (Fig. 7a) makes *flp-7* an attractive candidate as an upstream sensory signal in arousal and sensitization.

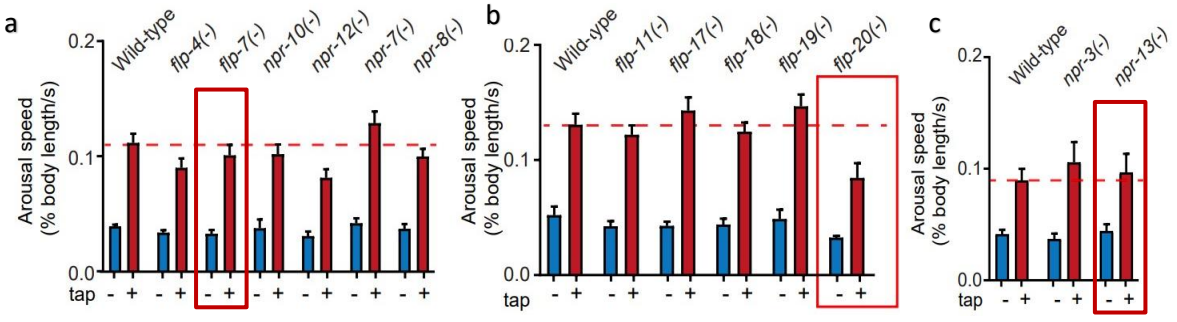

Figure 6: Locomotion assay in the candidate screen for mutants with defective arousal responses. The blue bars represent speed (% body lengths/second) before mechanical stimulation with plate taps while the red bars depict the average speed 10 seconds after taps. The dashed red line marks the Wild-type's arousal speed. Adopted from Chew, Tanizawa, *et al.* (2018).

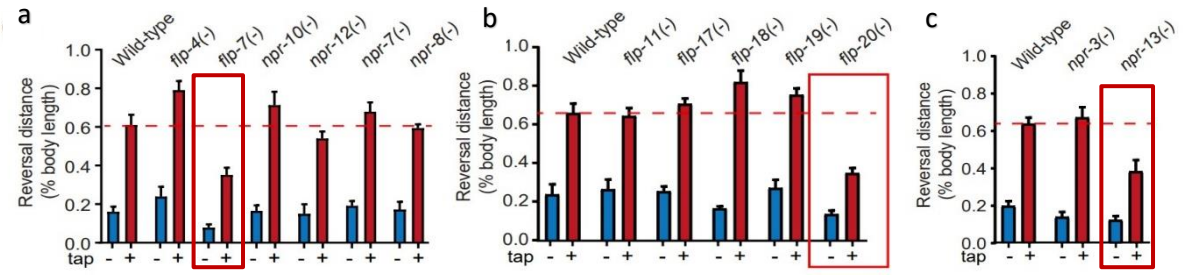

Figure 7: Candidate screen for cross-modal sensitization mutant strains. The escape response was measured in reversal distance (% body length) following optogenetic activation of ASH using blue light. The plus and minus signs refer to the administration of plate tap stimulation or not. Adopted from Chew, Tanizawa, *et al.* (2018).

3.2.3 The prolactin releasing hormone receptor homologue NPR-13

The NPY/RFamide neuropeptide receptor *npr*-13 was one of the neuropeptide GPCRs that displayed a pronounced decline in ASH-mediated cross modal sensitization following mechanical stimulation (Fig. 7c). It is homologous to the human prolactin releasing hormone receptor (PRLHR) (Kim *et al.*, 2018). Although not much is known about its cellular function, a behavioral mutant database identified it as a potential candidate for altered motion phenotypes. In this database, a partial deletion *npr-13* mutant, *npr-13(tm1504)*, showed different locomotion features compared to the wild-type strain (N2). These differences include body bend frequency, turning frequency, head bending angle, nose movement, and more (Yemini *et al.*, 2013). In addition, according to the CenGen RNA sequencing database, *npr-13* is expected to be mostly expressed in premotor and motor neurons (Taylor *et al.*, 2021). This combined with the locomotor database, the altered sensory sensitization (Chew, Tanizawa, *et al.*, 2018), and its homology with PRLHR, make *npr-13* a potential downstream candidate for arousal and sensitization.

Research outline

Proper adaptations to differing external conditions requires communication and coordination of neuronal networks to orchestrate the needed response in accordance with one's internal state. This is needed to elicit proper behavioral responses when exposed to certain environmental conditions, especially aversive cues. Also, this is important to cross-modulate the activity of different sensory neurons for immediate and future stimulation. Modulation of neuronal circuits is not limited to physical wiring and includes other long-range signaling molecules like neuropeptides (Chew, Tanizawa, *et al.*, 2018; Metaxakis *et al.*, 2018). A detailed understanding of how these wireless signals modulate behavior is not well understood. This project aims at shedding light on the neuropeptidergic circuitry driving arousal and sensitization in *C. elegans.*

Chew, Tanizawa, *et al.* (2018) highlighted an afferent neuropeptide signaling pathway mediating arousal responses to aversive mechanical and chemical cues. However, other afferent and efferent circuits driving this behavior need to be investigated.

We aim to investigate the potential functions of two candidate genes in mediating locomotory arousal responses to an aversive tap stimulation. These genes were chosen based on a genetic screen for arousal defective mutants performed previously by Chew, Tanizawa, *et al.* (2018). Both candidates, *npr-13* and *flp-7*, have been implicated in impaired ASH-dependent cross-modal sensitization after tap delivery. Although they have demonstrated non-defective locomotor arousal after mechanical stimulation, these results were based on partial deletion mutants. We will build full knockout mutants of both genes to assay in locomotory arousal assays. This would help in validating the observed phenotypes.

Mutants of the two candidate genes will also be assayed for hyperoxia-induced escape responses. RNA sequencing expression data shows that both candidates are expressed in oxygen sensing neurons. This suggests that they might be involved in receiving and integrating oxygen-related information.

Furthermore, we will further analyze the cellular expression of both these genes. Confirming the expression of these candidates in certain neurons *in vivo* would allow for better understanding of the underlying circuitry involved. *In vivo* cellular expression will be analyzed using green fluorescent protein (GFP) expressing reporter lines for both genes.

Materials and Methods

1. *C. elegans* maintenance and handling

1.1 *C. elegans* strains

Wild type N2-Bristol worms and multiple mutant strains listed in Table 1 were used to investigate arousal in *C. elegans*. All strains were maintained at 20°C.

Table 1: List of *C. elegans* mutant strains (N/A: not applicable).

Strain	*Genotype*	*Source*	*Description*
LSC1894	*lite-1(ce314) X*	Schoofs lab	Point mutation (substitution): G/A.
AQ2235	*lite-1(ce314) ljIs114[gpa-13p::FLPase, sra-6p::FTF::ChR2::YFP] X*	(Chew, Tanizawa, et al., 2018)	*lite-1:* point mutation; *ljIs114:* Transgene expressing Channelrhodopsin2 (ChR2) in the ASH neurons (*ASH::ChR2*). The transgene is present on the X chromosome.
AQ2755	*lite-1(ce314) X;ljIs124[gpa-13p::FLPase, sra-6p::FTF::ChR2::YFP] non-X*	(Chew, Tanizawa, et al., 2018)	*lite-1:* point mutation; *ljIs124:* Transgene expressing ChR2 in the ASH neurons (*ASH::ChR2*). The transgene is not on the X chromosome.
AQ2786	*flp-20(ok2964) lite-1(ce314) X; ljIs124 non-X*	(Chew, Tanizawa, et al., 2018)	Uncharacterized mutation in the FLP-20 gene; *lite-1:* point mutation; *ljIs124*: *ASH::ChR2*.
VG266	*frpr-3(gk240031) V (backcrossed 3x); lite-1(ce314) ljIs114 X*	(Chew, Tanizawa, et al., 2018)	Point mutation (substitution) in the FRPR-3 gene: T/A; *lite-1:* point mutation; *ljIs124*: *ASH::ChR2*.
RB1990	*flp-7(ok2625) X*	*Caenorhabditis* Genetics Centre (CGC)	Partial gene deletion of 548bp.

YTB291	*flp-7(ok2625) lite-1(ce314) X*	Schafer lab	*flp-7:* partial deletion; *lite-1:* point mutation.
IBE304	*flp-7(ok2625) lite-1(ces314) X;ljIs124 non-X*	This project	*flp-7*: partial deletion; *lite-1*: point mutation; *ljIs124: ChR2::ASH*.
IBE346	*flp-7(ibt7) X*	This project	CRISPR-mediated KO.
IBE414	*flp-7(ibt7) lite-1(ce314) X*	This project	*flp-7* KO; *lite-1*: point mutation.
PHX5413	*flp-7(syb5413[flp-7::SL2::GFP::H2B]) V*	SUNY Biotech	*flp-7* expression reporter strain with GFP as a marker.
LSC1329	*npr-13(tm1504) V (backcrossed 4x)*	Schoofs lab	Partial gene deletion of 1104bp.
IBE344	*npr-13(tm1504) V;lite-1(ce314) X*	This project	*npr-13:* partial deletion; *lite-1*: point mutation.
IBE303	*npr-13(tm1504) V;lite-1(ce314) ljIs114 X*	This project	*npr-13*: Partial deletion; *lite-1*: point mutation; *ljIs114: ChR2::ASH.*
IBE412	*npr-13(ibt6) V (backcrossed 2x)*	This project	CRISPR-mediated KO.
PHX5215	*npr-13(syb5215[npr-13::SL2::GFP::H2B]) V*	SUNY Biotech	*npr-13* expression reporter strain with GFP as a marker.
IBE154	*npr-1(ad609) X (backcrossed 6x)*	Beets lab	Point mutation (substitution): C/T.

1.2 Culturing conditions and growth medium

All strains in this project were grown and maintained on Nematode Growth Medium (NGM) seeded with *Escherichia coli* (*E. coli*) OP50 bacteria. This bacteria was cultivated in 2x Yeast Extract Tryptone (2xTY) medium broth. All solution and buffer preparation steps used are described in Appendix #.

1.2.1 Preparation of Nematode Growth Medium plates

For general growth and propagation of *C. elegans* strains, medium-sized (55mm) Nematode Growth Medium (NGM) agar plates were used. To prepare 1L of NGM, 17g of Bacto™ Agar (BD Biosciences), 3g of sodium chloride (Sigma-Aldrich), and 2.5g of Bacto™ Peptone (Gibco™) were dissolved in 800mL of AD water and autoclaved. A bottle with 200mL of AD water was also autoclaved. After autoclaving, the bottles were placed in a 60°C oven to cool down. Under the laminar flow cabinet, the 200mL AD water was added to the reagents containing bottle to reach a final volume of 1L. Then, 1mL of 1M $CaCl_2$ solution, 1mL of 1M $MgSO_4$ solution, 1mL of 5mg/mL cholesterol in ethanol solution, and 25mL of 1M phosphate buffer were added. The solution bottle was gently swirled to mix the added contents. Finally, using a pipette controller and a 50mL serological pipette (Greiner CELLSTAR®), 12mL of NGM agar was poured in 55mm petri dishes and left to solidify under the laminar flow. Once solid, plates were inverted, placed in a clean box, and stored at 4°C.

1.2.2 Preparation of *E. coli* OP50 culture

Under the laminar flow cabinet, around 40mL 2xTY medium broth was transferred to a 50mL autoclaved glass tube and inoculated with a single colony of *E. coli* OP50 from a streaked plate. Then, the tube was closed with a designated metal cap and sealed with parafilm tape. Once sealed, the tube is securely placed in a shaking incubator (37°C) overnight. The following morning, the media was ready to be used right away or stored at 4°C for later use. A new *E. coli* OP50-inoculated 2xTY medium broth was prepared every two weeks.

1.2.3 Seeding of Nematode Growth Medium plates

Pre-acclimated NGM plates were seeded with liquid *E. coli* OP50 culture in 2xTY broth. Under laminar flow, a stepper pipette (Eppendorf Multipette® plus) and a 5mL stepper pipette tip (Eppendorf) were used to dispense 150 µL of culture in the middle of the plate. Then, the culture was evenly spread using a sterilized glass spreader. Special care was taken to not spread the bacterial lawn to the edges of the plate. Keeping the lawn in the center, lowers the chances that worms would crawl up the sides, dry and eventually die (Stiernagle, 2006). The seeded plates were left open in the laminar flow to dry. Once dry, the plates were closed, inverted, and left at room temperature for the bacteria to grow overnight. The next morning, plates were ready to be used or stored at 4°C until needed.

1.2.4 Propagation of *C. elegans* hermaphrodites

For general maintenance of *C. elegans* strains, worms were frequently transferred to freshly seeded NGM plates. If plates are not regularly transferred, the bacterial food lawn will be

depleted, and worms will be starved. Starved worms can not be used for our experimental purposes. Thus, worms were regularly transferred to avoid starvation. Otherwise, if worms were starved, they were used in experiments after at least two weeks of being out of the starvation phase.

In general, transferring can be done with two methods: 'picking' and 'chunking'. In both methods, new seeded NGM plates are placed at room temperature to acclimate before transfers.

Picking involves the transfer of a specific number of worms on to freshly seeded NGM agar plates. A worm picker (platinum wire attached to a glass Pasteur-pipette with a hammer-tapered end) was used to individually select worms. Using a stereomicroscope (Nikon SMZ 745), adult worms were picked, and gently allowed to crawl onto a new plate. An average of 8 adult worms per medium plate were transferred.

Chunking is especially useful to transfer worms from overly starved plates where the bacterial lawn is completely depleted. Many worms and/or eggs are transferred onto a new plate by cutting out a piece of the old plate agar. Using a sterile scalpel, a small agar piece of the worms-containing plate is removed and placed upside down on a new plate. The inverted chunk allows the worms to crawl onto the new plate.

1.2.5 Generation and maintenance of *C. elegans* males

The frequency of male *C. elegans* is quite low (<0.002) calling for a slightly different culturing procedure (Hodgkin, 1983). When *C. elegans* males of certain genotypes were not available, males were generated by heat shock or by setting up a cross (as described in section 2.1 of *Materials and Methods)*. To generate males by heat shock, 8-10 L4 hermaphrodites were incubated for 6 hours at 30°C, then they were kept at 16°C overnight. The following morning, the plate was moved and kept at 20°C. Otherwise, since *C. elegans* males are XØ and hermaphrodites are XX, normal segregation of the sex chromosomes during mating would result in 50% male progeny (Anderson *et al.*, 2010). To maintain male worms' population, 20-30 male worms are transferred using a picker along with 2-3 L4 hermaphrodites onto a new plate under the stereomicroscope.

1.3 Freezing *C. elegans* strains

C. elegans strains were frozen for long-term storage that can be thawed and recovered at any time in the future. This allows for the indefinite storage of worm strains that are not currently in use and acts as a backup in case of breeding problems.

A liquid freezing solution was used for long-term storage. The freezing solution contained 30mL glycerol (Sigma-Aldrich), 0.112g K_2HPO_4 (Sigma-Aldrich), 0.592g KH_2PO_4 (Sigma-Aldrich), 0.585g NaCl (Sigma-Aldrich), and100mL of Milli-Q water. The solution was autoclaved before use. Since L1 worms freeze the best, four medium (55mm) plates that were freshly starved and uncontaminated were used for freezing. The worms were washed off the NGM agar plates using a total of 3mL S-Basal solution into a 15mL Falcon tube. An equal amount of the freezing solution was then added to the Falcon tube. The content of the Falcon tube was equally aliquoted into labeled 1.8mL cryo-vials (Thermo Scientific). The cryo-vials were placed in a Styrofoam box at -80°C to allow for gradual drop in temperature.

To check for successful freezing, one tube was thawed after two weeks. The content of the tube was transferred onto a seeded plate at room temperature. If worms started crawling after a couple of hours, freezing was properly done, and the remaining tubes were moved to the permanent storage box. Whereas if the worms did not recover, freezing the strain was redone.

2. *C. elegans* genetics

2.1 Crossing *C. elegans* mutants and transgenic strains

C. elegans mutants and transgenic strains were built by crossing necessary strains. Small-sized petri dishes (35mm) filled with 5mL NGM agar (as described in section 1.2.1 of *Materials and Methods*) were used to carry out crosses. From an *E. coli* OP50-seeded plate, bacteria were scooped up using the picker and placed in the middle of the crossing plate. Then, 8-10 males and 3-4 L4 hermaphrodites were transferred on the food patch and were transferred onto a new plate daily for 3-4 days. Depending on the genotype desired, males or hermaphrodites were picked from the progeny of the 3rd day transferred plate and singled out for further genotyping and generating homozygous strains. When transgenic strains were used, the homozygosity of the transgene in the progeny was checked using a fluorescent microscope (Leica M165 FC). All plates were grown and maintained at 20°C.

2.2 Generating CRISPR-mediated knockout mutants

Generating precise genome edits helps researchers examine the relationship between the function of a specific gene and an observed phenotype. In this project, genome editing techniques were used to make gene knockout mutants. The CRISPR-Cas9 system was used for this purpose. For every targeted gene, two guide RNAs and a repair template were designed to create two double-stand cuts surrounding the gene-of-interest. To facilitate screening for mutants, a co-CRISPR approach was followed. In this screening strategy a second locus with a visible phenotype is simultaneously edited to serve as an editing marker.

2.2.1 Designing crRNA and repair template

In the CRISPR-Cas9 system, the Cas9 is an endonuclease that binds a small RNA molecule referred to as the guide RNA that's used to recognize particular DNA sequences (Jinek *et al.*, 2012). This RNA molecule consists of two RNAs: a *trans*-activating CRISPR RNA (tracrRNA) required to activate the Cas9 enzyme and a CRISPR RNA (crRNA) homologous to the target sequence (Dickinson & Goldstein, 2016). To produce error-free genome edits, homology directed repair (HDR) mechanism was achieved using a repair template. Therefore, for every CRISPR-mediated knockout mutant a gene-specific crRNA and repair template were designed.

crRNA. For the CRISPR-Cas9 system to successfully find its target, a crRNA sequence is required. For generating a knockout of our gene-of-interest, two crRNA sequences were used to perform two double stranded breaks (DSBs). The ideal location for a target sequence was determined by locating an upstream Protospacer Adjacent Motif (PAM)-site (5'-NGG-3'). This is essential as the Cas9 enzyme binds the PAM sequence first and only then interrogates DNA for potential target sites (Sternberg *et al.*, 2014). Downstream of every Protospacer Adjacent Motif or PAM-site (5'-NGG-3'), a 20bp gRNA sequence was designed to act as a crRNA. To check for off-target effects, the sequences were analyzed using the program CRISPOR (Tefor Infrastructure). Then, the crRNAs were ordered from Integrated DNA Technologies (IDT).

Repair template. The repair template sequence consisted of 35 base pairs upstream of the first PAM sequence and 35 base pairs downstream of the second PAM sequence. Then, the 70 base pairs repair template was ordered from Sigma.

The gene mutation *dpy-10* was used as a marker. Both the crRNA and the repair template for *dpy-10* were preordered in the lab and stored at -20°C.

2.3 Preparing CRISPR-Cas9 injection mix

On the same day of the microinjection, the injection mix is prepared and stored at 4°C. Initially, two separate mixes are prepared, one mix for the *dpy-10* gene and the second for the gene-of-interest (Table 2). For the *dpy-10* mix, the components listed in Table 2 are added into a 1.5mL Eppendorf tube and incubated for 10 minutes at 37°C. Then 2.2µL of the repair template (0.5µg/µL) and 2.05µL of Milli-Q water were added. The mixture was kept on ice while preparing the second mix. In the second mix, the components of the gene-of-interest were added into a 1.5mL Eppendorf tube (Table 2). The tube was incubated for 10 minutes at 37°C. Next, 1.1µL of the repair template (1µg/µL) and 2.99µL of Milli-Q water were added.

Finally, both mixes were added into a single tube, spun at maximum speed for 2 minutes, and kept on ice ready for microinjection.

Table 2: Description of the volumes and stock concentrations of CRISPR-Cas9 injection mixes.

	dpy-10 mix		Gene-of-interest mix	
Component	Volume	Concentration	Volume	Concentration
Cas9	0.25µL	5.00µg/µL	0.25µL	5.00µg/µL
TracrRNA	0.26µL	3.77µg/µL	0.26µL	3.77µg/µL
crRNA	0.24µL	2.33µg/µL	2x 0.2µL	1.40µg/µL
		10 minutes incubation at 37°C		
Repair template	2.20µL	0.50µg/µL	1.10µL	1.00µg/µL
Milli-Q water	2.05µL		2.99 µL	

2.4 CRISPR-Cas9 microinjection

The day before the injection, in the late afternoon, two plates with 30-40 L4 hermaphrodites were picked. One of the plates was placed at 16°C and the other at 20°C overnight. This allows the worms to grow to young adults which is the best developmental stage to perform injections on. The following day, depending on the time of injection, the plate with the suitable developmental stage was chosen for injection.

To perform the microinjection, agarose pads are used to mount the worms. Mounting pads were prepared by transferring a drop of melted 2% agarose on a glass coverslip (60x24mm), flattened with another slide on top, and carefully the top slide was removed leaving a dry agarose pad. In an open container, the slides were placed at 37°C overnight.

Microinjections were done by trained personnel in the lab (Elke Vandewyer and Marijke Christiaens) with needles made from pulled glass capillaries (1.5mm). The needles were loaded with 2µL of injection mix using a Microloader™ (Eppendorf). The microinjection setup consisted of the Eppendorf InjectMan NI 2 and FemtoJet making up the semi-automatic electronic microinjector, and the Zeiss Axio Observer.A1 microscope for mounting and manipulating the worms. The worms were injected in the distal core cytoplasm of the gonadal arm, transferred onto a new seeded plate, and placed in the incubator at 20°C.

2.5 Screening and validation of knockout mutants

The injected worms were stored at 20°C and checked every day after the injection for laid progeny. After three days, the surviving worms would have laid eggs which can be screened. An overview of the screening approach can be found in figure 8.

Screening the progeny (F1) of the injected worms was made easier by having *dpy-10* as a co-injection marker which serves as an indicator of successful injection. Another advantage of co-injecting *dpy-10* is that homozygous and heterozygous mutants confer different phenotypes. The *dpy-10* heterozygotes (mut/+) show a left rolling phenotype while *dpy-10* homozygotes (mut/mut) show a dumpy roller phenotype (Arribere *et al.*, 2014b). This facilitates segregating away the *dpy-10* mutation in the background of the desired mutant animals. Thus, the progeny was screened for worms with the roller (twisting around body axis) and dumpy (stumpy) phenotype. Worms that showed either phenotype was singled out on a new seeded plate and genotyped for the mutation of interest (as described in section 1.3 of *Materials and Methods*) after laying progeny (F3). Once homozygous mutants are confirmed by genotyping, the samples were sent for sequencing.

Sequencing of the homozygous mutants was performed to confirm the CRISPR-mediated gene edit. The worms were genotyped following the same steps in section 3.1 of *Materials and Methods* but only half of the PCR product was used for gel electrophoresis. Then, ~13µL of the PCR product was used for DNA extraction using the Wizard® SV Gel and PCR Clean-Up System (Promega). The purified sample was diluted to a final concentration that depended on the size of the amplicon as shown in table 3. Finally, in a 1.5 mL Safe-Lock micro centrifuge tube (VWR) 10µL of the DNA sample and 4µL of the sequencing primer were mixed and sent out for sequencing.

Table 3: Required template DNA concentrations for sequencing by Ready2 Run.

PCR product size (bp)	Required concentration (ng/µL)
200 – 500	10
500 – 1,000	20
1,000 – 2,000	40

Once the mutant's homozygosity is confirmed, the subsequent backcrossing approach depended on the *dpy-10* genotype of the isolated animal. If the homozygous mutants were also homozygous for the *dpy-10* mutation (stumpy), they were first outcrossed with N2 worms to generate *dpy-10* heterozygotes. Then, roller animals (F1) were genotyped to confirm the heterozygosity of the gene-of-interest. Once confirmed, hermaphrodites were singled out on separate agar plates to lay progeny. The laid offspring (F2) were screened for

non-roller non-dumpy animals which were also singled out for genotyping the gene-of-interest. The isolated non-roller non-dumpy that's homozygous for the gene-of-interest was backcrossed at least twice before being used for any behavioral experiments. In the case of a heterozygous *dpy-10* (rollers) mutants, non-roller non-dumpy animals were isolated from the progeny for further backcrossing with N2 animals as mentioned above.

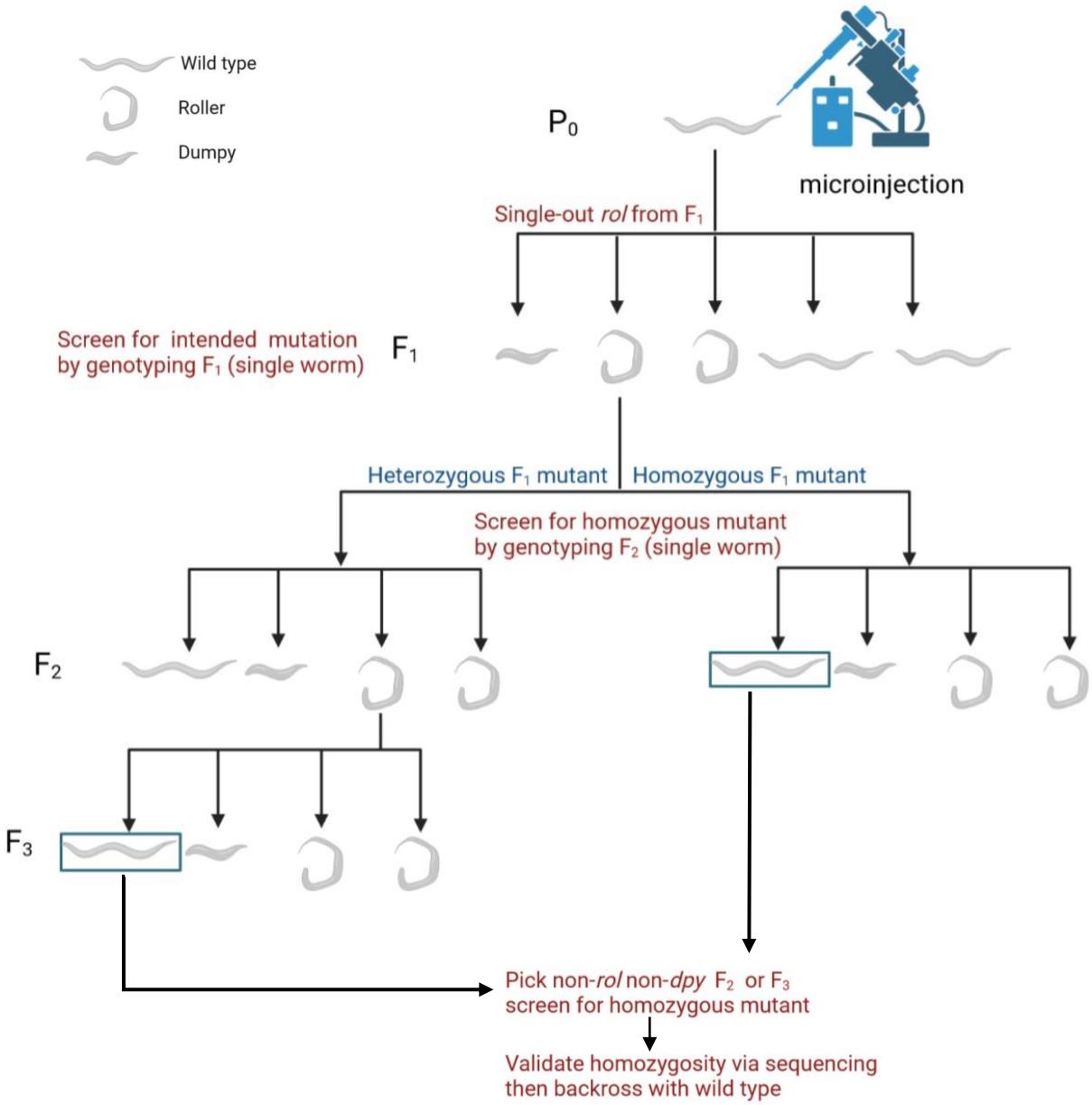

Figure 8: CRISPR-mediated gene knockout generation screening scheme. The same screening approach was followed if a dumpy mutant was singled out from F_1. In this case, once a homozygous mutant was confirmed, the dumpy mutation was segregated away by backcrossing. Scheme was generated using Biorender.com

3. Molecular biology techniques

3.1 Genotyping by PCR and agarose gel electrophoresis

Different strains genotypes were checked using a polymerase chain reaction (PCR) followed by an agarose gel electrophoresis. Following general primer design guidelines, as different primer sets were designed for every strain. Every genotyping process consisted of the genetic material extraction, amplification of the gene-of-interest using gene-specific primers, and performing gel electrophoresis.

Primer design. Primers were designed using the online tool Primer-BLAST by the National Center for Biotechnology Information (NCBI) according to general primer design guideline. Their GC content was between 40% and 60%, length between 19bp and 24bp, and the annealing temperature differences of primer pairs were < 5°C.

Primer reconstitution. To prepare a 100µM stock solution, the primer tube was centrifuged for 1 minute and resuspended in Milli-Q water. The amount of Milli-Q water added to prepare a 100µM stock solution depended on the oligo yield information per primer. The oligo yield (nmol) was multiplied by 10 to calculate the amount of Milli-Q water to be added. For example:

> If the oligo yield = 30.5nmol
> 100 nmol / 1 mL = 30.5nmol /? mL
> (1mL x 30.5 nmol) / 100 nmol = 0.305mL = 305µL Milli-Q water was added to the tube.

After adding the adequate amount of Milli-Q water, the tube is vortexed well. For the PCR reactions, a concentration of 10µM is required, thus the stock is diluted accordingly to prepare a working stock.

gDNA extraction. Proteinase K was used to lyse the worms and extract their genetic material. Proteinase K (1mg/mL, Tritirachium album, Sigma-Aldrich) and PCR template buffer (Worm lysis buffer) were thawed. 100µL of worm lysis buffer was added to 5µL of proteinase K. Then, 5µL of this mixture were transferred into every sample vial. Using a sterilized picker, depending on the experiment, single or multiple worms were picked into each sample vial. Every sample vial was checked under the stereomicroscope to confirm that the worms were transferred into the mixture. Next, the vials were placed at -80°C or on dry ice for 15 minutes to open the cuticula of the worms. Then, the sample vials were placed in a thermocycler (Biometra) to extract the genetic material using the following program (Table 4).

Table 4: Description of temperatures and time used for worm lysis.

Release of genomic DNA	60°C	60 min
Inactivation of proteinase k	95°C	15 min
Pause	4°C	

Worm PCR. The gene-of-interest was amplified using a thermocycler and a program that depended on the primers used, PCR reaction mix, and size of the amplicon. The 5µL worm lysis samples were split in half to amplify with the forward primer along with a reverse or poison primer. Forward, reverse, and poison primers (10µM), and REDTaq ReadyMix PCR Reaction Mix (Sigma-Aldrich) or OneTaq Hot Start Quick-Load 2X Master Mix with Standard buffer (NEB) were thawed on ice. Once thawed, the primers pair, PCR reaction mix, gDNA sample, and Milli-Q water were mixed to prepare a 25µL reaction per sample. Then, samples were placed in a thermocycler with the optimal PCR program (Table 5). The annealing temperature varied depending on the primers used. When new primers sets were designed, a gradient PCR was performed to choose the optimal annealing temperature.

Table 5: Description of PCR program used for worm PCR.

Initial denaturation	95°C	2 min
Denaturation	95°C	45-60 sec
Hybridization	Annealing temp.	2 min
Extension	72°C	1 min/Kb
➔ 30 cycles		
Final extension	72°C	5 min
Pause	4°C	

Agarose Gel electrophoresis. To resolve the amplified DNA fragments, a 1% agarose solution was prepared by mixing 1g of agarose (Sigma-Aldrich) and 100mL of Tris-acetate-EDTA (TAE) buffer. To dissolve the agarose, the solution was heated in the microwave for 30 seconds intervals until completely dissolved. To visualize the DNA bands, 5µL of the fluorescent nucleic acid dye, GelRed (10000x in Dimethylsulfoxide (DMSO), Biotum) was added, and the agarose solution was gently swirled. The size and number of gel casting trays and combs were chosen depending on the number of samples to be analyzed. Once the poured agarose gel solidified, it was removed from the tray and the combs were pulled out. Then, the agarose gel was placed in an electrophoresis chamber (Biorad PowerPac™ Basic) filled with TAE buffer. Depending on the size of the comb used, the volume of sample loaded varied between 7-12µL. In every lane, the first and last wells were pipetted with 3µL of 1Kb Pluss DNA ladder (Invitrogen). Finally, the gel-holding chamber is connected to a power supply, at 120V, to allow the DNA fragments to separate. The running time varied between

60-80 minutes. To view the results, Proxima 2500-T gel imaging system (Isogen Life Sciences) was used.

4. Behavioral assays

4.1 Locomotor (Tap) Assay

To investigate locomotor arousal defectiveness in mutant worms, a tracking setup on low peptone plates was used, with speed as the main parameter for readout. The use of low peptone agar plates facilitated the tracking of worms as the OP50 *E. coli* lawn is not thick. The same NGM agar recipe (described in section 1.2.1 of *Materials and Methods*) was followed except for the amount of Bacto^{TM} Peptone added, which was 0.13g/L instead of 2.5g/L. Every assay replicate was planned over the course of three days. On the first day, 15-25 low peptone plates were seeded with a 30µL OP50 *E. coli* drop in the middle of the plate. The drop of bacteria was not spread and was left in the laminar flow until it was dry. Once dry, the plates were covered, inverted, and placed in a clean box at room temperature. On the second day, 10 L4 hermaphrodites of each strain to be tested were transferred onto the seeded plate at around 5:00 p.m. The plates were stored at 20°C to be assayed the next day (third day).

4.1.1 Locomotor tracking setup

To track the locomotor activity of worms, the low peptone NGM plate was uncovered and inversely placed on the stereoscope's (Nikon SMZ745T) stage. The worms were tracked using a Dinolite camera mounted on the stereoscope and the recording software DinoCapture 2.0. At the beginning of every experiment the focus was manually adjusted for optimal recording and the settings were set to 5 frames per second. Each plate was recorded for around five and a half minutes. First, the plate was left on the stage for at least two minutes without disturbance, then, the recording was started. 30 seconds into the recording, 5 taps were administered manually on the bottom of the plate using the blunt end of a wooden chopstick. Taps were applied in less than three seconds. The animals were recorded for 5 more minutes following the tap stimulation.

4.2 Oxygen sensing response Assay

To assess whether mutant strains have a defective arousal response following exposure to 21% oxygen, worms were tracked for about 6 minutes under different oxygen conditions. The assay was carried out using a synchronized population of 1 days old hermaphrodites. Therefore, one day before performing the assay, 30-35 L4 hermaphrodites were transferred on acclimated seeded plate (procedure described in sections 1.2.1 and 1.2.3 of *Materials and Methods)*. In addition, NGM agar plates with 2.5 peptone were seeded to be used as the assay

plates. To seed the assay plates, a 20µL drop of liquid OP50 *E. coli* inoculate was dispensed in the center of a pre-acclimated plates. The small drop was spread into a 1cm^2 patch using a short tip spreader made from a glass Pasteur pipette. Once dried, the plates were inverted and kept at room temperature overnight.

4.2.1 Oxygen sensing tracking setup

The shape of the bacterial patch was adjusted to fit the size of the behavioral chamber chip. This was done using a 1cm^2 hollow frame made from Polydimethylsiloxane (PDMS) which served as a stamp. Using the stereoscope, the PDMS stamp was gently pressed against the bacterial lawn to remove any bacteria outside the 1cm^2 square. The stamping step was performed multiple times until almost all the unwanted bacterial lawn was removed. Then, 20-30 young adult hermaphrodites were transferred onto the stamped assay plates. To keep the bacterial patch intact, the transferred worms were gently allowed to crawl on the bare agar side into the food patch.

In the gas response setup consisted of four 50mL syringes (BD) filled with the desired gas. Two gas syringes were filled with 7% oxygen (Air Liquide) and the rest were filled with 21% oxygen (Air Liquide) from the appropriate gas flask. The gas-filled syringes were mounted onto the PHD ULTRA™ Syringe Pump (Harvard Apparatus) and attached to the Valvebank® perfusion controller (Automate Scientific). The worms were allowed to acclimate on the stereoscope's stage for at least 6 minutes without disturbance. The gas chamber chip was gently laid surrounding the worms. To track changes in locomotor in response to different concentrations of oxygen, a specific program was used. The program spanned exactly eight minutes with alternating 7% and 21% oxygen gas concentrations as shown below.

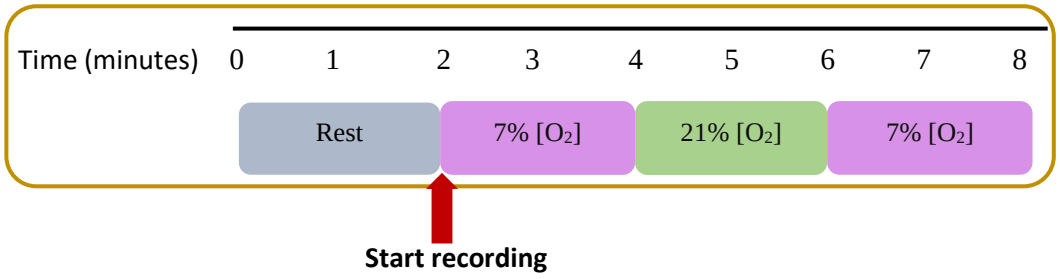

Figure 9: Illustration of the gas responses experiment timeline.

A Dinolite camera mounted on the stereoscope set at 2 frames per second and the DinoCapture 2.0 were used for video acquisition.

4.3 Data analysis

4.3.1 Tap assay data acquisition and analysis

The recordings were analyzed using the multi-worm behavior tracker Tierpsy (version 1.5.3a+18aaba9). The Tierpsy Tracker was developed by the MRC-LMS Behavioral Phenomics Group to track a high number of worms with the resolution of a single worm tracker (Javer *et al.,* 2018). The tracking data from Tierpsy was processed using a custom Python script (Written by Keertana Venkatesh). Using this script, the speed trace for the worms tracked was plotted. This was further quantified and compared by calculating the arousal integral and the arousal speed. Arousal integral refers to the area under the curve for the first 20 seconds post stimulus delivery. This was calculated using Graphpad Prism (version 9.3.1) wherein the baseline for every genotype is taken as the speed before stimulus delivery. The arousal speed is the average speed 10 seconds post stimulus delivery. The speed without stimulus is taken as the average speed 10 seconds before stimulus delivery.

Statistical analysis was performed using Graphpad Prism (version 9.3.1). To compare the difference in mean between two or more independent groups, an unpaired t-test or One-Way ANOVA test was performed, respectively. When analyzing more than two strains, a Tukey's multiple comparisons test was performed to achieve pairwise significance comparisons. Adjusted P-values smaller than 0.05 were deemed statistically significant.

4.3.2 Oxygen responses' data analysis

Worm tracking videos were processed using the Zen Tracker (version 2.14). This is a multi-worm tracker that can be used to extract different behavioral outputs like speed and turns. In this experiment we were interested in speed as the main parameter. Under the microfluidic chip, only worms on the food patch were considered for further analysis. This is to avoid any differences in locomotory behaviors associated with food. The exported data was then manually processed to calculate the average speed when exposed to different oxygen concentrations. The average speed at 7% oxygen conditions was calculated using the average plate speed between 40-100 seconds for each trial. Whereas the average speed at 21% oxygen was calculated from the time range of 160-220 seconds for every trial. Using Graphpad Prism (version 9.3.1), a One-Way ANOVA test and a Tukey test were used for pairwise significance comparisons. Tests with a P-value smaller than 0.05 were considered statistically significant.

5. Imaging

To visualize expression patterns of different neuropeptides and neuropeptide receptors, images of reporter strains were taken. To image the fluorescent reporter lines, 2% agarose

pads were prepared. Around four worms were picked and placed in a drop of M9 buffer solution on the dry agarose pad. Then, to paralyze the worms, a drop of sodiumazide (1M; Sigma-Aldrich) was added. Finally, the slides were covered with a coverslip. The images of the GFP reporter strains were done using the confocal microscope ZEISS LSM 900. Images were taken at a magnification of 63X.

Results

1. Generation of transgenic strains and CRISPR-Cas9-based genome editing

To investigate cross-modal sensitization, Chew, Tanizawa, *et al.* (2018) exposed worms to plate taps which served as the arousing stimuli. Then, ChR2-expressing ASH neurons were optogenetically activated using blue light. Therefore, to perform this experiment, assayed worms should have ChR2 expressed in their ASH neurons and to be intrinsically insensitive to blue light stimulation. A new strain with the *ASH::ChR2* transgene (*ljIs114* or *ljIs124*) and *lite-1* mutation background were built for each candidate, *flp-7* and *npr-13*. A partial deletion mutant strain of each candidate was used to build new transgenic strains. The *npr-13* partial deletion mutant in figure 10 is used as an example of our crossing scheme to build the new transgenic strains. The same approach was followed to build the *flp-7(ok2625) lite-1(ce314); ljIs124* strain. However, steps 1-3 were skipped since we used a *flp-7* partial deletion mutant that already had the *lite-1(ce314)* allele.

To further validate any observed phenotype, we generated complete gene knockout mutants for both *flp-7* and *npr-13*. Gene deletion was done using CRISPR-Cas9 with guide RNAs spanning the whole gene sequence (as described in section 2.2 of *Materials and Methods*). We were able to successfully generate three knockout mutants, two for *flp-7* and one for *npr-13* (complete gene sequences can be found in *Appendix 3*).

For the *flp-7* knockout, we originally deleted the *flp-7* gene in a wild type (N2) background to generate the IBE346 strain. However, *flp-7* and *lite-1* genes are very close to one another on the X chromosome, with a genetic distance that is less than 1 centiMorgan (cM). This means that the recombination frequency is even lower than 1% between these two genes. Thus, it would be very laborious to build this strain by crossing in the *lite-1* mutation. To avoid this, we generated another *flp-7* knockout strain in the *lite-1(ce314)* background strain itself instead of N2.

The final confirmation of the knockout was done by sequencing. All knockout mutants had the intended gene sequence deleted from their genome. Once confirmed, knockout strains were backcrossed with the wild-type strain (N2) at least twice before being used in any behavioral assays.

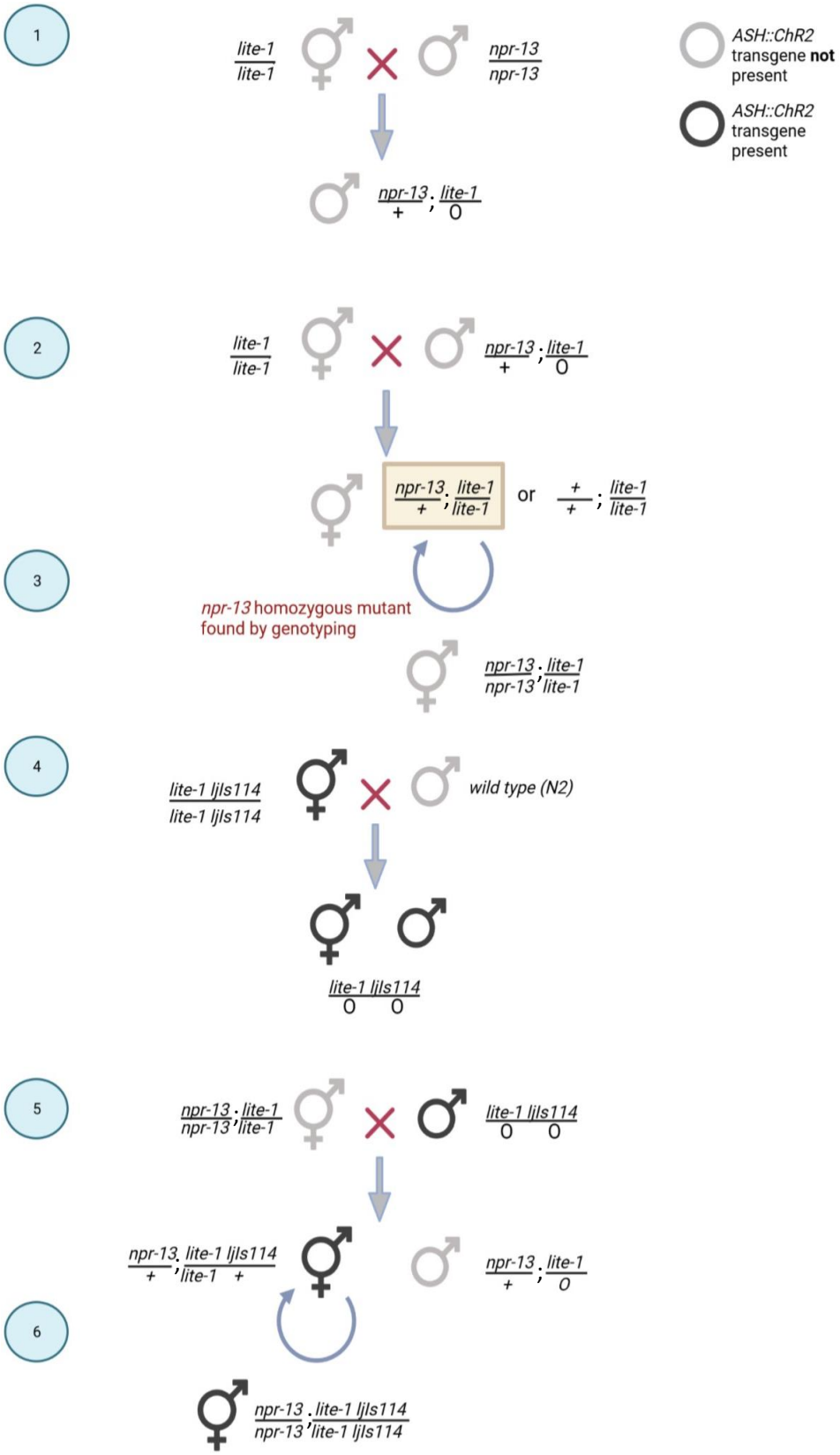

Figure 10: *npr-13* partial deletion mutant crossing scheme to generate *npr-13(tm1504);lite-1(ce314) ljIs114*. Black symbols indicate animals with the *ASH::ChR2* transgene (*ljIs114*) which have a fluorescent marker for screening. Curved arrows indicate self-fertilization. For ease of visualization, allele information was not included in the scheme. Depicted genotypes: *lite-1 = lite-1(ce314)*; *npr-13 = npr-13(tm1504)*. "+" indicates

wild-type allele and “O” is used for the hemizygosity of the male’s sex chromosome. Scheme generated using Biorender.com

2. Control strains respond similarly to mechanical stimulation

To evaluate locomotor arousal, worms were exposed to five plate taps in less than three seconds. Then, the data obtained from the tracking software was quantified in the form of speed traces, arousal integrals and average arousal speeds.

Besides the wild-type strain N2, two other strains were used as a control in the tap response assay. These strains have the *lite-1* mutation and the *ASH::ChR2* transgene (on the X chromosome or not) in their background. When assaying mutant strains with the *ASH::ChR2* transgenic background and *lite-1* mutation, the appropriate control with the same background was used for comparison and statistical analysis. In addition, *flp-20* and *frpr-3* were included as control strains with altered arousal responses. All control strains were compared to confirm their expected arousal responses and the adequacy of the assay setup.

To elucidate whether the *lite-1(ce314)* allele, *ljIs114* transgene, and *ljIs124* transgene affected arousal responses, they were compared to the wild-type strain, N2. As shown in Figure 11, these strains exhibited very similar arousal responses following mechanosensory (taps) stimulation. The hyperactivity state seems to be maintained for a slightly longer time period in the *lite-1(ce314);ljIs114* strain (Fig. 11a). This is evident in the slightly larger arousal integral (Figure 11c). On the contrary, the average speed after stimulation is a bit lower for the *lite-1(ce314) ljIs114* (Fig. 11b). This indicates a faster drop in speed after tap. Nonetheless, no statistically significant difference in locomotor arousal was found among these three control strains. Their similar response to plate taps allows for their use as the wild-type control when compared to mutant strains with the same background. Note that plate taps initiate an escape response in *C. elegans* with worms travelling backwards for some distance before moving forward again (Rankin *et al.*, 1990). This backward locomotion accounts for the sharp increase in speed immediately after taps delivery (Fig. 11a).

The requirement of the neuropeptide *flp-20* and its receptor *frpr-3* in locomotor arousal was also confirmed (Fig. 11). Both mutants showed defective hyperactivity following tap stimulation as predicted from Chew, Tanizawa, *et al.* (2018). This is evident in the speed trace, arousal speed, and the arousal integral (Fig. 11).

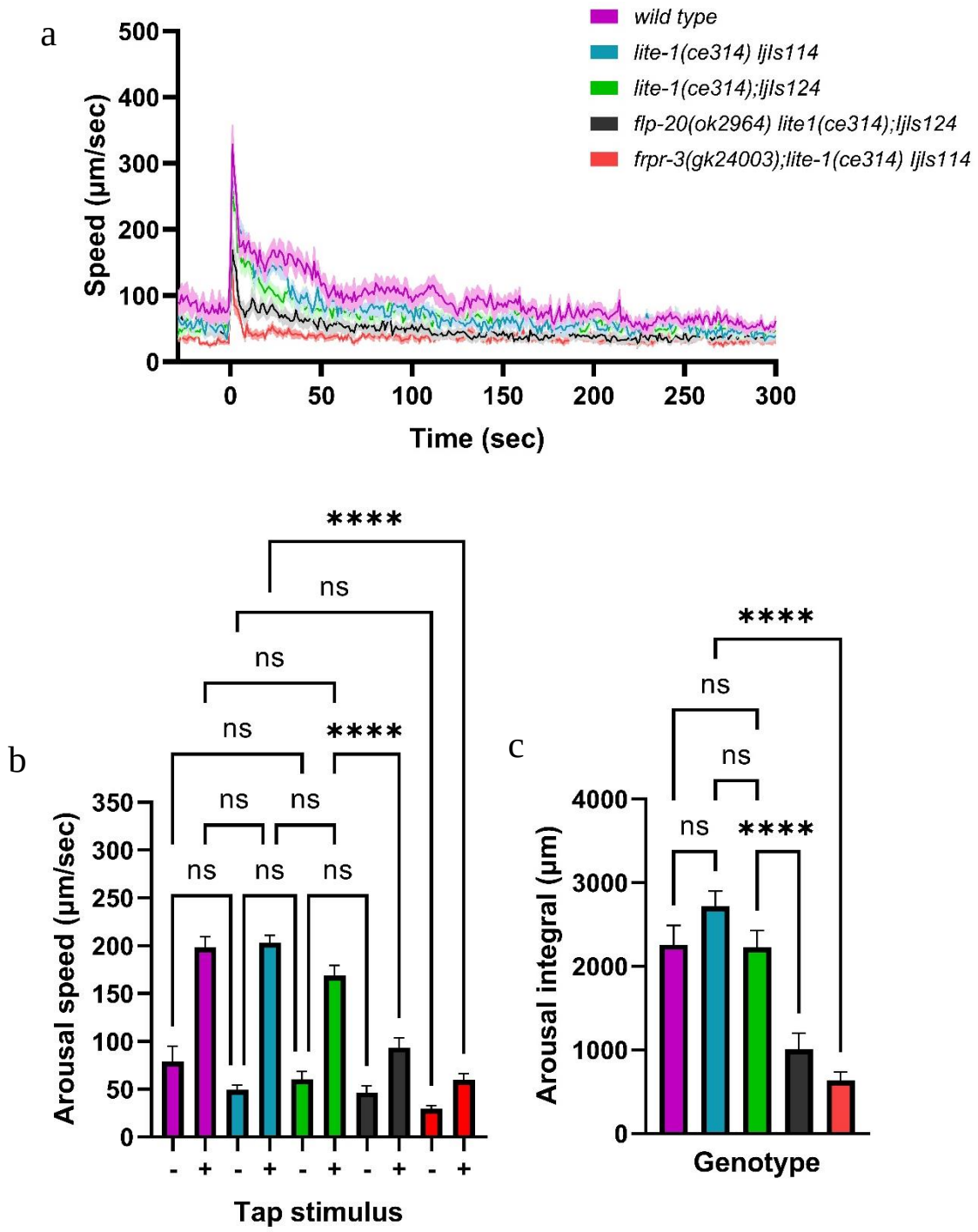

Figure 11: Locomotor arousal responses comparison of all control strains used. (a) Speed trace (µm/sec). The tap stimulus was delivered at t = 0. Each speed trace represents the compiled average speeds of all experimental trials. **(b)** Quantification of the average speed 10 second before (-) and after (+) taps administration. **(c)** The arousal integral (µm) was quantified as the total area under the speed trace curve in the first 30 seconds after tap delivery. Around 5-10 animals were assayed in each trial. Number of trials: wild type = 9; *lite-1(ce314) ljIs114* = 9; *lite-1(ce314);ljIs124* = 10; *flp-20(ok2964) lite-1(ce314);ljIs124* = 11; *frpr-3(gk24003);lite-1(ce314) ljIs114* = 9. Error bars signify mean ± Standard Error of the Mean (SEM). Statistical differences in mean were obtained using Tukey's multiple comparisons test. All p-values > 0.05 were deemed non-significant (ns).

Hereafter, the *lite-1(ce314) X; ljIs124 non-X* and *lite-1(ce314) ljIs124 X* transgenic strains will be referred to as the "wild-type control" when compared to strains with the same transgenic background.

3. FLP-7 does not have a role in locomotor arousal

To investigate the involvement of *flp-7* in locomotor arousal, two mutant strains of the *flp-7* gene were assayed. The two mutant strains assayed were a partial deletion mutant, *flp-7(ok2625),* and a partial deletion mutant with the *lite-1(ce314)* allele and *ASH::ChR2* transgene, *flp-7(ok2625) lite-1(ce314); ljIs124*. The partial deletion mutants seemed to have a slightly higher speed overall (Fig. 12). This slight shift in speed is evident in the *flp-7(ok2625)* speed trace (Fig. 12a) and post-tap arousal speed (Fig. 12b) when compared with the wild-type strain (N2). The increase in arousal speed after stimulation is significantly higher than the post-tap arousal speed of the controls (p-value = 0.0237).

Nevertheless, the arousal extent did not differ between the *flp-7* partial deletion mutant and wild type. This can be extrapolated from the non-significant difference in the arousal integral (area under the curve) between the two strains (p-value = 0.3836). The quantification of the arousal integral takes into account the baseline speed of the assayed strain (described in section 4.3.1 of *Materials and Methods*). Although the baseline speed of *flp-7(ok2625)* is higher than wild type, the overall arousal integral did not differ. This suggests that *flp-7* has no role in mediating locomotor arousal responses.

The second assayed *flp-7* mutant has an additional mutation and transgene in its background. This strain has a single base pair mutation in the *lite-1* gene (*lite-1(ce314)*) and a transgene expressing the optogenetic actuator ChR2 in the ASH neurons. These strains were assayed as they will be used to investigate ASH-dependent sensory sensitization (as described in section 3.2.1. of the *Introduction*). Like the partial deletion mutant without the transgene, this *flp-7* mutant did not have an altered arousal response compared to its wild type (Fig. 13). This further confirms that the transgene these mutants have did not affect the locomotor arousal response.

Although two *flp*-7 strains were assayed, to confirm our findings, a complete *flp-7* gene KO should be tested.

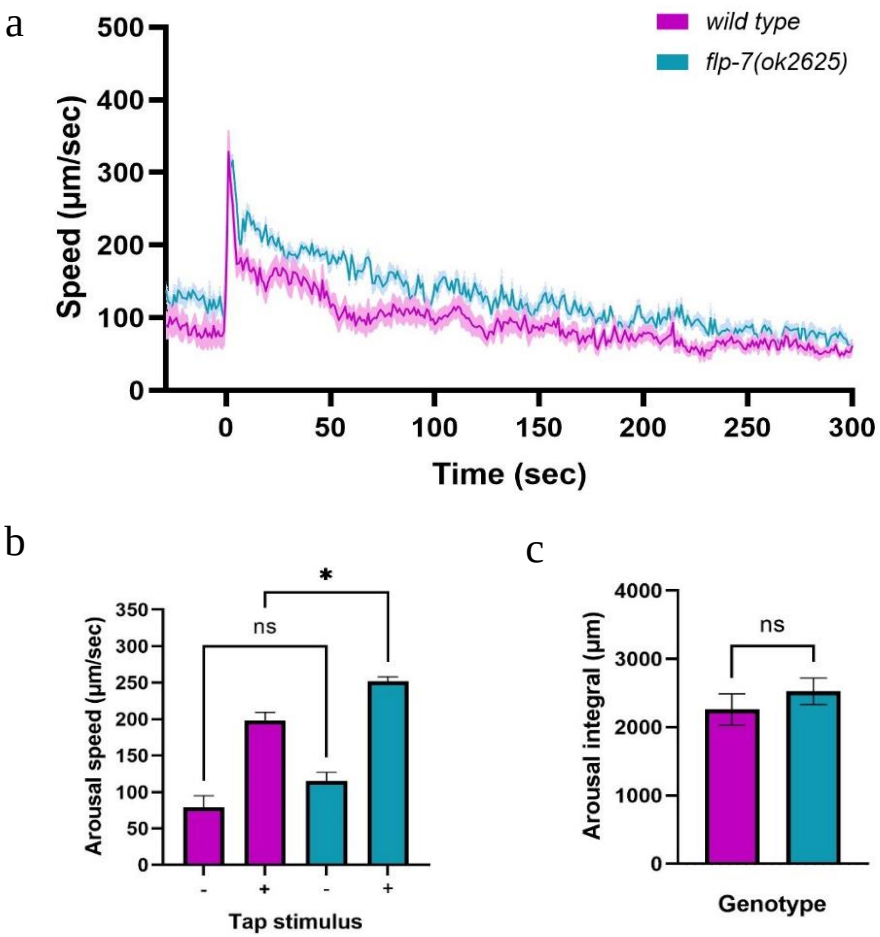

Figure 12: Locomotor arousal assay for the candidate FMR-amide neuropeptide FLP-7. (a) Speed trace (µm/sec) of both the control strain, N2, and the mutant *flp-7(ok2625)*. **(b)** Average arousal speed before (-) and after (+) taps stimulation. **(c)** The arousal integral (µm). Around 5-10 animals were assayed in each trial. Number of trials: wild type = 9; *flp-7(ok2625)* = 8. In all three panels, Error bars signify mean ± SEM. Here, statistical difference in mean was obtained using an unpaired t-test. All p-values > 0.05 were deemed non-significant (ns).

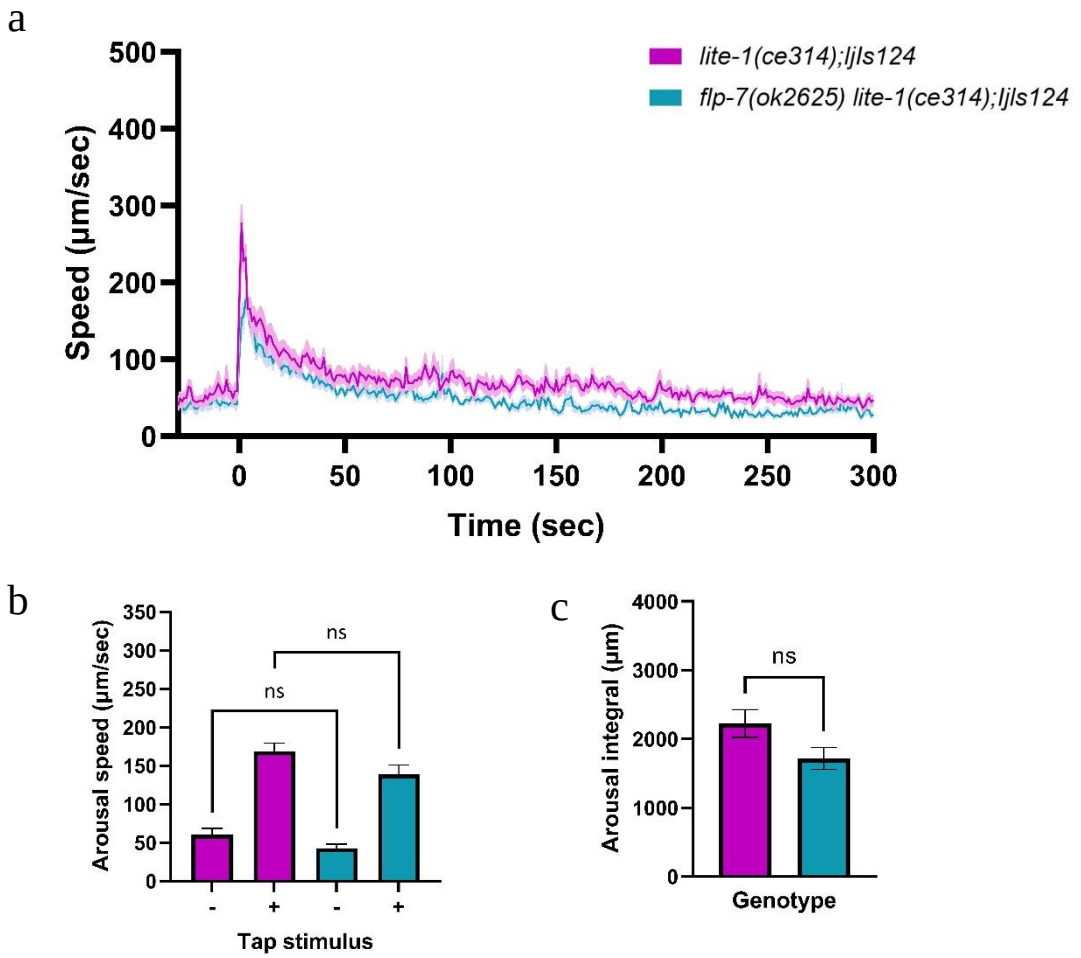

Figure 13: Locomotor arousal assay for *flp-7* mutants with the *lite-1(ce314)* allele and *ASH::ChR2* transgene. (a) Speed traces (µm/sec). **(b)** Average arousal speed before (-) and after (+) taps stimulation. **(c)** Arousal integral (µm). Around 5-10 animals were assayed in each trial. Number of trials: *lite-1(ce314);ljIs124* = 10; *flp-7(ok2625) lite-1(ce314);ljIs124* = 9; *flp-20(ok2964) lite-1(ce314);ljIs124* = 11. In all three panels, Error bars signify mean ± SEM. Statistical difference in mean was obtained using an unpaired t-test. All p-values > 0.05 were deemed non-significant (ns).

4. NPR-13 may not be involved in regulating locomotor arousal

The same locomotor arousal tracking setup and data processing was used to investigate whether the neuropeptide receptor *npr-13* was involved in arousal behaviors. Hyperactivity after mechanical (tap) stimulation was investigated in a partial deletion mutant and a knockout strain (Fig. 14). Compared to wild type, both, the partial deletion mutant *npr-13(tm1504)* and the *npr-13 KO* mutant showed very similar baseline average arousal speed (p-value = 0.3021 and 0.9046, respectively) (Fig. 14b).

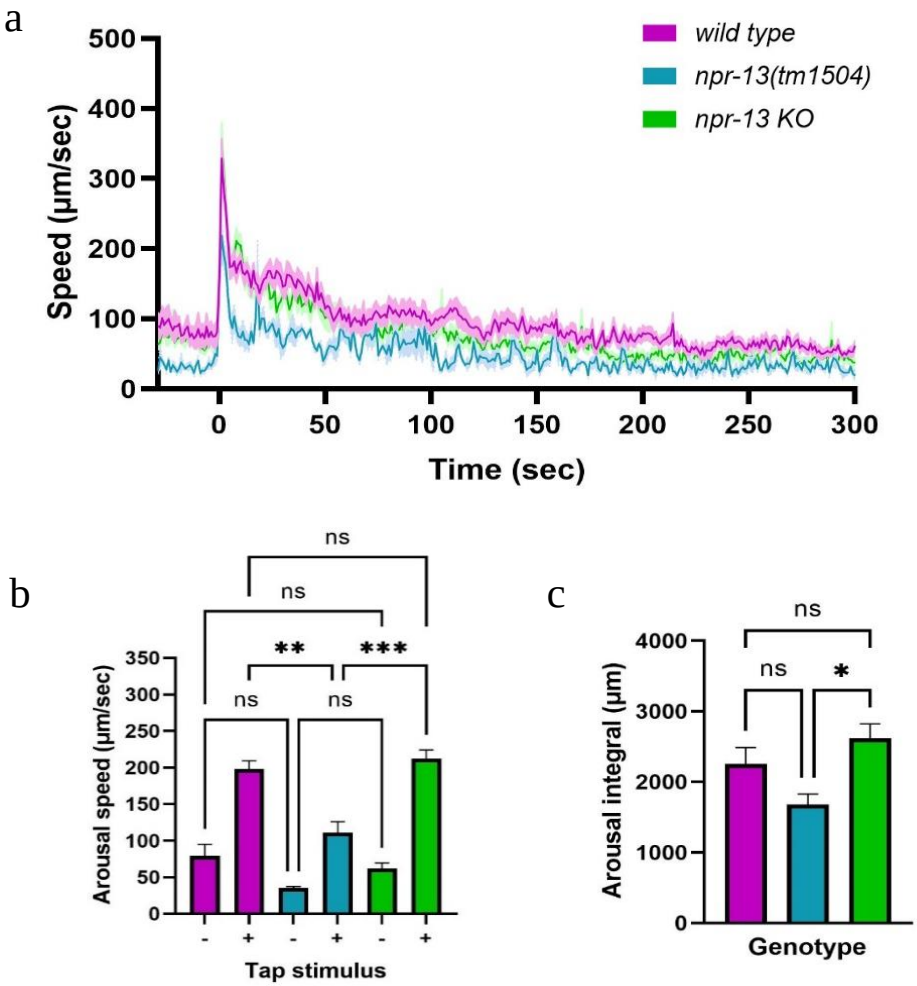

Figure 14: Locomotor arousal assay of the Prolactin releasing hormone homologue *npr-13* mutants. (a) Speed traces (µm/sec). **(b)** Average arousal speed before (-) and after (+) taps stimulation. **(c)** Arousal integral. Around 5-10 animals were assayed in each trial. Number of trials: wild type = 9; *npr-13(tm1504)* = 4; *npr-13 KO* = 9. All error bars indicate mean ± SEM. Tukey's multiple comparisons test was used with p-values > 0.05 considered non-significant (ns).

Surprisingly, the partial deletion mutant, *npr-13(tm1504)*, had significantly lower post-taps speed compared to both the control and *npr-13 KO* (Fig. 14b). The arousal response of *npr-13(tm1504)* was not only lower but also dropped quickly. This is apparent in the peak width of the speed trace (Fig. 14a) and the difference in arousal integral (Figure 14c). The difference in the arousal response between the partial deletion mutant and complete gene knockout indicates allele specific effects. The observed altered arousal response in the *npr-13(tm1504)* allele seems to be specific to this strain as we were not able to replicate the altered phenotype in the knockout strain.

An *npr-13(tm1504)* with *ASH::ChR2* transgene was also assayed (Fig. 15). This mutant had a significantly reduced initial response after mechanical stimulation with a baseline speed like

the control strain (Fig. 15a-b). In addition, this *npr-13* mutant had an arousal response that did not last for long which is clear in the reduced arousal integral size (Fig. 15c).

Compared to the non-transgenic *npr-13* mutant, this mutant showed similar arousal defect hereby confirming that the transgene background has no effect on this response (Fig. 14 and 15).

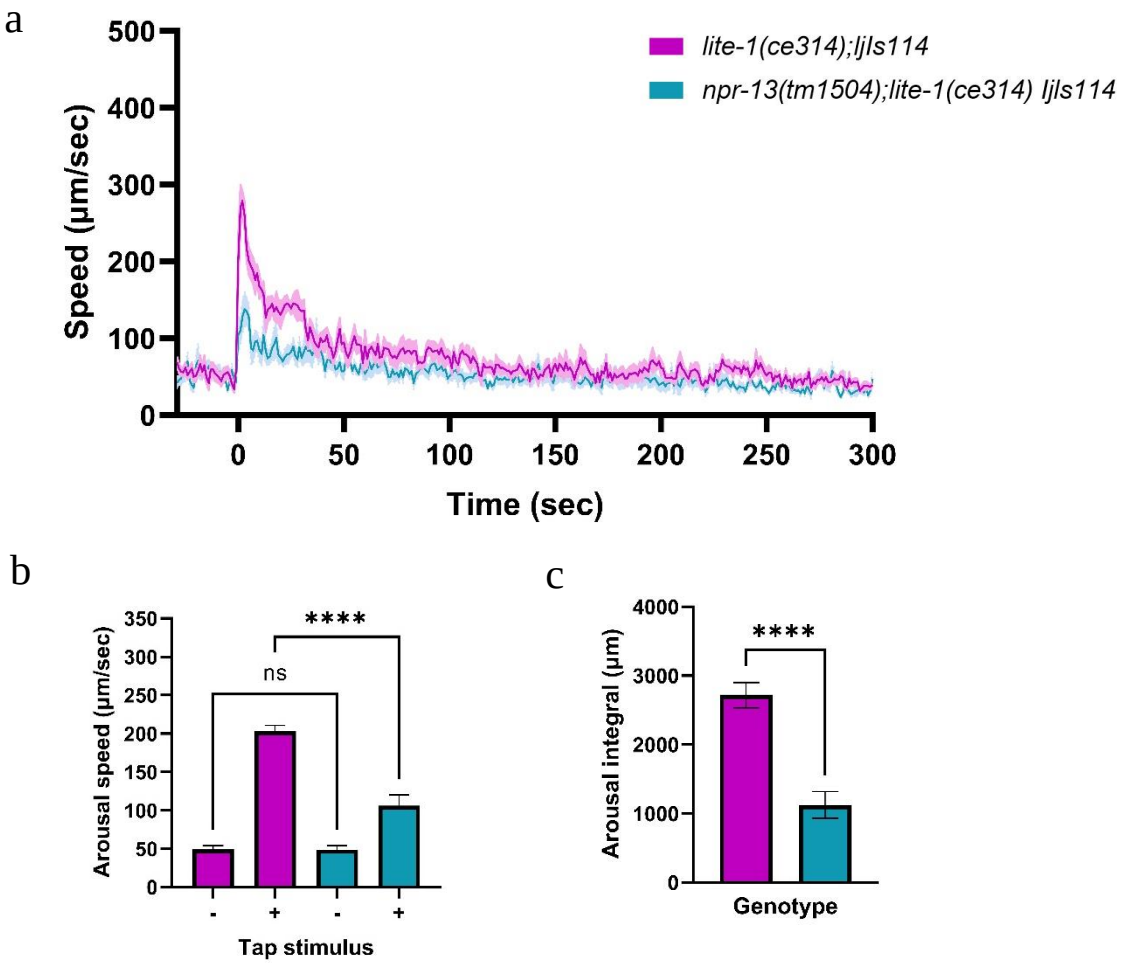

Figure 15: Locomotor arousal assay for *npr-13* mutants with the *lite-1(ce314)* allele and *ASH::ChR2* transgene. (a) Speed traces (µm/sec). **(b)** Average arousal speed before (-) and after (+) taps stimulation. **(c)** Arousal integral. Around 5-10 animals were assayed in each trial. Number of trials: *lite-1(ce314) ljIs114* = 8; *npr-13(tm1504);lite-1(ce314) ljIs114* = 8. Error bars indicate mean ± SEM. Statistical difference in mean was obtained using an unpaired t-test. All p-values > 0.05 were deemed non-significant (ns).

5. FLP-7 may be involved in oxygen avoidance responses

Based on *C. elegans* single-cell (sc)-RNA-sequencing data, both *flp-7* and *npr-13* are expressed in cells implicated in the oxygen sensing circuit. This suggests a potential regulatory role in the circuit.

When exposed to atmospheric oxygen levels, *flp-7(ok2625)* mutants demonstrated a hyperactivity response with a similar trend to *npr-1* mutants (Fig. 16). *npr-1* mutants were used as a positive control strain that elicits a strong response to 21% oxygen exposure, whereas the wild-type N2 strain was used as a negative control due to the *npr-1* gain-of-function mutation in its background (Chang *et al.*, 2006). This mutation makes the wild type insensitive to otherwise noxious oxygen levels. Like *npr-1* mutants, the *flp-7(ok2625)* mutant had a pronounced increase in speed after exposure to 21% oxygen levels (Fig. 16b). This acceleration was not significantly different between the *flp-7(ok2625)* and *npr-1* mutants. All assayed strains exhibited almost the same levels of speed when exposed to 7% oxygen conditions (Fig. 16b).

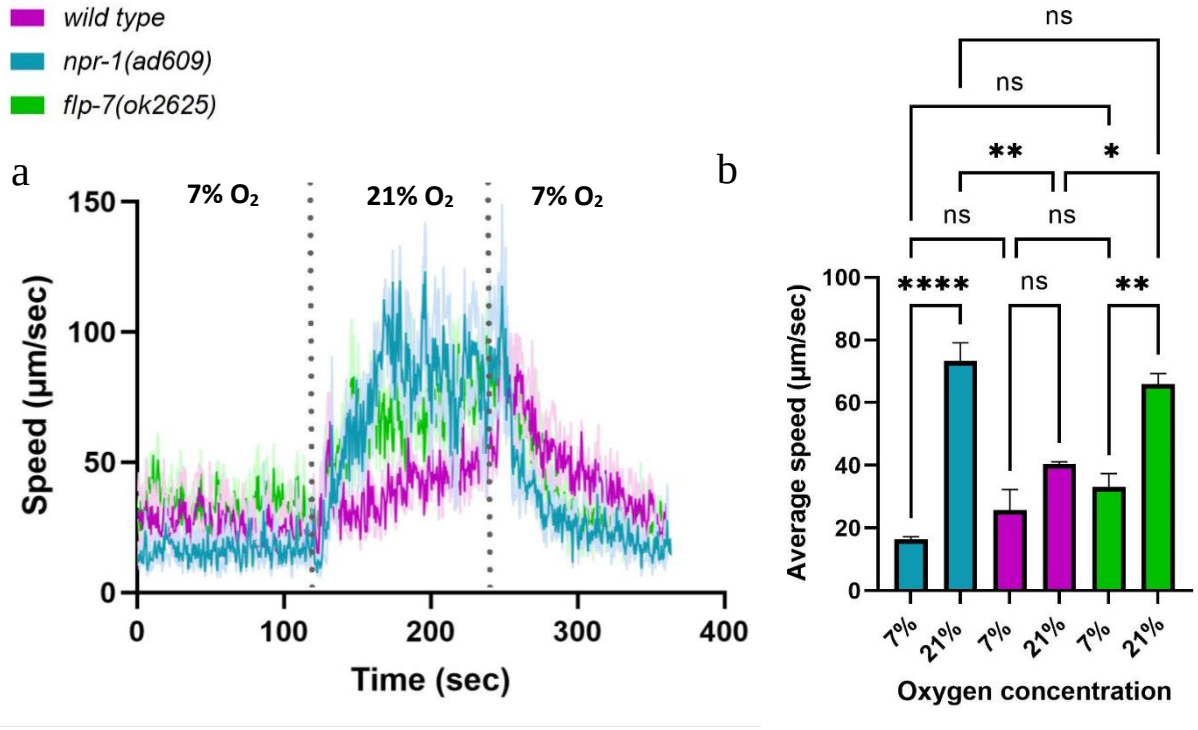

Figure 16: Oxygen-avoidance assay for *flp-7* mutant. (a) Average speed trace (µm/sec) of *flp-7(ok2625)* mutants compared to the positive control *npr-1* and the negative control N2. **(b)** Average speed at 7% and 21% oxygen concentration exposure. Dashed lines indicate oxygen concentration changes. Three trials were conducted for each strain assayed. Every trial had an average of 25-30 worms tracked. Pairwise significance comparisons were done using the Tukey's multiple comparisons test with p-values > 0.05 were deemed non-significant (ns).

On the contrary, the *npr-13* knockout mutant had a smaller response to 21% oxygen exposure that was similar to the wild-type strain N2 (Fig. 17). Although *npr-13 KO* mutants accelerated when in a 21% oxygen environment, this increase in speed did not significantly differ from the wild-type N2 speed in the same conditions (Fig. 17b). In addition, the speed traces of both the N2 and *npr-13 KO* follow the same trend (Fig. 17a).

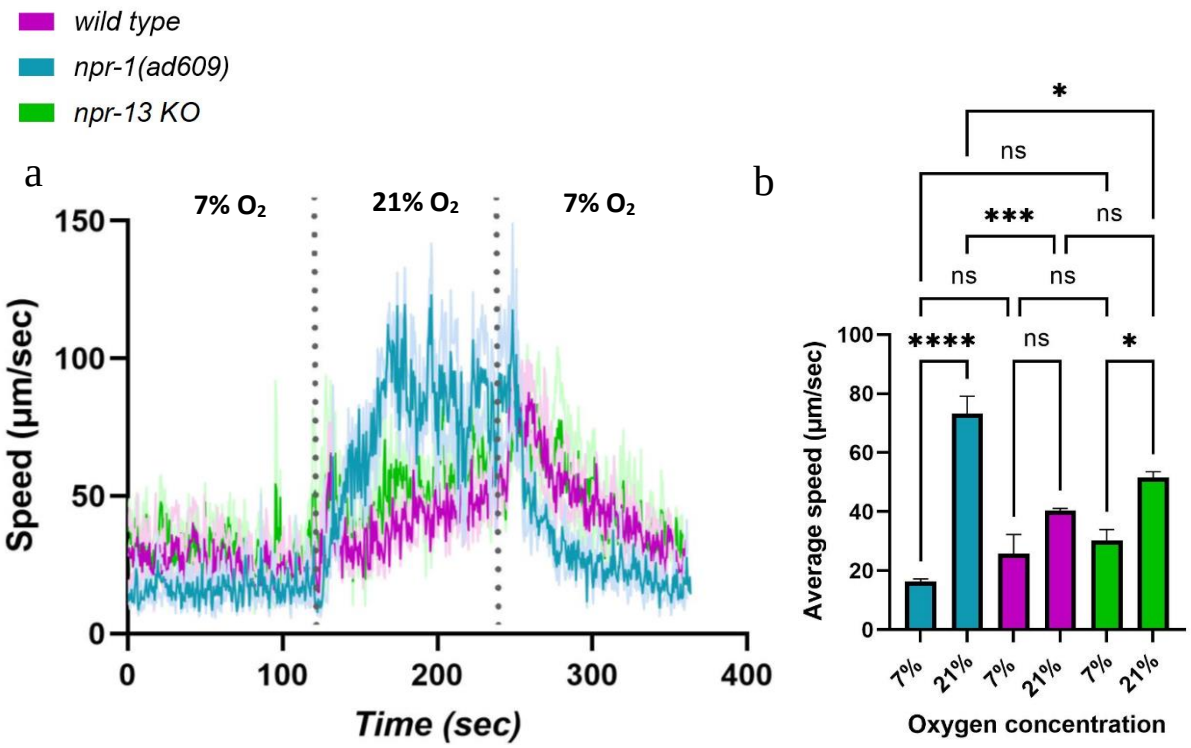

Figure 17: Oxygen-avoidance assay for *npr-13* knockout mutant. (a) Average speed trace (µm/sec) of *npr-13 KO* mutant compared to the positive control *npr-1* and the negative control N2. **(b)** Quantification of average speed at 7% and 21% oxygen levels. Dashed lines indicate oxygen concentration changes. Three trials were conducted for each strain assayed. Every trial had an average of 25-30 worms tracked. Pairwise significance comparisons were done using the Tukey's multiple comparisons test with p-values >0.05 considered as non-significant (ns).

6. FLP-7 and NPR-13 expression pattern

In addition to generating mutant strains and performing behavioral assays, neuropeptides' gene expression patterns can help unfold potential signaling pathways. A reporter strain generated by SUNY biotech for each candidate was obtained. Each is an endogenous reporter line with a CRISPR-mediated GFP tag at the end of the gene sequence. As seen in figures 18 and 19, the reporter expression is confined to the nucleus. This is because the expressed transgene, *flp-7::SL2::GFP::H2B* and *npr-13::SL2::GFP::H2B*, have a histone-tagged GFP reporter.

As predicted from the CenGen database, both *flp-7* and *npr-13* are expressed in a number of head and tail neurons (Fig. 18 and 19) (Taylor *et al.*, 2021). To confirm the expression patterns of each gene, the neuronal polychromatic atlas of landmarks (NeuroPal) (Yemini *et al.*, 2021) along with location information will be used to accurately identify neurons. The newly developed NeuroPal transgene is a multicolor reporter that contains four discriminable fluorophores that are expressed at four or more levels. The unique combination of these

reporters yields 41 neuron-specific reporters that overlap in a selective manner (Yemini *et al.*, 2021). This color-coded atlas can be co-expressed with gene expression reporter lines since it does not interfere with common fluorescent reporter signals like GFP (Yemini *et al.*, 2021). This compatibility allows for the accurate identification of cellular gene expression in the *C. elegans'* nervous system.

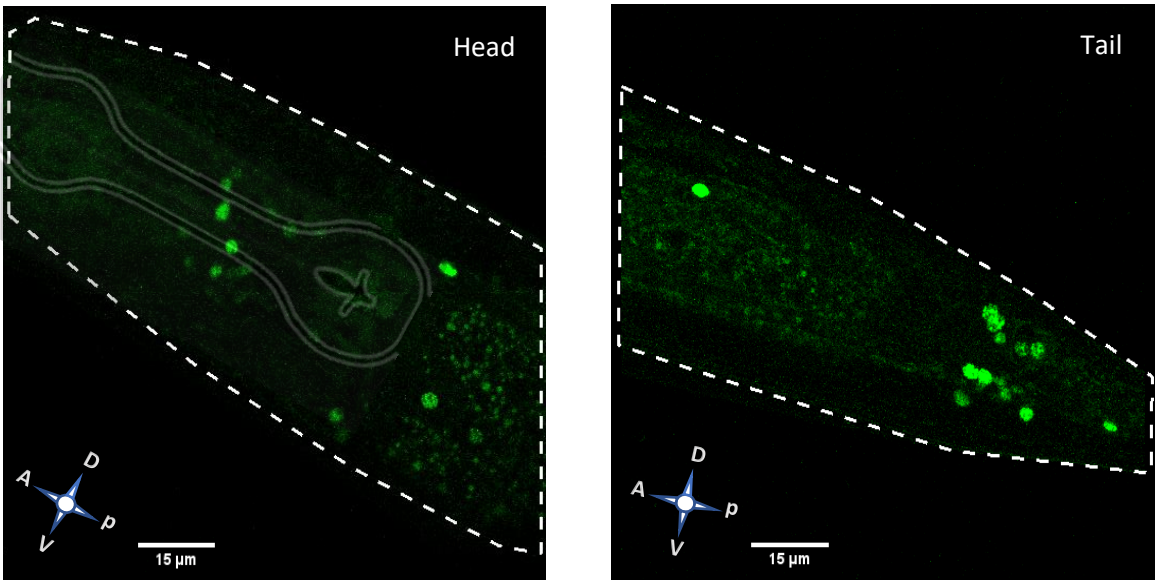

Figure 18: Expression pattern of *flp-7* reporter strain. The reporter strain has GFP as an expression marker in the head (left panel) and tail (right panel). Images were obtained using the ZEISS LSM 900 confocal microscope.

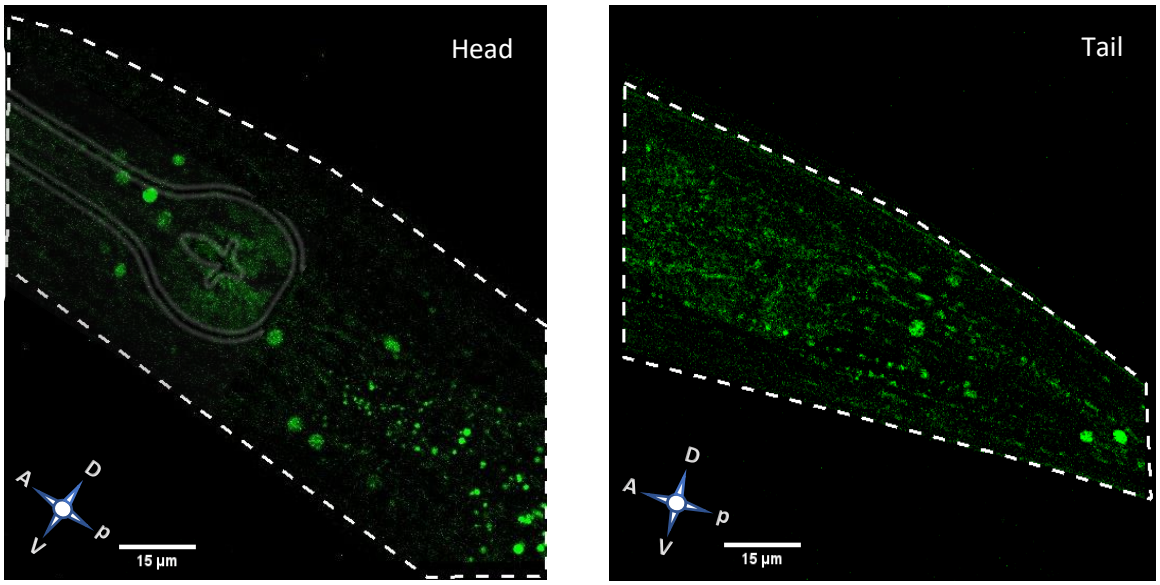

Figure 19: *npr-13* expression localization using a reporter strain. Images of the expression marker GFP were taken for the head (left panel) and tail (right panel). The confocal microscope ZEISS LSM 900 was used to acquire these images.

Discussion

1. *flp-7* and *npr-13* are not involved in tap-induced hyperactivity

Mechanical stimulation, specifically plate taps, leads to locomotor arousal in the form of increased speed. This noxious cue acts as an arousing stimuli wherein further chemical stimulation becomes sensitized. The complete underlying molecular and cellular features of this behavioral state are yet to be elucidated. We sought to shed more light on possible molecular players involved in arousal and sensitization in *C. elegans*.

Based on previous work done in our lab, two candidates, *flp-7* and *npr-13*, were chosen as potential regulators of arousal based on their defective cross-modal sensitization as shown in figure 7. Although both candidates showed normal locomotor arousal responses (Fig. 6), we wanted to confirm these results using both partial deletion and knockout mutants. It's noteworthy that all assayed mutants had the ability to perceive tap stimulation, as they all exhibited a sharp reversal response upon stimulation. This escape response is reflected in the immediate and robust increase in speed in the collected speed traces.

To evaluate our assay setup, the requirement of *flp-20* and *frpr-3* for locomotor arousal and all intended controls were assayed and compared. As expected, both *flp-20* and *frpr-3* mutants showed defective arousal response after tap delivery (Fig. 11). Also, strains with the *lite-1(ce314)* allele and *ASH::ChR2* transgene had similar arousal responses compared to the wild-type strain N2. This allowed us to use these transgenic strains as controls where appropriate.

Our results showed both candidate responses to be comparable to their corresponding controls. This suggests the non-involvement of either candidate in mediating this arousal response.

1.1 *flp-7* mutants have normal arousal response to tap stimulation.

flp-7 is an FMRFamide-related neuropeptide that has only been implicated in regulating lipid metabolism, however, not much is known about other possible functions (Palamiuc *et al.*, 2017). Two strains with a partial deletion of the *flp*-7 gene were assayed. One strain only had the *flp-7(ok2625)* allele while the other also had the *lite-1(ce314)* allele and *ASH::ChR2* transgene. As expected from Chew, Tanizawa, *et al.* (2018) (Fig. 6), *flp-7* does not seem to be involved in locomotor arousal after mechanical stimulation. The only significant difference was the post-taps speed in the partial deletion mutant without the transgene. However, as shown in figure 12, the baseline speed of this strain is higher than wild type. This is taken into consideration in the arousal integral calculation which is comparable between this strain and its control (Fig. 12c). In addition, more trials need to be conducted since the number of

assayed worms per trial was not consistent. Although our planned protocol had 10 worms simultaneously tracked, not all transferred worms stayed in the field-of-view throughout the assay.

It's noteworthy that the *flp-7(ok2625)* strain used in the experiment, was not backcrossed before being assayed. It is necessary to backcross strains with the appropriate wild-type strain several times to make any conclusions about observed phenotypes. This is especially important when assigning a certain phenotype or behavior to a mutant strain as other mutations might be present in the background. Burnett *et al.* (2011) demonstrated the necessity of backcrossing mutant strains in their work on SIR-2. Previous publications claimed that the overexpression *sir-2* increased lifespan in *C. elegans* (Tissenbaum & Guarente, 2001). A decade later, Burnett *et al.* (2011) were able to demonstrate that this promotion of longevity in *sir-2* overexpression strains diminished after several backcrossing with wild type. Hence, the *flp-7(ok2625)* strain needs to be backcrossed several times with a wild-type strain to draw any conclusions.

Although *flp-7* seems to not be involved in hyperactivity after taps stimulation, its role in ASH-dependent cross-modal sensitization is yet to be explored. Based on the CenGen database, *flp-7* is expressed in a number of sensory neurons like PVM (1583.159 transcripts per million (TPM)), PHA (718.342TPM), and AVM (363.493TPM) among others. It is also expressed in the ASH neurons (221.257TPM) (Taylor *et al.*, 2021). While exploring this RNA sequencing database, to ensure we had expression data with acceptable false discovery rate, we opted for the use of threshold 2. In CenGen, threshold 2 has a positive true rate of 81% and a false discovery rate of 14%. This allowed to assess the expression pattern data more confidently with a threshold that was not too stringent nor with high false positive calls.

Predicated on the expression of *flp-7* in various sensory neurons combined with the observed defective cross-modal sensitization phenotype, we hypothesize that *flp-7* might be part of the sensory signal mediating ASH sensitization. Also, since *flp-7* is expressed in the ASH neurons themselves, it might play a role in ASH-mediated locomotor sensitization. This is a response seen in worms in which ASH is repeatedly activated and requires the neuropeptide receptor *pdfr-1* (Ardiel *et al.*, 2017). Both hypotheses can be delved into by performing cell-specific rescue experiments and repeated stimulation of ASH in *flp-7* mutants.

Finally, the involvement of *flp-7* in regulating arousal responses after tap stimulation can further be concluded by assaying CRISPR-mediated *flp-7* knockout mutants. This would allow us to confidently exclude *flp-7* as an effector of mechanosensory-induced hyperactivity.

1.2 The neuropeptide receptor *npr-13* is not required for locomotor arousal.

npr-13 is a predicted homologue of the human PRLHR with no confirmed functions besides the defective cross-modal sensitization reported by Chew, Tanizawa, *et al.* (2018). Although previous reports showed *npr-13* mutants to have normal arousal responses after tap stimulation, the opposite was seen in our mutants (Fig. 14 and 15). Both *npr-13* strains with and without the optogenetic transgene had abnormal locomotor arousal. The arousal abnormality in these strains can be attributed to the *npr-13(tm1504)* strain itself based on the strains' origin and the control strains comparisons. First, we built the optogenetic strain (*npr-13(tm1504);lite-1(ce314) ljIs114*) using the same *npr-13(tm1504)* strain. Second, both *npr-13* partial deletion strains (with and without the transgene) showed a response with the same trend when compared to their respective control strain. Based on this, our data suggests that the defect in arousal originates from the *npr-13(tm1504)* strain itself.

The role of *npr-13* in tap-evoked hyperactivity can be more confidently deduced, if the *npr-*13 knockout mutant showed the same defective arousal phenotype. Surprisingly, the *npr-13 KO* mutant had an arousal response that was almost identical to wild type. This strain was sequenced for the complete gene deletion and backcrossed twice. Therefore, based on the substantial difference in responses between the partial deletion and knockout mutant, we can not conclude that *npr-13* is required for tap-evoked locomotor arousal.

To shed more light on what is causing the arousal defect in the *npr-13(tm1504)* strain, its complete genome can be sequenced. By sequencing this strain's genome, we might be able to find the mutation in the background that is responsible for the observed phenotype.

2. Oxygen-sensing circuit might involve *flp-7* but not *npr-13*

C. elegans perceive atmospheric oxygen levels (21%) as an aversive cue. This cue elicits a locomotor escape response that may last until oxygen levels are optimal again. Based on the CenGen sc-RNA-sequencing database (Taylor *et al.*, 2021), the *flp-7* gene is expected to be expressed in the three main oxygen sensing neurons, AQR, PQR, and URX. From the expected 102 neuronal cells to be expressing the *flp-7* gene, AQR is among the top ten neurons showing most abundant expression.

The neuropeptide receptor *npr-13* is also expressed in neurons that have been implicated with oxygen-evoked responses, however at much lower levels compared with *flp-7*. Using the same expression level threshold, *npr-13* is expected to be expressed in SDQ, RMG, and ADL neurons (Taylor *et al.*, 2021). Compared to the expression levels of the neuropeptides encoding genes in the CenGen database, the detected neuropeptide receptor-encoding genes

had limited expression with the exception of a few genes (Taylor *et al.*, 2021). This explains the multiple fold difference in the expression levels of FLP-7 and NPR-13 encoding genes.

The expression pattern reported by CenGen made *flp-7* and *npr-13* strong candidates for potential roles in the *C. elegans'* oxygen-sensing circuit. Therefore, to test whether *flp-7* or *npr-13* may be involved in hyperoxia-evoked responses, they were tracked while exposed to favorable (7%) and threatening (21%) oxygen levels (as described in section 2.4.1. of *Materials and Methods*).

2.1 *flp-7* might be a repressor of hyperoxia avoidance responses

Our data demonstrates that the neuropeptide *flp-7* is involved in oxygen-evoked escape responses to hyperoxia (Fig. 16). When *flp-7* mutant worms were exposed to a 7-21% rise in oxygen levels, a shift in their behavioral state was observed. The increase in oxygen levels elicited a change in locomotor activity observed as a sustained increase in speed that drops back to baseline at 7% oxygen concentration. Considering that this partial mutant strain originates from a wild-type N2 strain, it has an *npr-1* gain-of-function allele. Based on these results, *flp-7* could act as a repressor of the oxygen-sensing circuit as the effect of the *npr-1* gain-of-function seems to be overridden in the *flp-7* mutants. To further investigate this effect, experiments at the level and downstream of *npr-1* regulation need to be done. Possible interactions between *npr-1* and *flp-7* can be elucidated by using ligand-receptor pair screenings. On the circuit level, whether *flp-7* and *npr-1* affect the same pathway, can be investigated by generating double mutants and performing aerotaxis assays. If their phenotypic effect is not additive, then *flp-7* and *npr-1* might be modulating the same hyperoxia-induced escape response. Also, using cell-specific reporters, ablating techniques, and rescue experiments would shed more light on the cellular secretion of *flp-7*.

Based on our results, *flp-7* mutants showed almost normal levels of acceleration after tap delivery. Considering that these worms were grown and maintained in ambient oxygen conditions, it is plausible that these growth conditions have affected their responses to tap stimulation. To assess whether this might be the case, *flp-7* mutants cultured at favorable 7% oxygen levels should be assayed and compared to worms maintained at 21% oxygen concentration.

Besides the escape response, *flp-7* might be involved in the crosstalk between the oxygen sensory circuit and gut metabolism. *flp-7* induces intestinal fat loss by interacting with its receptor *npr-22* leading to the transcriptional activation of a lipolytic enzyme called ATGL-1 (Palamiuc *et al.*, 2017). In *C. elegans*, fat oxidation has been shown to be stimulated by the oxygen sensors URX (Witham *et al.*, 2016). Witham *et al.* (2016) proposed a neuroendocrine axis that involves the regulation of intestinal fat storage based on the availability of oxygen.

The environment's oxygen levels serve as an indication of food availability. The availability of bacteria, *C. elegans'* main food source, drops the local oxygen concentration due to bacterial respiration. A higher concentration of oxygen indicates low or depleted food and vice versa. In a model according to Witham *et al.* (2016), the activity level of the URX neurons depends on the integration of both internal fat reserve and external oxygen cues. When the food source is depleted and oxygen levels are high (21%), *gcy-36* becomes very active. Under these conditions, the intestine sends a fat sufficiency signal mediated by the activation of GPA-6. Eventually, URX activation leads to fat loss in the intestine as long as the fat stores are not depleted. This crosstalk ensures that fat is metabolized for energy only in the absence of food and the availability of fat reserve.

In *C. elegans*, the gut is not directly innervated by the nervous system; neuroendocrine modulators are needed to relay the information between the two sites (Witham *et al.*, 2016). This model combined with the expected expression pattern of *flp-7* and its role in fat oxidation, make *flp-7* a potential neuroendocrine signal between URX and the gut.

To fully decipher *flp-7*'s role in oxygen-evoked responses and potentially a neuroendocrine axis that relays oxygen availability to the gut, more research is needed. This includes assaying *flp-7* knockout mutants, cell-specific knockdowns, neuronal activity recordings, and measurements of fat content. In addition, to understand the neural mechanism by which *flp-7* mediates its modulatory effects, its receptor(s) need to be identified and assayed. This includes assaying the cognate receptor candidate *dmsr-7* which was discovered to interact with *flp-7* in a cell culture-based *in vitro* screen done in the host lab (Unpublished data from Isabel Beets). Also, the neuropeptide receptor *npr-22* which mediates *flp-7* fat loss signal should be assayed (Palamiuc *et al.*, 2017).

2.2 *npr-13* may not be involved in oxygen-elicited escape responses

The *npr-13 KO* strain had a similar oxygen response pattern to the wild type. Although our data suggests an increase in average speed at 21% oxygen compared to 7% oxygen levels, this data is based on three trials. More trials need to be conducted to confirm the significance of this speed increase. Nonetheless, based on our current data, *npr-13* might not affect the avoidance response in hyperoxic conditions as a negative regulator. To better understand the function of *npr-13* in oxygen-related responses, more experiments (like reversing rate) need to be conducted. These effects would be very hard to detect with the *npr-1* gain-of-function background these mutants have. Aerotaxis assays with *npr-1* and *npr-13* double mutants may shed more light on the role of *npr-13* in the oxygen sensing circuit. Additionally, *npr-13* might modulate non-oxygen related activities of the oxygen-implicated neurons SDQ, RMG, and ADL. This is yet to be studied.

The cognate ligands of *npr-13* are yet to be discovered. Deorphanizing *npr-13* would help to better understand the roles this neuropeptide receptor might be involved in. Possible interaction partners along with localization experiments would shed more light on the function of *npr-13* in *C. elegans*.

Conclusion

Our work has contributed to elucidate potential roles of the neuropeptide *flp-7* and the neuropeptide receptor *npr-13* in arousal responses. In tap-evoked arousal, both candidates seemed not to be involved in the hyperactivity response. Based on the *npr-13* knockout behavioral responses, we were able to eliminate it as a candidate mediating responses in this arousal paradigm. However, since the *npr-13* partial deletion mutants showed a defective locomotor response, there might be a mutation in this strain's background that we do not know of yet. All data acquired using this strain can not be used to confidently assign a phenotype to the NPR-13 gene. To help explain the observed phenotype of the *npr-13(tm1504)* allele, its whole genome can be sequenced.

In oxygen-evoked escape responses, *flp-7* might play a role in repressing hyperoxia-induced hyperactivity. Further work is needed to investigate its secretion source, receptor, and cell targets in the oxygen-sensing circuit. Since all of our assayed strains were cultured at atmospheric oxygen levels, it would be interesting to perform the taps assay using *flp-7* mutants that have been maintained at 7% oxygen concentration.

Although *npr-13* CenGen expression data indicates that this neuropeptide receptor might be involved in the oxygen-sensing circuit, our assayed knockout mutant was insensitive to a 7-21% change in oxygen concentration. This does not exclude possible roles in promoting oxygen-evoked escape responses since this strain has an *npr-1* gain-of-function allele. This allele makes animals almost non-responsive to hyperoxic conditions. Therefore, generating an *npr-1;npr-13* double mutant might help uncover possible functions of *npr-13* in the oxygen circuit.

Finally, the roles of *npr-13* and *flp-7* in the ASH-dependent sensory sensitization pathway still need to be investigated. As described in the *Introduction* section 3.2.1, ASH neurons will be optogenetically activated using blue light with or without prior-tap stimulation. This will allow us to confirm the diminished average speeds portrayed by Chew, Tanizawa, *et al.* (2018) in *flp-7* and *npr-13* mutants. In addition, investigating possible interactions between the afferent *flp-20/frpr-3* pathway and our candidates will help delineate the underlying circuitry mediating arousal and sensitization in *C. elegans*.

This project further highlights the role of neuropeptidergic signaling in altering behavioral states in *C. elegans*. It also sheds the light on the dearth of knowledge in the functions of the *C. elegans'* large neuropeptide repertoire. Follow-up experiments for both candidate genes will help further conclude their implications in arousal.

References

1. Cited webpages

WormBase: www.wormbase.org

CenGen: www.cengen.org

Biorender: www.biorender.com

2. Bibliography

Ahnaou, A., & Drinkenburg, W. H. I. M. (2011). Neuromedin U2 receptor signaling mediates alteration of sleep–wake architecture in rats. *Neuropeptides*, *45*(2), 165–174. https://doi.org/10.1016/J.NPEP.2011.01.004

Alcedo, J., & Prahlad, V. (2020). Neuromodulators: an essential part of survival. *Journal of Neurogenetics*, *34*(3–4), 475–481. https://doi.org/10.1080/01677063.2020.1839066

Allen, E., Ren, J., Zhang, Y., Alcedo, J., & Biology, E. (2015). Sensory systems: their impact on *C. elegans* survival. *Neuroscience*, *18*(296), 15–25. https://doi.org/10.1016/j.neuroscience.2014.06.054.Sensory

Altun, Z.F. and Hall, D.H. (2011). Nervous system, general description. In *WormAtlas*. doi:10.3908/wormatlas.1.18

Anderson, J. L., Morran, L. T., & Phillips, P. C. (2010). Outcrossing and the Maintenance of Males within *C. elegans* Populations. *Journal of Heredity*, *101*(Suppl 1), S62–S74. https://doi.org/10.1093/JHERED/ESQ003

Ardiel, E. L., Yu, A. J., Giles, A. C., & Rankin, C. H. (2017). Habituation as an adaptive shift in response strategy mediated by neuropeptides. *Npj Science of Learning*, *2*(9). https://doi.org/10.1038/s41539-017-0011-8

Arribere, J. A., Bell, R. T., Fu, B. X. H., Artiles, K. L., Hartman, P. S., & Fire, A. Z. (2014). Efficient marker-free recovery of custom genetic modifications with CRISPR/Cas9 in *Caenorhabditis elegans*. *Genetics*, *198*(3), 837–846. https://doi.org/10.1534/GENETICS.114.169730/-/DC1

Asahina, K., Watanabe, K., Duistermars, B. J., Hoopfer, E., González, C. R., Eyjólfsdóttir, E. A., Perona, P., & Anderson, D. J. (2014). Tachykinin-expressing neurons control male-specific aggressive arousal in drosophila. *Cell*, *156*(1–2), 221–235. https://doi.org/10.1016/j.cell.2013.11.045

Babcock, D. T., Landry, C., & Galko, M. J. (2009). Cytokine Signaling Mediates UV-Induced Nociceptive Sensitization in Drosophila Larvae. *Current Biology*, *19*(10), 799–806. https://doi.org/10.1016/j.cub.2009.03.062

Bargmann, C. I., Hartwieg, E., & Horvitz, H. R. (1993). Odorant-selective genes and neurons mediate olfaction in *C. elegans*. *Cell*, *74*(3), 515–527. https://doi.org/10.1016/0092-8674(93)80053-H

Bargmann, C.I. Chemosensation in *C. elegans* (2006), *WormBook*, ed. The *C. elegans* Research Community, WormBook, doi/10.1895/wormbook.1.123.1, http://www.wormbook.org

Bentley, B., Branicky, R., Barnes, C. L., Chew, Y. L., Yemini, E., Bullmore, E. T., Vértes, P. E., & Schafer, W. R. (2016). The Multilayer Connectome of *Caenorhabditis elegans*. In *PLoS Computational Biology* (Vol. 12, Issue 12). https://doi.org/10.1371/journal.pcbi.1005283

Bounoutas, A., & Chalfie, M. (2007). Touch sensitivity in *Caenorhabditis elegans*. *Pflugers Archiv European Journal of Physiology*, *454*(5), 691–702. https://doi.org/10.1007/S00424-006-0187-X/FIGURES/4

Bozorgmehr, T., Ardiel, E. L., McEwan, A. H., & Rankin, C. H. (2013). Mechanisms of plasticity in a *Caenorhabditis elegans* mechanosensory circuit. *Frontiers in Physiology*, *4*(88). https://doi.org/10.3389/FPHYS.2013.00088/BIBTEX

Branch, A. F., Navidi, W., Tabuchi, S., Terao, A., Yamanaka, A., Scammell, T. E., & Behn, C. D. (2016). Progressive Loss of the orexin neurons reveals dual effects on wakefulness. *Sleep*, *39*(2), 369–377. https://doi.org/10.5665/sleep.5446

Brenner, S. (1974). The Genetics of *Caenorhabditis elegans*. *Genetics*, *77*, 71–94.

Bretscher, A. J., Kodama-Namba, E., Busch, K. E., Murphy, R. J., Soltesz, Z., Laurent, P., & de Bono, M. (2011). Temperature, Oxygen, and Salt-Sensing Neurons in *C. elegans* Are Carbon Dioxide Sensors that Control Avoidance Behavior. *Neuron*, *69*(6), 1099–1113. https://doi.org/10.1016/J.NEURON.2011.02.023

Burbach, J. P. H. (2011). What Are Neuropeptides? *Methods in Molecular Biology*, *789*, 1–36. https://doi.org/10.1007/978-1-61779-310-3_1

Burnett, C., Valentini, S., Cabreiro, F., Goss, M., Somogyvári, M., Piper, M. D., Hoddinott, M., Sutphin, G. L., Leko, V., McElwee, J. J., Vazquez-Manrique, R. P., Orfila, A. M., Ackerman, D., Au, C., Vinti, G., Riesen, M., Howard, K., Neri, C., Bedalov, A., … Gems, D.

(2011). Absence of effects of Sir2 overexpression on lifespan in *C. elegans* and Drosophila. *Nature*, *477*(7365), 482–485. https://doi.org/10.1038/nature10296

Busch, K. E., Laurent, P., Soltesz, Z., Murphy, R. J., Faivre, O., Hedwig, B., Thomas, M., Smith, H. L., & De Bono, M. (2012). Tonic signaling from O2 sensors sets neural circuit activity and behavioral state. *Nature Neuroscience*, *15*(4), 581–591. https://doi.org/10.1038/nn.3061

C. elegans Sequencing Consortium (1998). Genome sequence of the nematode *C. elegans*: a platform for investigating biology. *Science*, *282*(5396), 2012–2018. https://doi.org/10.1126/science.282.5396.2012

Carew, T. J., Castellucci, V. F., & Kandel, E. R. (1971). An analysis of dishabituation and sensitization of the gill-withdrawal reflex in *aplysia*. *International Journal of Neuroscience*, *2*(2), 79–98. https://doi.org/10.3109/00207457109146995

Chalfie, M., & Thomson, J. N. (1979). Organization of neuronal microtubules in the nematode *Caenorhabditis elegans*. *Journal of Cell Biology*, *82*(1), 278–289. https://doi.org/10.1083/jcb.82.1.278

Chalfie, M., Sulston, J. E., White, J. G., Southgate, E., Thomson, J. N., & Brenner, S. (1985). The Neural Circuit for Touch Sensitivity in *Caenorhabditis*. *Journal of Neuroscience*, *5*(4), 956–964.

Chang, A. J., Chronis, N., Karow, D. S., Marletta, M. A., & Bargmann, C. I. (2006). A Distributed Chemosensory Circuit for Oxygen Preference in *C. elegans*. *PLOS Biology*, *4*(9), e274. https://doi.org/10.1371/JOURNAL.PBIO.0040274

Chang, Y. J., Burton, T., Ha, L., Huang, Z., Olajubelo, A., & Li, C. (2015). Modulation of locomotion and reproduction by FLP neuropeptides in the nematode *Caenorhabditis elegans*. *PLoS ONE*, *10*(9), 1–16. https://doi.org/10.1371/journal.pone.0135164

Chen & Chalfie, M. (2014). Modulation of *C. elegans* Touch Sensitivity Is Integrated at Multiple Levels. *The Journal of Neuroscience*, *34*(19), 6522–6536. https://doi.org/10.1523/JNEUROSCI.0022-14.2014

Chew, Y. L., Tanizawa, Y., Cho, Y., Zhao, B., Yu, A. J., Ardiel, E. L., Rabinowitch, I., Bai, J., Rankin, C. H., Lu, H., Beets, I., & Schafer, W. R. (2018). An Afferent Neuropeptide System Transmits Mechanosensory Signals Triggering Sensitization and Arousal in *C. elegans*. *Neuron*, *99*(6), 1233-1246.e6. https://doi.org/10.1016/j.neuron.2018.08.003

Chiba, C. M., & Rankin, C. H. (1990). A Developmental Analysis of Spontaneous and Reflexive Reversals in the Nematode *Caenorhabditis elegans*. *Journal of Neurobiology*, *21*(4), 543–554. https://doi.org/10.1002/neu.480210403

Chiu, C. N., Rihel, J., Lee, D. A., Singh, C., Mosser, E. A., Chen, S., Sapin, V., Pham, U., Engle, J., Niles, B. J., Montz, C. J., Chakravarthy, S., Zimmerman, S., Salehi-Ashtiani, K., Vidal, M., Schier, A. F., & Prober, D. A. (2016). A Zebrafish Genetic Screen Identifies Neuromedin U as a Regulator of Sleep/Wake States. *Neuron*, *89*(4), 842–856. https://doi.org/10.1016/j.neuron.2016.01.007

Coates, J. C., & De Bono, M. (2002). Antagonistic pathways in neurons exposed to body fluid regulate social feeding in *Caenorhabditis elegans*. *Nature*, *419*(6910), 925–929. https://doi.org/10.1038/nature01170

Cook, S. J., Jarrell, T. A., Brittin, C. A., Wang, Y., Bloniarz, A. E., Yakovlev, M. A., Nguyen, K. C. Q., Tang, L. T. H., Bayer, E. A., Duerr, J. S., Bülow, H. E., Hobert, O., Hall, D. H., & Emmons, S. W. (2019). Whole-animal connectomes of both *Caenorhabditis elegans* sexes. *Nature*, *571*(7763), 63–71. https://doi.org/10.1038/s41586-019-1352-7

Corsi, A. K., Wightman, B., & Chalfie, M. (2015). A Transparent Window into Biology: A Primer on *Caenorhabditis elegans*. *Genetics*, *200*(2), 387–407. https://doi.org/10.1534/GENETICS.115.176099

Couillault, C., Pujol, N., Reboul, J., Sabatier, L., Guichou, J. F., Kohara, Y., & Ewbank, J. J. (2004). TLR-independent control of innate immunity in *Caenorhabditis elegans* by the TIR domain adaptor protein TIR-1, an ortholog of human SARM. *Nature Immunology*, *5*(5), 488–494. https://doi.org/10.1038/ni1060

Croll, N. A. (1975). Components and patterns in the behaviour of the nematode *Caenorhabditis elegans*. *Journal of Zoology*, *176*(2), 159–176. https://doi.org/10.1111/j.1469-7998.1975.tb03191.x

De Bono, M., & Bargmann, C. I. (1998). Natural Variation in a Neuropeptide Y Receptor Homolog Modifies Social Behavior and Food Response in *C. elegans*. *Cell*, *94*(5), 679–689. https://doi.org/10.1016/S0092-8674(00)81609-8

Diao, F., Elliott, A. D., Diao, F., Shah, S., & White, B. H. (2017). Neuromodulatory connectivity defines the structure of a behavioral neural network. *ELife*, *6*, e29797. https://doi.org/10.7554/ELIFE.29797

Dickinson, D. J., & Goldstein, B. (2016). CRISPR-Based Methods for *Caenorhabditis elegans* Genome Engineering. *Genetics*, *202*(3), 885–901. https://doi.org/10.1534/GENETICS.115.182162

Dieringer, N., Koester, J., & Weiss, K. R. (1978). Adaptive changes in heart rate of *Aplysia californica*. *Journal of Comparative Physiology, A*, *123*(1), 11–21. https://doi.org/10.1007/BF00657339

Edwards, S. L., Charlie, N. K., Milfort, M. C., Brown, B. S., Gravlin, C. N., Knecht, J. E., & Miller, K. G. (2008). A Novel Molecular Solution for Ultraviolet Light Detection in *Caenorhabditis elegans*. *PLOS Biology*, *6*(8), e198. https://doi.org/10.1371/JOURNAL.PBIO.0060198

Fernandes de Abreu, D. A., Caballero, A., Fardel, P., Stroustrup, N., Chen, Z., Lee, K. H., Keyes, W. D., Nash, Z. M., López-Moyado, I. F., Vaggi, F., Cornils, A., Regenass, M., Neagu, A., Ostojic, I., Liu, C., Cho, Y., Sifoglu, D., Shen, Y., Fontana, W., … Ch'ng, Q. L. (2014). An Insulin-to-Insulin Regulatory Network Orchestrates Phenotypic Specificity in Development and Physiology. *PLOS Genetics*, *10*(3), e1004225. https://doi.org/10.1371/JOURNAL.PGEN.1004225

Frooninckx, L., Rompay, L. Van, Temmerman, L., Sinay, E. Van, Beets, I., Janssen, T., Husson, S. J., & Schoofs, L. (2012). Neuropeptide GPCRs in *C. elegans*. *Frontiers in Endocrinology*, *3*, 1–18. https://doi.org/10.3389/fendo.2012.00167

Gabel, C. V, Gabel, H., Pavlichin, D., Kao, A., Clark, D. A., & Samuel, A. D. T. (2007). Neural Circuits Mediate Electrosensory Behavior in *Caenorhabditis elegans*. *The Journal of Neuroscience*, *27*(28), 7586–7596. https://doi.org/10.1523/JNEUROSCI.0775-07.2007

Garey, J., Goodwillie, A., Frohlich, J., Morgan, M., Gustafsson, J. A., Smithies, O., Korach, K. S., Ogawa, S., & Pfaff, D. W. (2003). Genetic contributions to generalized arousal of brain and behavior. *Proceedings of the National Academy of Sciences of the United States of America*, *100*(19), 11019–11022. https://doi.org/10.1073/pnas.1633773100

Gold, M. S., & Gebhart, G. F. (2010). Nociceptor sensitization in pain pathogenesis. *Nature Medicine*, *16*(11), 1248–1257. https://doi.org/10.1038/nm.2235

Gong, J., Yuan, Y., Ward, A., Kang, L., Zhang, B., Wu, Z., Peng, J., Feng, Z., Liu, J., & Xu, X. Z. S. (2016). The *C. elegans* Taste Receptor Homolog LITE-1 Is a Photoreceptor. *Cell*, *167*(5), 1252–1263. https://doi.org/10.1016/J.CELL.2016.10.053

Goodman, M. B., Ernstrom, G. G., Chelur, D. S., O'Hagan, R., Yao, C. A., & Chalfie, M. (2002). MEC-2 regulates *C. elegans* DEG/ENaC channels needed for mechanosensation. *Nature*, *415*(6875), 1039–1042. https://doi.org/10.1038/4151039a

Govindaraju, S. R., Curry, B. D., Bain, J. L. W., & Riley, D. A. (2006). Comparison of continuous and intermittent vibration effects on rat-tail artery and nerve. *Muscle and Nerve*, *34*(2), 197–204. https://doi.org/10.1002/MUS.20578/FORMAT/PDF

Gray, J. M., Karow, D. S., Lu, H., Chang, A. J., Chang, J. S., Ellis, R. E., Marletta, M. A., & Bargmann, C. I. (2004). Oxygen sensation and social feeding mediated by a *C. elegans* guanylate cyclase homologue. *Nature*, *430*(6997), 317–322. https://doi.org/10.1038/nature02714

Hammarlund, M., Watanabe, S., Schuske, K., & Jorgensen, E. M. (2008). CAPS and syntaxin dock dense core vesicles to the plasma membrane in neurons. *Journal of Cell Biology*, *180*(3), 483–491. https://doi.org/10.1083/JCB.200708018

Hilliard, M. A., Apicella, A. J., Kerr, R., Suzuki, H., Bazzicalupo, P., & Schafer, W. R. (2005). In vivo imaging of *C. elegans* ASH neurons: cellular response and adaptation to chemical repellents. *The EMBO Journal*, *24*(1), 63–72. https://doi.org/10.1038/SJ.EMBOJ.7600493

Hodgkin, J. (1983). Male Phenotypes and Mating Efficiency in *Caenorhabditis elegans*. *Genetics*, *103*(1), 43–64. https://doi.org/10.1093/genetics/103.1.43

Hubbard, C. S., Ornitz, E., Gaspar, J. X., Smith, S., Amin, J., Labus, J. S., Kilpatrick, L. A., Rhudy, J. L., Mayer, E. A., & Naliboff, B. D. (2011). Modulation of nociceptive and acoustic startle responses to an unpredictable threat in men and women. *PAIN®*, *152*(7), 1632–1640. https://doi.org/10.1016/J.PAIN.2011.03.001

Husson, S. J., Clynen, E., Baggerman, G., Janssen, T., & Schoofs, L. (2006). Defective processing of neuropeptide precursors in *Caenorhabditis elegans* lacking proprotein convertase 2 (KPC-2/EGL-3): Mutant analysis by mass spectrometry. *Journal of Neurochemistry*, *98*(6), 1999–2012. https://doi.org/10.1111/J.1471-4159.2006.04014.X/FORMAT/PDF

Iannacone, M. J., Beets, I., Lopes, L. E., Churgin, M. A., Fang-Yen, C., Nelson, M. D., Schoofs, L., & Raizen, D. M. (2017). The RFamide receptor DMSR-1 regulates stress-induced sleep in *C. elegans*. *ELife*, *6*, 1–20. https://doi.org/10.7554/eLife.19837

Iliff, A. J., Wang, C., Ronan, E. A., Hake, A. E., Guo, Y., Li, X., Zhang, X., Zheng, M., Liu, J., Grosh, K., Duncan, R. K., & Xu, X. Z. S. (2021). The nematode *C. elegans* senses airborne sound. *Neuron*, *109*(22), 3633–3646. https://doi.org/10.1016/J.NEURON.2021.08.035

Im, S. H., Takle, K., Jo, J., Babcock, D. T., Ma, Z., Xiang, Y., & Galko, M. J. (2015). Tachykinin acts upstream of autocrine Hedgehog signaling during nociceptive sensitization in Drosophila. *ELife*, *4*(NOVEMBER2015), 1–27. https://doi.org/10.7554/eLife.10735

Jacob, T. C., & Kaplan, J. M. (2003). The EGL-21 Carboxypeptidase E Facilitates Acetylcholine Release at *Caenorhabditis elegans* Neuromuscular Junctions. *The Journal of Neuroscience*, *23*(6), 2122–2130. https://doi.org/10.1523/JNEUROSCI.23-06-02122.2003

Jarrell, T. A., Wang, Y., Bloniarz, A. E., Brittin, C. A., Xu, M., Thomson, J. N., Albertson, D. G., Hall, D. H., & Emmons, S. W. (2012). The connectome of a decision-making neural network. *Science*, *337*(6093), 437–444. https://doi.org/10.1126/SCIENCE.1221762/SUPPL_FILE/1221762S1.MOV

Javer, A., Currie, M., Lee, C. W., Hokanson, J., Li, K., Martineau, C. N., Yemini, E., Grundy, L. J., Li, C., Ch'ng, Q. L., Schafer, W. R., Nollen, E. A. A., Kerr, R., & Brown, A. E. X. (2018). An open-source platform for analyzing and sharing worm-behavior data. *Nature Methods*, *15*(9), 645–646. https://doi.org/10.1038/s41592-018-0112-1

Jinek, M., Chylinski, K., Fonfara, I., Hauer, M., Doudna, J. A., & Charpentier, E. (2012). A programmable dual-RNA-guided DNA endonuclease in adaptive bacterial immunity. *Science*, *337*(6096), 816–821. https://doi.org/10.1126/SCIENCE.1225829/SUPPL_FILE/JINEK.SM.PDF

Jones, B. E. (2020). Arousal and sleep circuits. *Neuropsychopharmacology*, *45*, 6–20. https://doi.org/10.1038/s41386-019-0444-2

Kim, W., Underwood, R. S., Greenwald, I., & Shaye, D. D. (2018). OrthoList 2: A New Comparative Genomic Analysis of Human and *Caenorhabditis elegans* Genes. *Genetics*, *210*(2), 445–461. https://doi.org/10.1534/GENETICS.118.301307

Koch, U. T., & Koester, J. (1982). Time sharing of heart power: Cardiovascular adaptations to food-arousal in *Aplysia*. *Journal of Comparative Physiology, B*, *149*(1), 31–42. https://doi.org/10.1007/BF00735712

Laurent, P., Soltesz, Z., Nelson, G., Chen, C., Arellano-Carbajal, F., Levy, E., & de Bono, M. (2015). Decoding a neural circuit controlling global animal state in *C. elegans*. *ELife*, *2015*(4), 1–39. https://doi.org/10.7554/eLife.04241

Lebestky, T., Chang, J. S. C., Dankert, H., Zelnik, L., Kim, Y. C., Han, K. A., Wolf, F. W., Perona, P., & Anderson, D. J. (2009). Two Different Forms of Arousal in Drosophila Are Oppositely Regulated by the Dopamine D1 Receptor Ortholog DopR via Distinct Neural Circuits. *Neuron*, *64*(4), 522–536. https://doi.org/10.1016/j.neuron.2009.09.031

Li, C. (2005). The ever-expanding neuropeptide gene families in the nematode *Caenorhabditis elegans*. *Parasitology*, *131*, S109–S127. https://doi.org/10.1017/S0031182005009376

Li, C. and Kim, K. Neuropeptides (2008), WormBook, ed. The *C. elegans* Research Community, WormBook, doi/10.1895/wormbook.1.142.1, http://www.wormbook.org.

Li, C., & Kim, K. (2014). Family of FLP peptides in *Caenorhabditis elegans* and related nematodes. *Frontiers in Endocrinology*, *5*(OCT), 1–16. https://doi.org/10.3389/fendo.2014.00150

Libersat, F., & Pflueger, H. J. (2004). Monoamines and the Orchestration of Behavior. *BioScience*, *54*(1), 17–25. https://doi.org/10.1641/0006-3568(2004)054[0017:MATOOB]2.0.CO;2

Lim, M. A., Chitturi, J., Laskova, V., Meng, J., Findeis, D., Wiekenberg, A., Mulcahy, B., Luo, L., Li, Y., Lu, Y., Hung, W., Qu, Y., Ho, C. Y., Holmyard, D., Ji, N., McWhirter, R., Samuel, A. D. T., Miller, D. M., Schnabel, R., … Zhen, M. (2016). Neuroendocrine modulation sustains the *C. elegans* forward motor state. *ELife*, *5*(e19887). https://doi.org/10.7554/ELIFE.19887

Lingueglia Eric, Champigny Guy, Lazdunski Michel, B. P. (1995). Cloning of the amiloride-sensitive FMRFamide peptide-gated sodium channel. *Nature*, *378*, 730–733.

Littlejohn, N. K., Seban, N., Liu, C. C., & Srinivasan, S. (2020). A feedback loop governs the relationship between lipid metabolism and longevity. *ELife*, *9*(e58815). https://doi.org/10.7554/ELIFE.58815

Matsunaga, Y., Iwasaki, T., & Kawano, T. (2017). Diverse insulin-like peptides in *Caenorhabditis elegans*. *International Biology Review*, *1*(1). https://doi.org/10.18103/IBR.V1I1.1276

Maulik, M., Mitra, S., Bult-Ito, A., Taylor, B. E., & Vayndorf, E. M. (2017). Behavioral phenotyping and pathological indicators of Parkinson's disease in *C. elegans* models. *Frontiers in Genetics*, *8*, 77. https://doi.org/10.3389/FGENE.2017.00077/BIBTEX

Metaxakis, A., Petratou, D., & Tavernarakis, N. (2018). Multimodal sensory processing in *Caenorhabditis elegans*. *Open Biology*, *8*(180049). https://doi.org/10.1098/rsob.180049

Mochizuki, T., Crocker, A., Mccormack, S., Yanagisawa, M., Sakurai, T., & Scammell, T. E. (2004). Behavioral State Instability in Orexin Knock-Out Mice. *The Journal of Neuroscience*, *24*(28), 6291–6300. https://doi.org/10.1523/JNEUROSCI.0586-04.2004

Moroz, L. L. (2011). *Aplysia*. *Current Biology*, *21*(2), 60–61. https://doi.org/10.1016/j.cub.2010.11.028

Munk, C., Isberg, V., Mordalski, S., Harpsøe, K., Rataj, K., Hauser, A. S., Kolb, P., Bojarski, A. J., Vriend, G., & Gloriam, D. E. (2016). GPCRdb: the G protein-coupled receptor database – an introduction. *British Journal of Pharmacology*, *173*(14), 2195–2207. https://doi.org/10.1111/BPH.13509

Muschamp, J. W., Dominguez, J. M., Sato, S. M., Shen, R. Y., & Hull, E. M. (2007). A role for hypocretin (orexin) in male sexual behavior. *Journal of Neuroscience*, *27*(11), 2837–2845. https://doi.org/10.1523/JNEUROSCI.4121-06.2007

Nagel, G., Brauner, M., Liewald, J. F., Adeishvili, N., Bamberg, E., & Gottschalk, A. (2005). Light Activation of Channelrhodopsin-2 in Excitable Cells of *Caenorhabditis elegans* Triggers Rapid Behavioral Responses. *Current Biology*, *15*(24), 2279–2284. https://doi.org/10.1016/J.CUB.2005.11.032

Nagel, G., Szellas, T., Huhn, W., Kateriya, S., Adeishvili, N., Berthold, P., Ollig, D., Hegemann, P., & Bamberg, E. (2003). Channelrhodopsin-2, a directly light-gated cation-selective membrane channel. *Proceedings of the National Academy of Sciences of the United States of America*, *100*(24), 13940–13945. https://doi.org/10.1073/PNAS.1936192100/SUPPL_FILE/6192FIG5B.PDF

Nath, R. D., Chow, E. S., Wang, H., Schwarz, E. M., & Sternberg, P. W. (2016). *C. elegans* stress-induced sleep emerges from the collective action of multiple neuropeptides. *Current Biology*, *26*(18), 2446. https://doi.org/10.1016/J.CUB.2016.07.048

Nigon, V.M., and Félix, M.A. (2017). History of research on *C. elegans* and other free-living nematodes as model organisms., WormBook, ed. The *C. elegans* Research Community, WormBook, doi/10.1895/wormbook.1.181.1, http://www.wormbook.org

Nuttley, W. M., Harbinder, S., & Van der Kooy, D. (2001). Regulation of Distinct Attractive and Aversive Mechanisms Mediating Benzaldehyde Chemotaxis in *Caenorhabditis elegans*. *Learning & Memory*, *8*(3), 170–181. https://doi.org/10.1101/LM.36501

O'Hagan, R., Chalfie, M., & Goodman, M. B. (2004). The MEC-4 DEG/ENaC channel of *Caenorhabditis elegans* touch receptor neurons transduces mechanical signals. *Nature Neuroscience*, *8*(1), 43–50. https://doi.org/10.1038/nn1362

Palamiuc, L., Noble, T., Witham, E., Ratanpal, H., Vaughan, M., & Srinivasan, S. (2017). A tachykinin-like neuroendocrine signalling axis couples central serotonin action and nutrient sensing with peripheral lipid metabolism. *Nature Communications*, *8*(1), 1–14. https://doi.org/10.1038/ncomms14237

Peymen, K., Watteyne, J., Borghgraef, C., Van Sinay, E., Beets, I., & Schoofs, L. (2019). Myoinhibitory peptide signaling modulates aversive gustatory learning in *Caenorhabditis elegans*. *PLOS Genetics*, *15*(2), e1007945. https://doi.org/10.1371/JOURNAL.PGEN.1007945

Pfaff, D. (2006). Toward a Universal Theory of Brain Arousal in *Brain Arousal and Information Theory: Neural and Genetic Mechanisms* (pp. 1-25). Harvard University Press.

Pfaff, D., Ribeiro, A., Matthews, J., & Kow, L. M. (2008). Concepts and mechanisms of generalized central nervous system arousal. *Annals of the New York Academy of Sciences, 1129*, 11–25. https://doi.org/10.1196/annals.1417.019

Pierce-Shimomura, J. T., Morse, T. M., & Lockery, S. R. (1999). The Fundamental Role of Pirouettes in *Caenorhabditis elegans* Chemotaxis. *The Journal of Neuroscience*, *19*(21), 9557–9569.

Pocock, R., & Hobert, O. (2010). Hypoxia activates a latent circuit for processing gustatory information in *C. elegans*. *Nature Neuroscience*, *13*(5), 610–614. https://doi.org/10.1038/nn.2537

Prober, D. A., Rihel, J., Onah, A. A., Sung, R. J., & Schier, A. F. (2006). Hypocretin/orexin overexpression induces an insomnia-like phenotype in zebrafish. *Journal of Neuroscience*, *26*(51), 13400–13410. https://doi.org/10.1523/JNEUROSCI.4332-06.2006

Raizen, D. M., Zimmerman, J. E., Maycock, M. H., Ta, U. D., You, Y., Sundaram, M. V., & Pack, A. I. (2008). Lethargus is a *Caenorhabditis elegans* sleep-like state. *Nature*, *451*(31), 569–572. https://doi.org/10.1038/nature06535

Rankin, C. H., Beck, C. D. O., & Chiba, C. M. (1990). *Caenorhabditis elegans*: A new model system for the study of learning and memory. *Behavioural Brain Research*, *37*(1), 89–92. https://doi.org/10.1016/0166-4328(90)90074-O

Richmond, J. E., & Broadie, K. S. (2002). The synaptic vesicle cycle: exocytosis and endocytosis in *Drosophila* and *C. elegans*. *Current Opinion in Neurobiology*, *12*(5), 499–507. https://doi.org/10.1016/S0959-4388(02)00360-4

Rogers, C., Reale, V., Kim, K., Chatwin, H., Li, C., Evans, P., & De Bono, M. (2003). Inhibition of *Caenorhabditis elegans* social feeding by FMRFamide-related peptide activation of NPR-1. *Nature Neuroscience*, *6*(11), 1178–1185. https://doi.org/10.1038/nn1140

Russell, J., Vidal-Gadea, A. G., Makay, A., Lanam, C., & Pierce-Shimomura, J. T. (2014). Humidity sensation requires both mechanosensory and thermosensory pathways in *Caenorhabditis elegans*. *PNAS*, *111*(22), 8269–8274. https://doi.org/10.1073/pnas.1322512111

Sahbaie, P., Shi, X., Guo, T. Z., Qiao, Y., Yeomans, D. C., Kingery, W. S., & Clark, J. D. (2009). Role of Substance P Signaling in Enhanced Nociceptive Sensitization and Local Cytokine Production after Incision. *Pain*, *145*(3), 341–349. https://doi.org/10.1016/J.PAIN.2009.

Salio, C., Lossi, L., Ferrini, F., & Merighi, A. (2006). Neuropeptides as synaptic transmitters. *Cell and Tissue Research*, *326*(2), 583–598. https://doi.org/10.1007/S00441-006-0268-3

Shaw, Paul J., Cirelli Chiara, Greenspan J. Ralph, T. G. (2000). Correlates of Sleep and Waking in *Drosophila melanogaster*. *Science*, *287*(March), 1834–1837.

Sieburth, D., Madison, J. M., & Kaplan, J. M. (2006). PKC-1 regulates secretion of neuropeptides. *Nature Neuroscience*, *10*(1), 49–57. https://doi.org/10.1038/nn1810

Sorribes, A., Þorsteinsson, H., Arnardóttir, H., Jóhannesdóttir, I. Þ., Sigurgeirsson, B., Polavieja, G. G. de, & Karlsson, K. Æ. (2013). The ontogeny of sleep-wake cycles in zebrafish: a comparison to humans. Frontiers in Neural Circuits, 7(178). https://doi.org/10.3389/FNCIR.2013.00178

Steiner, D. F. (1998). The proprotein convertases. *Current Opinion in Chemical Biology*, *2*(1), 31–39. https://doi.org/10.1016/S1367-5931(98)80033-1

Sternberg, S. H., Redding, S., Jinek, M., Greene, E. C., & Doudna, J. A. (2014). DNA interrogation by the CRISPR RNA-guided endonuclease Cas9. *Nature*, *507*(7490), 62–67. https://doi.org/10.1038/nature13011

Stiernagle, T. (2006). Maintenance of *C. elegans*. In *WormBook : the online review of C. elegans biology* (pp. 1–11). https://doi.org/10.1895/WORMBOOK.1.101.1

Susswein, A. J., Weiss, K. R., & Kupfermann, I. (1978). The effects of food arousal on the latency of biting in *Aplysia*. *Journal of Comparative Physiology*, *123*(1), 31–41. https://doi.org/10.1007/BF00657341

Taylor, S. R., Santpere, G., Weinreb, A., Barrett, A., Reilly, M. B., Xu, C., Varol, E., Oikonomou, P., Glenwinkel, L., McWhirter, R., Poff, A., Basavaraju, M., Rafi, I., Yemini, E., Cook, S. J., Abrams, A., Vidal, B., Cros, C., Tavazoie, S., … Miller, D. M. (2021). Molecular topography of an entire nervous system. *Cell*, *184*(16), 4329-4347.e23. https://doi.org/10.1016/J.CELL.2021.06.023

Thacker, C., & Rose, A. M. (2000). A look at the *Caenorhabditis elegans* Kex2/Subtilisin-like proprotein convertase family. *BioEssays*, *22*(6), 545–553. https://doi.org/10.1002/(SICI)1521-1878(200006)22:6<545::AID-BIES7>3.0.CO;2-F

Tissenbaum, H. A., & Guarente, L. (2001). Increased dosage of a sir-2 gene extends lifespan in *Caenorhabditis elegans*. *Nature*, *410*(6825), 227–230. https://doi.org/10.1038/35065638

Tomioka, M., Adachi, T., Suzuki, H., Kunitomo, H., Schafer, W. R., & Iino, Y. (2006). The insulin/PI 3-kinase pathway regulates salt chemotaxis learning in *Caenorhabditis elegans*. *Neuron*, *51*(5), 613–625. https://doi.org/10.1016/J.NEURON.2006.07.024

Turek, M., Besseling, J., Spies, J.-P., König, S., & Bringmann, H. (2016). Sleep-active neuron specification and sleep induction require FLP-11 neuropeptides to systemically induce sleep. *ELife*, *5*, e12499. https://doi.org/10.7554/ELIFE.12499

Tyree, S. M., Borniger, J. C., & de Lecea, L. (2018). Hypocretin as a hub for arousal and motivation. *Frontiers in Neurology*, *9*, 1–16. https://doi.org/10.3389/fneur.2018.00413

Van Bael, S., Watteyne, J., Boonen, K., De Haes, W., Menschaert, G., Ringstad, N., Robert Horvitz, H., Schoofs, L., Husson, S. J., & Temmerman, L. (2018). Mass spectrometric evidence for neuropeptide-amidating enzymes in *Caenorhabditis elegans*. *Journal of Biological Chemistry*, *293*(16), 6052–6063. https://doi.org/10.1074/JBC.RA117.000731/ATTACHMENT/A9B0AAE7-C13E-49C3-B2BA-CC2CA7ADB4FE/MMC1.ZIP

Van Bael, S., Zels, S., Boonen, K., Beets, I., Schoofs, L., & Temmerman, L. (2018). A *Caenorhabditis elegans* Mass Spectrometric Resource for Neuropeptidomics. *Journal of the American Society for Mass Spectrometry*, *29*(5), 879–889. https://doi.org/10.1007/S13361-017-1856-Z/SUPPL_FILE/JS8B05803_SI_002.DOCX

Vidal-Gadea, A., Ward, K., Beron, C., Ghorashian, N., Gokce, S., Russell, J., Truong, N., Parikh, A., Gadea, O., Ben-Yakar, A., & Pierce-Shimomura, J. (2015). Magnetosensitive neurons mediate geomagnetic orientation in *Caenorhabditis elegans*. *ELife*, *4*(e07493). https://doi.org/10.7554/ELIFE.07493

Way, J. C., & Chalfie, M. (1989). The mec-3 gene of *Caenorhabditis elegans* requires its own product for maintained expression and is expressed in three neuronal cell types. *Genes and Development*, *3*, 1823–1833.

White, J. G., Southgate, E., Thomson, J. N., & Brenner, S. (1986). The structure of the nervous system of *Caenorhabditis elegans* (Vol. 314). https://pubmed.ncbi.nlm.nih.gov/22462104/

Wicks, S. R., & Rankin, C. H. (1995). Integration of Mechanosensory Stimuli in *Caenorhabditis elegans*. *The Journal of Neuroscience*, *15*(3), 2434–2444.

Wicks, S. R., Roehrig, C. J., & Rankin, C. H. (1996). A dynamic network simulation of the nematode tap withdrawal circuit: predictions concerning synaptic function using behavioral criteria. *The Journal of Neuroscience*, *16*(12), 4017–4031. https://doi.org/10.1523/JNEUROSCI.16-12-04017.1996

Witham, E., Comunian, C., Ratanpal, H., Skora, S., Zimmer, M., & Srinivasan, S. (2016). *C. elegans* Body Cavity Neurons Are Homeostatic Sensors that Integrate Fluctuations in Oxygen Availability and Internal Nutrient Reserves. *Cell Reports*, *14*(7), 1641–1654. https://doi.org/10.1016/J.CELREP.2016.01.052

Yemini, E., Jucikas, T., Grundy, L. J., Brown, A. E. X., & Schafer, W. R. (2013). A database of *Caenorhabditis elegans* behavioral phenotypes. *Nature Methods*, *10*(9), 877–879. https://doi.org/10.1038/nmeth.2560

Yemini, E., Lin, A., Nejatbakhsh, A., Varol, E., Sun, R., Mena, G. E., Samuel, A. D. T., Paninski, L., Venkatachalam, V., & Hobert, O. (2021). NeuroPAL: A Multicolor Atlas for Whole-Brain Neuronal Identification in *C. elegans*. *Cell*, *184*(1), 272-288.e11. https://doi.org/10.1016/j.cell.2020.12.012

Yokogawa, T., Hannan, M. C., & Burgess, H. A. (2012). The dorsal raphe modulates sensory responsiveness during arousal in zebrafish. *The Journal of Neuroscience*, *32*(43), 15205–15215. https://doi.org/10.1523/JNEUROSCI.1019-12.2012

Zheng, S., Chiu, H., Boudreau, J., Papanicolaou, T., Bendena, W., & Chin-Sang, I. (2018). A functional study of all 40 *Caenorhabditis elegans* insulin-like peptides. *The Journal of Biological Chemistry*, *293*(43), 16912–16922. https://doi.org/10.1074/JBC.RA118.004542

Witvliet, D., Mulcahy, B., Mitchell, J. K., Meirovitch, Y., Berger, D. R., Wu, Y., Liu, Y., Koh, W. X., Parvathala, R., Holmyard, D., Schalek, R. L., Shavit, N., Chisholm, A. D., Lichtman, J. W., Samuel, A. D. T., & Zhen, M. (2021). Connectomes across development reveal principles of brain maturation. *Nature*, *596*(7871), 257–261. https://doi.org/10.1038/s41586-021-03778-8

Appendices

1. Risk Analysis

The host lab in which experiments were conducted has a safety level of 1. During the experiments, exposure is limited to the non-pathogenic organisms, *E. coli* OP50 and *C. elegans*. Throughout this project, protective gear like gloves and a lab coat were used during experimental work. Following general lab rules and safety measures, food and drinks consumption and storing in the lab is forbidden. Moreover, hands are washed with soap and disinfected after leaving the lab area and lab coats are not allowed in rooms designated for storing and consuming food.

Volatile materials were handled under the laminar flow cabinet. Before using the flow cabinet, the cabinet, materials, and worn gloves are disinfected with 70% ethanol. Biohazardous waste is deposited in designated containers. Depending on the type of waste, a properly labeled jerrycan or plastic box is used for disposal. Lower risk solid biological waste is deposited in properly labeled cardboard boxes with a yellow liner plastic bag. In the case of reusable equipment, the autoclave is used for disinfection. The autoclave is started under supervision and proper protective gear like heat resistant gloves are used to handle autoclaved objects. Extra precautionary measures were taken when certain products are in use. These products are discussed in more detail below.

GelRed is a nucleic acid stain used as an alternative to ethidium bromide with risks that are still unclear. GelRed is only handled in the designated gel electrophoresis area where a specific lab coat is worn. All materials and equipment used in this area are not transferred out of this zone or used for other purposes in the lab. To avoid contamination, any objects or samples brought into this area remain there or are discarded in an appropriate biohazardous waste container. Physical contact must be avoided.

Calcium chloride ($CaCl_2$) is a severe eye irritant for which it is recommended to wear eye and face protection. In case of contact, rinse with water for few minutes.

Cholesterol should not be ingested or come in contact with skin or eyes. After skin, eye or mouth contact, it should be rinsed off with water thoroughly.

Acetic acid is highly flammable and can cause serious eye damage and skin burns. Protective gear should be worm when handled. In case of skin or eye contact, it should be rinsed off with plenty of water and a doctor should be consulted. If swallowed, rinse the mouth several times and call the poison center.

Disodium Ethylenediaminetetraacetic acid (EDTA) is very harmful when inhaled and is a skin and eye irritant. It should be handled under the flow cabinet or with a proper mask. It should be rinsed off thoroughly in case of contact.

Ethanol (EtOH) is highly flammable and can cause eye irritation upon contact. It should be stored in a tightly closed container away from heat or hot surfaces.

Hydrochloric acid (HCl) is extremely corrosive and can cause severe eye damage, skin burns, and respiratory irritation. It should be handled in a well-ventilated area or under the flow cabin. In case of contact, it should be rinsed off with water for several minutes.

2. Solutions and buffers

$CaCl_2$: Volume 200mL; Concentration 1M

1. Weigh 147g of $CaCl_2$ (147.01g/mol, Sigma-Aldrich) and add to a 500mL Duran bottle.
2. Add 200mL of Milli-Q water into the Duran bottle.
3. Swirl to mix well.
4. Autoclave the solution.
5. Under the laminar flow cabinets, aliquots of 50 mL in Falcon tubes (50mL) are prepared.

2xTY medium Broth: Volume 200mL

1. Weigh the following reagents:
    a. 3.2 g of Bactotryptone (Gibco)
    b. 2 g of Yeast extract (Sigma-Aldrich)
    c. 1 g of NaCl (58.44g/mol, Sigma-Aldrich)
2. Add the weighed reagents to a 500mL Duran bottle.
3. Add 200mL of AD water.
4. Swirl the bottle to mix the reagents with the water.
5. Autoclave the broth.

Cholesterol in ethanol: Volume 200mL; Concentration 5mg/mL

1. Weigh 1 g of Cholesterol (386.65g/mol, Sigma-Aldrich) and add to 500mL Duran bottle.
2. Add 200mL of 100% ethanol absolute (VWR Prolabo Chemicals).
3. Swirl to mix well.
4. Under the laminar flow cabinets, aliquots of 50mL in Falcon tubes (50mL) are prepared.

Worm Lysis buffer (PCR template buffer): Volume 100mL

1. Measure and combine the following reagents:
    a. 1mL of 1% Gelatin
    b. 5mL of KCl
    c. 0.25mL of 1M $MgCl_2$
    d. 1mL of 1M Tris in HCl (pH 8.3)
    e. 4.5mL of 10% NP-40
    f. 4.5mL of 10% Tween 20

2. Add 83.75mL of Milli-Q water to make a 100mL of lysis buffer.
3. Aliquot 100µL in PCR tubes.
4. Store in a box at -20°C.

$MgSO_4$: Volume 200mL; Concentration 1M

1. Weigh 49.3g of $MgSO_4$ (246.5g/mol, Supelco®) and add to a 500mL Duran bottle.
2. Fill up the Duran bottle with 200mL of Milli-Q water.
3. Swirl to mix well.
4. Autoclave the solution.
5. Under the laminar flow cabinets, aliquots of 50mL in Falcon tubes (50mL) are prepared.

Phosphate buffer: Volume 200mL; Concentration 1M

1. Weigh 21.77g of KH_2PO_4 (136.09g/mol, Sigma-Aldrich) and add to a 500mL Duran bottle.
2. Weigh 6.97g of K_2HPO_4 (174.18g/mol, VWR Prolabo Chemicals) and add to the same Duran bottle.
3. Add 200mL of Milli-Q water.
4. Swirl to mix well.
5. Autoclave the buffer.

TAE buffer (50x): Volume 1L

1. In a plastic bottle, weight and add the following reagents:
    a. 242g of Trizma base (121.14g/mol, Sigma-Aldrich)
    b. 18.61g of Disodium EDTA (372.24 g/mol, Sigma-Aldrich)
2. Add 700mL of AD water and place on stirrer until dissolved.
3. Add 57.1mL of acetic acid (60.05g/mol, Sigma-Aldrich) and swirl to homogenize.
4. Fill the bottle up to 1L with AD water.

Tris solution: Volume 100mL; Concentration 5mM; pH 7.5

1. Weigh 0.06g of Trizma Base (121.14g/mol, Sigma-Aldrich).
2. Dissolve in 60mL AD water.
3. While on stirrer, add HCl (36.46g/mol, Vel) to adjust the pH to 7.5.
4. Add AD water to reach 100mL.

3. CRISPR-Cas9 knockout mutants

The following are wild type and gene knockout sequences of both *flp-7* and *npr-13*. These mutants were generated using the CRISPR-Cas9 system as described in section 2.2 of *Materials and Methods*.

Repair template
PAM sequence
Exon

Wild type *flp-7*

TTTTTGACTTTTCAACTTTTCTCCTCATTTTTTCTCGATTGAAATTTCAATTTTTAA
ACCACTCCGCGTCATGTTTGGAAACATGACGTCATCGAAAAATACCATCTCGTTT
TCATTCAAAGACTTTTAGAAATGCTTGGATCCCGCTTCCTTCTTCTTGCTCTTGGT
CTCCTAGTTTTGGTATTGGCCGAGGAATCAGCCGAACAACAAGTTCAAGAACCA
ACTGAGTGAGTTGAGATTTATTGATATTATGTTGTTCTTGTTGTCGTGATTTGTTG
AGTGAATAAATTTATTTTATTATTCTGAATGAACTCCTATTTTTTCTATTTTTTATA
TTTTTCAGACTCGAGAAGTCAGGAGAGCAACTCTCAGAGGAGGACTTGTGAGTT
GTTATTATTCAGAAAAAACTTTATTCTCACACTATGCACTTTTAGAATTGACGAG
CAAAAGCGTACTCCAATGCAACGCTCATCAATGGTTCGGTTCGGACGGTCACCA
ATGCAACGCTCATCCATGGTTAGATTCGGAAAGCGTTCGCCAATGCAAAGGTCCT
CAATGGTTCGCTTTGGAAAACGGTCGCCAATGCAACGATCTTCAATGGTGCGTTT
TGGAAAACGTTCACCGATGGAGCGTTCGGCTATGGTTCGCTTTGGAAGATCACCT
ATGGACCGATCGAAAATGGTCCGATTTGGTAGATCATCAATTGATCGCGCTTCTA
TGGTTCGGTACGTATTGACGTGAAAAGTATTTTGTGAATAAAGCTGAAGTTCAGA
CTCGGAAAACGGACACCAATGCAGAGATCATCGATGGTCCGTTTTGGCAAACGT
TCGATGGAATTTGAGATGCAATCAAACGAGAAGAACATCGAGGACAGCGAATAA
ACAAGTACATGCAAACACCTTGATTACCAAGAACAAAACGGTCTCACATTGTAG
TTTAATCTCGTTCTACGGCCTATTCTTACCTTTTTCATTTATGTATTTTTTTT

Mutant *flp-7(ibt7)*

TTTTTGACTTTTCAACTTTTCTCCTCATTTTTTCTCGATTGAAATTTCAATTTTTAA
ACCACTCCGCGTCCTCCACGGCCTATTCTTACCTTTTTCATTTATGTATTTTTTTT

Wildtype *npr-13*

CATCTTCCTTATTCTCCATTTTCTAATCATCTTCGACTTCTTCTTCTTCTACGCCTT
CCTGACTCCTCCCACACTCCTCATCCTTCTAGTACGTCGGTTAAAAAGGACTCAG
ACATCACACTTCTTTGTTTTAGGATCAAAAAGAAAATCAGTATAAAATGGGTGAT

GCTGAATCTCATCATTGTATAGATGTGAACGCCATTCTTCAGCAGTTCAATGATT
GGACAGTCCTCTTTGAAGTTCGGGTAAATTAATTTATGATTTCAGAGATCTTAAA
GCGAGTGATTCAGTGAAACTTCTTTATTTTTTCTAGACAACACTTTTTTGTTTGGA
ATTTTCACTTAGATTATTATGAAATTTAATAATCTAAACTTACATAACTATAAGTC
TGAAAACAAAGCTTGAAAACTTCACCTTCTAAACCTAGGCATATTACCCTGCGTA
TCTAAAATCCTCCTATCTGAAATTTCAAACTGAAGTGCTCAGAAAAAAATGAAA
AAAGTTCTGAATGCTTTTTGGATATTAAAAGTTAAAAAAGTTGATTAAAAGTTAG
TGTCCGAATTAATCCGAAGATTTCAAAAATTAATGAAGTTTATTTTGCACATTATT
TTAAAAAATTAAACTAGAAATGAATAAAAACTAATTTCTTAAACTCTATTTTTCT
GCAAACCACCTTGAAATCAATCAATGATCATAAATTTTCAAAAATTTGTTTAAAA
TTTGTACCTGAAATTTATTGCTCGGAAACTCATCATCAAAATAACTGTAACAATT
TTCAGCTTGGATATTCAGTACTATACTTTCTCATATTAATAATCGGATTGGTTGGA
AATGGGCTATTGATCACTTCAATTTTAATGCGAAAGAAACTTTCCGTGGCAAACA
TATTCTTGATAAACCTGGCAGTTTCTGATTTGGTAAGTTTTCAAGATTTTATTTGA
ATTGAACTTTGAAAGTTCCTGGCTCAAGATCAGAATCAAAATTATAATTTTAATG
TCAACCAAAAACGTCATACATTATTTCCAGCTTCTTTGCATCACGGCGGTGCCGA
TCACTCCAGTATTGGCGTTTATGAAGCGATGGATATTTGGAATAATTATGTGTAA
ATTGGTTCCAACTTGTCAGGCGTTTTCGGGTAAGAACGGGATCTAACCATTCGGA
ACAATTGAATTGTCCACTTTATCGTATTTGATAGGGAGAGCCGACCAAAAAGTAG
AAAGTGTCGCTTTTGAGGAAGTAAAGGGAAAAAGGGAAAACTTGAAGTTGATTT
TGATTACGAAAAAAACATTTTCGACTCTTTTTTTTTAGTGTTGTAACTCATATTTT
GGGTGGAGGTATACCTGTAGGTTGCAGGTGCCTAAATTAAAACCTGAATAAGTA
TAATACTGATTTCAAAACAATTCTATCCCAAATTAATTTAAGCTTTAAAGACCCT
CTGTGCCTGTTCTCAGGCGCTCGTCTTGAAAAATAGTTACGACTCTTGTGAAGAA
CAGAAGTCAGCATAAAATCTCAAAGCAGTAACATATTTTCAGCTGTTTTAAACAC
AAAGAAGCTTCAAATTTCAAAAATAAAAAACTCTGTACTGATTTTGCACACGAA
CTCTCTCCCCGAATCAATTCAATTTCCTAACTTTCAGTGCTCATTTCTTCATGGTC
TTTGTGTTACATCGCAATTGATAGATATCGAAGTATTGTGACGCCACTCCGGGAA
CCATGGTCTGATAGGCATGCAAGGGTAAGATTTGAAAATTTAGATGGGGTTCTGT
TAAAGTTGGGGTAGCTCCAGTTGGAAAAGTATTCAGAACTATTCATTTGGCACTA
AAGTAATAAAACATCAGAGTGAACCTTTTTTTTTTAAATTGGAAATGTTTTTATTT
ACTGTTAAAAAGCGGCAAAGCACTAATTTTTCTAAAATTACAAATTTTGGATGAT
GGGTCTTTGTGACCAATTTGAGGATTTTGAAAAAAACTCGCACGGGTGCTCCTCT
GTCAACTTACAGTAATTACGGAGTTTTCTGAAACCACTGTCTAAAGACGCATGGA
TTCATGAAAATAAGGCCTAGCTGCAAATAAAAAGTTTACGATATCATATTGGTGG
TTTTGGCCAACTTTTGACAGTGGGTTAAAATAAGTAAATTGGATATAAAACAGCC
GAAAACTAAAACAGCGTTGCAATAATTGTTTTCGCTTATTAGACCCTTCTGAATA
AACCCGTGCGCCTTTAGGCATGCGTTTCAGAAAGTTTCTTTGTAAACGTACGGAG

TTACACTAATAGAAGAAATACCGTATATATTTTCAAGTTTAGAACGTAGCTTTGC
GAGATTCAATTTAATTTTTAGTGCATTAAATACTTTAAATAATTAAATTTATTTCG
AAAATTCCCAAGCTTGAATAATTTTTCAAATATATTTTTCCAGTGGCTTCTGATGT
TCACATGGGTGGTCGCCTTCCTTGCTAGTTATCCTCTATATTACTCACAGAACTTG
AAAACAATGGTTATTGAAAATGTGACATTATGTGGAGATGTAAGTTTGAAAACCT
CAAAAATATCCAGCTAACATTCATTTGTTCCAGTTTTGCGGCGAGTTCAATTGGC
AGTCGGATGAAATATCCAAGTTGACATATACTACGAGTTTATTGATTATTCAGCT
GATTATTCCAGCAATTATCATGTCTTTTTGTTATTTAATGATTCTACAAAAGGTAT
TTTATCTATTGAGACGTTTTGAAATGGTCTATTTTTAGGTACAAACCGACTGGCTT
GTCGACGAGGGATCCATGTTGACTGCCGCACAACAGGTGAGACATAGACGGTAG
CAGATAGCGATAGGGTTTTCATAACGACACGGAAAACCGATTTTCCCGTCGGGG
GTATAGCTCAGTGGCAGAGCATTCGACTGCAGATCGAGAGGTCCCTGGTTCAACT
CCGGGTGCCCCCTAAATACTTTTTGGAATTTTTTTGCAAAATGTTTTTCACGATAA
TTATTTCAGGCTCAAACAGCAGTTCGAAAGCGACGAGTGATGTACGTGTTGATTC
TAATGGTTATTGTTTTTATGGCTTGCTGGTTCCCGTTGTCCGCCGTGAATTTGTTC
AGAGATCTCGGAATGCGATTCGAGTTCTGTCAAACTGTTTACAAGGTTTTAATGA
TGGACCAAATGTATTTCAAGTTGCTCAATGTGCACGTCATCGCGATGACTTCGAT
CGTATGGAATCCGGTGCTCTATTTCTGGATGAGCAAGGTATTTGCACATTTAGGT
ATTTAGAATTACAGTGTTTCATTCTGATTTTGATAGGTTAATGGAACTCAAAAATT
TTGAAGATGAAGAAGCCAATATGTGGGCGGTCATAGTTTTGATAGTTCCAGAAA
AAGCTACGCGCTTGGCTTTCTTTTTTGCAACACATTTTTGAGCTTATCGGAATTGT
TCAATAATTTTGATACATTTTTTGATGGTTGAAATTAGGATTTTTAAATTTAAATA
AACAATCGGACAGAGATAGTGAAAAAATACTCGCACTTCTTCCTAAAAAGATTT
ATAAAGATTTATTATTTTTCGTGCCCTGCCACTCTCGTACTGTCGACTGTCCGAAA
ATTAAAATTTCCGATAATATAAGTTCGATAAATAAAAATGTGCATACGTCTTTCA
AGCTCAAATGTTTTAAACTTCTCTGAATATTAGAAAAAAAAGATTAAATTTAACA
ATTTTTGAAATTTAGCAACCGGCTTCTGTCAAACTTTTGATTGCACCGCAACCCTG
GTTTCCAAGCTCAAATTGCTCCAAATCTTAGTTTTAGGCATTGTCTCAGAAAATG
ATATTAAAAATGATTTGCAATTGTTGAAACCTCTGATTTTCCGGAAACCGGTAAT
CTCCAAAATTTAGAAACACCCTAAACTTTTCATTCCCGGAATTCCCGATTTCTGG
GCACCGCTGGTTTACCAAAAACGATTACATTTGAAAATAAACCCTGTCCTCCCAA
CAATCATTTCATCTAATTTCCCCTAATTTTCAAATCTTCCAGCGTCATCGACGAGC
CCTGAAAGACGACATGACGTGGCTCACCAATGCTCGCCGTCATACAAACGTCGG
CGTTCTGTCTCGCTTCACACCTTCTCCATCAGTTTCAGTGGTTTACAGACGAACTC
TGGAGCGACATCTAGGTGTCAATCATTTCCGGTAAGAGACACTTTCTTCACGAGT
CTTTCTTGATTTTCGTCTTTTTGATGCCGCCGGCTAAATATGTGTGTGTGTGTATG
TGTGCTTAGGCTAAATATGATTATGGTGGTATTGGGTGGAAAAATGAGATAGAG
AGAGAATACACTCACATGCAACACTGATTCTAATTGACTTTTTATTCTGTTTCATA

GGGATCCGAGGGGAACAATTTTGATATGAAATGAGAAATATTTCAAAATTAAAA
TCATAGAAACCTCACAGAACATTTTTTACCAGCGTTGTGTTTTTTAGCCAACAAA
AATTACTTTTTAATCTGCATTTTTGAGAAATCTGCAAATGGATACTACAATTACCA
AAATTACAGTGAAACTGTTCCAAAAAAATTTGAAATTCTCTAGTTATCAAAAAGT
GGCAATACTCAGTTTTTACGCATCATTATTTAGAGCCCACCGAAAAAGTTCCAAG
GTCAGGTCTCCAAAAAGTTCACAATTTCTGGCCATCCCTTACAAAACTACAATTT
TAAATTTTTCAGCCGTGGCACACTTGCGGACCCGACATGCACTTCACGTGAACGA
AGTCTTCCGCGAGAACTTCAATCAAATTGTTTCCTTCTTGTTCCGCTTATGCCATT
ATGTCAATCTGTGACGAGGAAGAATAGTCATCTAGCAATCAATCGAGACGGGTA
AGTGATGTTACAGTTGATAGTCCTTGAAAGACATTTTTATGCAAATGGCGAAAAA
GAGAAGCCAGAAGCTCAATTGGAAAAAAAATTACAAAATGTAAAAGATGATTAG
GTATTCCCAATATTCTCATAAGTATTTTGTCAGCTGGAAATTTCTCGTAGATTTTC
CAAAAAAGCAAGCCGAACATCTTAAACAAGATTGTGCTGGAACATTTTCAAACT
TGTGGCTCTTTACTGTATTTTTTTTCTTGAAGAGATACATGAGCTGCAATTCTACG
AAATTTTCAATTGCCCAATATTCATCCAATATTTTAATTAAAATGTAGAAAACAA
TTTGGTACATCTGAAAAGTCTATATTTTGCCTGAAACGTATGAAGGCGCAAAAGT
TTAATGAAAGCTGCCAATAGGTGGAAAATGCCAGGTCATCAAAAACAACTGCAA
CATTTTCTGAACCCCTTTTCAAAATTTCCAATTAAAATGAAATTCATTTTCAGATC
AATCAATTATATTTCTGTAATTTAATATAAAGCCTCATGGAAAAATGTGGGGCAA
CATATTGTGATATTCCATTTTGCAGAATACACAAATTTAGCAGCTTGTTCATAATG
TGAAAAATGTAAAATAATTTTTTGAAGGAGTGTTTCAAATTTTTTTTTGTTTTTTT
TTTACAATGTGGGATTACACGTAAAAATATACCATGCGTTTCCTTTCTAGATCCCT
CCGGCAATATATACATTTTCCAAAGATCCCACACGAACATTTTATTTCTAATTAC
AGGATCGTCATTCCACAAGCCAATGGCTCAAGTCGTCGGCCGAGCAGCGTGAAT
ACCAATTCAACTCGAGACTGGTGACACCACCAACTTCTTTTTCATCATTTTCTCAT

Mutant *npr-13(ibt6)*

CATCTTCCTTATTCTCCATTTTCTAATCATCTTCGACTTCTTCTTCTTCTACGCCTT
CCTGACTCCTCCCACACTGACACCACCAACTTCTTTTTCATCATTTTCTCAT

AFDELING
Straat nr bus 0000
3000 LEUVEN, BELGIË
tel. + 32 16 00 00 00
fax + 32 16 00 00 00
www.kuleuven.be